NASA TECHNICAL NOTE

NASA TN D-3601

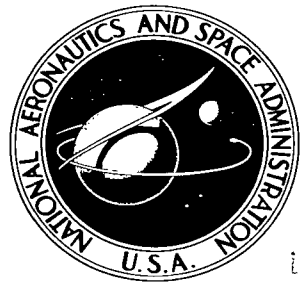

NASA TN D-3601

VELOCITY PROFILES AND EDDY VISCOSITY DISTRIBUTIONS DOWNSTREAM OF A MACH 2.22 NOZZLE EXHAUSTING TO QUIESCENT AIR

by James M. Eggers

Langley Research Center
Langley Station, Hampton, Va.

NATIONAL AERONAUTICS AND SPACE ADMINISTRATION • WASHINGTON, D. C. • SEPTEMBER 1966

NASA TN D-3601

VELOCITY PROFILES AND EDDY VISCOSITY DISTRIBUTIONS DOWNSTREAM OF A MACH 2.22 NOZZLE EXHAUSTING TO QUIESCENT AIR

By James M. Eggers

Langley Research Center
Langley Station, Hampton, Va.

NATIONAL AERONAUTICS AND SPACE ADMINISTRATION

For sale by the Clearinghouse for Federal Scientific and Technical Information
Springfield, Virginia 22151 – Price $2.50

VELOCITY PROFILES AND EDDY VISCOSITY DISTRIBUTIONS DOWNSTREAM OF A MACH 2.22 NOZZLE EXHAUSTING TO QUIESCENT AIR

By James M. Eggers
Langley Research Center

SUMMARY

An analytical and experimental study of compressible, turbulent, axisymmetric mixing was performed in order to validate or disprove recent formulations for the eddy viscosity function and to determine whether or not direct experimental determination of eddy viscosity distributions is feasible. The experimental study involved a Mach 2.22 axisymmetric nozzle exhausting to the atmosphere and operating at the design pressure ratio, with jet total temperature equal to ambient temperature. Total-pressure surveys were made across the jet at various axial stations from the nozzle exit plane downstream to 150 nozzle radii. The total-pressure surveys were reduced to velocity profiles and then, through the use of the momentum equation, to eddy viscosity distributions. An analytical study of the Mach 2.22 jet was performed for various eddy viscosity formulations by following the approach used by Walter R. Warren, Jr., in his PhD Thesis (Princeton Univ., 1957).

It was concluded that recent modifications of the eddy viscosity functions by incorporation of a density are unwarranted for the supersonic jet in quiescent air. It was also concluded, from inspection of the eddy viscosity distributions computed from the present experimental data, that the assumption of an eddy viscosity independent of the radial coordinate is not justified. Finally, general computational difficulties were found to make an experimental determination of the eddy viscosity coefficient subject to large uncertainties and possible errors.

INTRODUCTION

Although the phenomenon of mixing in turbulent, incompressible fluids is predictable for a wide variety of systems through the use of Prandtl's mixing theories, mixing in turbulent, compressible fluids is, in general, only beginning to be predictable. Recent interest in the problem of mixing in compressible, turbulent flow has been generated because of the application of the mixing phenomenon to a large number of flow problems, such as fuel and air mixing in hypersonic ramjet engines, mixing in fluid amplifiers, and prediction of rocket nozzle base pressures.

Analysis of mixing in turbulent, compressible flows has generally been attempted by modifying the incompressible eddy viscosity expressions of Prandtl either by the inclusion of a representative density or by transformations relating compressible flow to incompressible flow. The empirical constants required were taken from experiments involving mixing in incompressible flow. A wide variety of expressions for the eddy viscosity function have been suggested by various authors. For the downstream region of a jet in quiescent air, the expressions range from a formulation that produces an eddy viscosity which is constant throughout the flow field (see conclusion of ref. 1) to a formulation that produces a kinematic eddy viscosity which varies as the center-line velocity and the width of the mixing region (see ref. 2). Each author professes satisfactory agreement between his solution, which employs a particular eddy viscosity formulation, and the limited experimental data he considers. No criterion is yet available for selecting which of the suggested formulations for the eddy viscosity function is best for a given problem.

The simplest case of mixing in turbulent, compressible flow, that of a jet in quiescent air, is considered herein. A Mach 2.22 circular-cross-section nozzle was constructed from a design by using the method of characteristics and was operated at the design pressure ratio, with jet total temperature equal to ambient temperature. Surveys of total pressure were made across the jet at various axial stations from the nozzle exit plane downstream to 150 nozzle radii. The total-pressure surveys were reduced to velocity profiles and then, through the use of the momentum equation, to eddy viscosity distributions.

One purpose of the present report was to validate or disprove recent formulations for the eddy viscosity function, and another purpose was to establish whether or not experimental determination of eddy viscosity distributions is feasible. Experimental data for the Mach 2.22 jet were compared with the predictions of center-line velocity decay and jet spreading rate obtained by employing various formulations of eddy viscosity coefficient in an analysis similar to that of Warren.

SYMBOLS

Measurements for this investigation are given first in the International System of Units (SI) and parenthetically in the U.S. Customary System of Units.

A	function of jet exit properties defined by equation (A15)
$b_{0.1}, b_{0.9}$	radial distance to $\bar{u}^2 = 0.1$ and $\bar{u}^2 = 0.9$, respectively
B	function of jet exit properties defined by equation (A22)

c	function of density defined by equation (A8)
$\tilde{d}$	function of jet exit properties defined by equation (A9)
D	function of jet exit properties defined by equation (A23)
F	function of jet exit properties defined by equation (A47a)
G	function of jet exit properties defined by equation (A31)
H	function of jet exit properties defined by equation (A16)
K, K_1, K_2	empirical constants in various eddy viscosity formulations
l	Prandtl mixing length
m_x	integrated mass flow at x
M	Mach number
r	radial coordinate (see fig. 1)
r_i	radial dimension to edge of potential core (see fig. 1)
r_s	radial distance to surface of stream tube
$r_{0.1}, r_{0.9}$	radial distance to $\bar{u} = 0.1$ and $\bar{u} = 0.9$, respectively
T	static temperature
T_t	stagnation temperature
u	axial velocity component
U	center-line velocity nondimensionalized with respect to jet exit velocity
v	radial velocity component
V	function of jet exit properties and center-line velocity defined by equation (A38)
W	function of jet exit properties and center-line velocity defined by equation (A39)
x	axial coordinate (see fig. 1)

x_o	axial dimension to end of potential core (see fig. 1)
y_5	radial distance to point where the local mass flux per unit area is one-half the center-line value for the same axial station
α	function of jet exit properties and center-line velocity defined by equation (A29)
β	function of jet exit properties and center-line velocity defined by equation (A30)
γ	ratio of specific heats
δ	function of jet exit properties and center-line velocity defined by equation (A28)
ϵ	eddy kinematic viscosity
ϵ_2	function of jet exit properties and center-line velocity defined by equation (A36)
θ	function of jet exit properties and center-line velocity defined by equation (A34)
ρ	density
τ	turbulent shear stress defined by equation (C7)
φ	function of jet exit properties and center-line velocity defined by equation (A35)

Subscripts:

a	evaluated at ambient conditions
℄	evaluated on jet center line
r_s	evaluated at radial distance to surface of stream tube
y_5	evaluated at radial distance to point where the local mass flux per unit area is one-half the center-line value for the same axial station
1	evaluated at nozzle exit station

evaluated at radial distance to point where the local velocity is one-half the center-line value for the same axial station

A bar over a symbol denotes a quantity that is nondimensionalized with respect to jet exit properties r_1, u_1, and ρ_1 (for example, $\bar{r} = r/r_1$, $\bar{u} = u/u_1$, $\bar{\rho} = \rho/\rho_1$, $\bar{\epsilon} = \epsilon/u_1 r_1$, $\bar{x} = x/r_1$, and $\overline{\rho\epsilon} = \frac{\rho\epsilon}{\rho_1 u_1 r_1}$).

APPARATUS

Nozzle

The internal coordinates for the circular-cross-section Mach 2.22 nozzle were taken from reference 3. The nozzle coordinates were determined by the use of a computer program based on the three-dimensional characteristics method, and the nozzle was designed to have a minimum length with axial flow at the exit. The nozzle inviscid contours were not corrected for boundary-layer growth. The nozzle exit diameter was measured as 2.558 centimeters (1.007 in.) and the throat diameter as 1.793 centimeters (0.706 in.). Thus, the ratio of nozzle exit area to throat area is 2.035. This area ratio corresponds to a nozzle Mach number of 2.22 (actually 2.217, but the value 2.22 was believed to be of sufficient accuracy).

Instrumentation

The nozzle was installed in a blowdown facility and was connected to three bottles, each having a capacity of 28.32 cubic meters (1000 ft^3). Regulation of the total pressure upstream of the nozzle was accomplished by use of a pneumatically operated regulator valve. Monitoring of the upstream total pressure and total temperature was accomplished through the use of continuous recording devices and total-pressure and total-temperature probes installed in a settling chamber. A 2.07×10^6-N/m^2 (300-psi) pressure transducer was calibrated and installed to sense the upstream total pressure.

Total pressures from surveys were recorded on an x-y recorder, which was synchronously connected to the probe-traversing mechanism. This system allowed continuous direct recording of survey total pressure as a function of distance. Chart-to probe-travel calibrations used were 3:1, 2:1, and 1:1. At each survey station the chart-travel calibration that gave maximum profile size within the available chart travel of about 20.32 centimeters (8 in.) was used. Pressure transducers having ranges of 0 to 6.89×10^5 N/m^2 (0 to 100 psi), 0 to 3.45×10^5 N/m^2 (0 to 50 psi), 0 to 6.89×10^4 N/m^2 (0 to 10 psi), and 0 to 1.38×10^4 N/m^2 (0 to 2 psi) were calibrated and installed to sense the total pressures. The pressure transducer with the lowest range that the total-pressure range permitted was employed at a given survey station. The sensing end of

the total-pressure probe consisted of stainless-steel tubing with an outside diameter of 0.1524 centimeter (0.060 in.) and an inside diameter of 0.1016 centimeter (0.040 in.). A single-pass schlieren system, which allowed photographic monitoring of the jet, and a barometer completed the instrumentation.

Test Procedure

First attempts to adjust the jet flow to the design pressure ratio were unsuccessful. In these attempts the static pressure inside the nozzle exit lip was adjusted to match the ambient pressure; however, schlieren photographs indicated the jet was underexpanded. The area ratio of the nozzle, as determined from measurements, was then used to select the design pressure ratio for the nozzle, and this static- to total-pressure ratio (0.09064, which corresponds to Mach 2.22) was used for all subsequent nozzle operations. Pressures from the exit static taps were on the order of 1.38×10^4 N/m^2 (2 psi) below ambient pressure at this designation. A static-pressure survey near the nozzle exit indicated that the average static pressure was about 3.45×10^3 N/m^2 (0.5 psi) below ambient pressure and was fairly insensitive to upstream pressure changes of 4 to 5 percent. The flow in the region of the exit static taps was complicated by a shock wave which intersected the jet boundary just outside the nozzle exit. The extraneous shock which is evident in the schlieren photograph of figure 2, but not in the schlieren photograph of figure 3, is believed to have had an effect on the static-pressure readings of the exit tap. The effect of the shock, if any, on downstream flow development is not known; however, Warren (ref. 2) concluded that downstream region characteristics do not depend on the flow history in the core region. Thus, the effect of the extraneous shock wave, if any, would be expected to be confined to the immediate region downstream of the shock.

After adjustment of the jet flow to the design pressure ratio, total-pressure surveys were made across the jet at axial stations from the nozzle exit downstream to 150 nozzle radii. Verification that no detectable pressure lag existed in the system was accomplished by varying the rate of probe travel, stopping the probe while it was traversing, and traversing in both directions. Repeatability of the surveys was checked by repeating surveys under the same conditions on different days and was found to be within the accuracy of the measurements.

ACCURACY

Assumptions made during data analysis were that the total temperature was constant, that the profiles were symmetrical, and that the static pressure was constant throughout the flow field. The assumption that the total temperature was constant was valid since the difference between ambient and jet total temperature rarely exceeded

5.56° K (10° R). Profile symmetry was inspected by superimposing profiles and was found to be within the accuracy of the measurements.

The accuracy of the pressure transducers employed for the pressure measurements is commonly accepted as one-half of 1 percent of full range, but generally the accuracy is substantially better. Since the total pressure varies from zero to a maximum for a given survey, the percent error due to employing a given pressure transducer becomes a function of radial distance as well as axial distance from the nozzle. Inspection of reduced data from surveys performed at a given axial station during different runs indicated uncertainties of ±3/4 percent in $\bar{u}/U$ on the jet axis. The uncertainties increased with increasing radius to ±1 percent for $\bar{u}/U = 0.3$ and increased further to ±15 percent for $\bar{u}/U = 0.1$. These values are considered typical of the accuracy of the Mach 2.22 data presented herein.

THEORY

Theoretical analyses of compressible, turbulent jet mixing have been performed by Warren (ref. 2) and Kleinstein (ref. 1). The distinctly different analytical approach employed by each author warrants some discussion herein.

Kleinstein considers the differential system of boundary-layer equations expressing conservation of mass, momentum, specie, and energy; thus, his analysis is applicable to binary fluid systems. Under the assumption of Prandtl, Schmidt, and Lewis numbers near unity which reduce the momentum, specie, and energy equations to identical forms, Kleinstein transforms and linearizes the equations into the form of a heat conduction equation. The solution is then available in terms of the P-function (offset circular probability function). The solution relates the center-line decay of the jet properties to the transformed axial coordinate. The shape of the radial profiles is also specified by the solution for a given center-line property. An eddy viscosity functional relationship is then required to relate the transformed axial coordinate to the real axial coordinate. Kleinstein employs the following formulations for eddy viscosity for a jet in quiescent air:

$$\overline{\rho\epsilon} = \frac{K_1}{2}\bar{y}_5\bar{\rho}_{\text{¢}}U \tag{1}$$

$$\overline{\rho\epsilon} = \frac{K_2}{2}\bar{x} \tag{2}$$

Note that these formulations are written in the notation of the present paper and that the factor 1/2 is included for consistency with other eddy viscosity formulations considered herein. Equation (1) was applied for the region of developed flow downstream of the

potential core (see fig. 1 for jet flow field nomenclature used herein), and equation (2) was applied for the region of near two-dimensional mixing in the vicinity of the nozzle exit. A conclusion of Kleinstein was that a plot of nondimensional center-line velocity as a function of $\bar{\rho}_a^{1/2}\bar{x}$ was a universal plot independent of Mach number and the fluid considered. Discussion of this conclusion is found herein under "Presentation and Discussion of Data." The primary analytical attribute of Kleinstein's solution is its applicability for binary fluid problems and coaxial jet mixing as well as for the jet in quiescent air. Its chief weakness lies in the fact that the effect on the solution brought about by the linearization of the initial equations can not be foreseen.

Warren considers the integral system of equations expressing conservation of mass and conservation of momentum. Inasmuch as no specie conservation equation was employed, his solution is restricted to problems involving a single fluid. Warren develops his analysis by applying mass and momentum conservation, with a Crocco expression used to relate temperature to velocity, and by employing an assumed form of the velocity profile. The velocity profile assumed in the region of the potential core is

$$\bar{u} = \exp\left(-0.6932\frac{\bar{r}^2 - \bar{r}_i^2}{\bar{r}_5^2 - \bar{r}_i^2}\right) \tag{3}$$

and in the fully developed region downstream of the potential core is

$$\frac{\bar{u}}{U} = \exp\left(-0.6932\frac{\bar{r}^2}{\bar{r}_5^2}\right) \tag{4}$$

A criticism of Warren's analysis is that the velocity profile is discontinuous at the edge of the potential core. The eddy viscosity relationship was assumed to be

$$\bar{\epsilon} = \frac{K}{2}\left(\bar{r}_5 - \bar{r}_i\right) \tag{5}$$

for the core region within a potential core length from the nozzle exit and

$$\bar{\epsilon} = \frac{K}{2}\bar{r}_5 U \tag{6}$$

for the region downstream of the potential core. A combination of equations expressing mass and momentum conservation is then applied through equations (5) and (6) in order to relate $\bar{r}_5$ to $K\bar{x}$ in the core region and to relate the center-line velocity to $K\bar{x} - K\bar{x}_o$ (where $\bar{x}_o$ defines the potential core length) in the downstream region. Of course, empirical determination of K is necessary to complete the solution. An

apparent mathematical restriction exists in Warren's solution due to the inclusion of various terms in square root radicals. The restriction is removed in appendix A by rederiving Warren's solution. The primary analytical attribute of Warren's solution is its straightforwardness and simplicity of approach; of course, the solution is limited to mixing of a single fluid.

Because of its simplicity, Warren's method was expanded to encompass the formulations of the eddy viscosity, listed in table I, with the view to determining the differences in solution brought about by various assumptions for the eddy viscosity. The analytical development necessary to produce the solution for a given eddy viscosity formulation is summarized in appendix A.

TABLE I.- EDDY VISCOSITY FORMULATIONS

Formulation number	Core region	Developed region	Comments
1	$\bar{\epsilon} = \frac{K}{2}(\bar{r}_5 - \bar{r}_i)$	$\bar{\epsilon} = \frac{K}{2}\bar{r}_5 U$	Warren (ref. 2)
2	$\overline{\rho\epsilon} = \frac{K}{2}(\bar{r}_5 - \bar{r}_i)$	$\overline{\rho\epsilon} = \frac{K}{2}\bar{r}_5\bar{\rho}_\ell U$	Modification of reference 1
3	$\overline{\rho\epsilon} = \frac{K_2}{2}\bar{x}$	$\overline{\rho\epsilon} = \frac{K_1}{2}\bar{y}_5\bar{\rho}_\ell U$	Kleinstein (ref. 1)
4	$\overline{\rho\epsilon} = \frac{K}{2}(\bar{r}_5 - \bar{r}_i)\bar{\rho}_a$	$\overline{\rho\epsilon} = \frac{K}{2}\bar{\rho}_a\bar{r}_5 U$	Reference 4 (expression for developed region only)
5	$\bar{\epsilon} = \frac{K}{2}$	$\bar{\epsilon} = \frac{K}{2}$	Trivial solutions
6	$\overline{\rho\epsilon} = \frac{K}{2}$	$\overline{\rho\epsilon} = \frac{K}{2}$	Trivial solutions
7	$\overline{\rho\epsilon} = \frac{K}{2}(\bar{y}_5 - \bar{r}_i)$	$\overline{\rho\epsilon} = \frac{K}{2}\bar{y}_5\bar{\rho}_\ell U$	Modification of reference 1
8	$\bar{\epsilon} = \frac{K}{2}(\bar{r}_5 - \bar{r}_i)$	$\bar{\epsilon} = \frac{K}{2}$	Combination of formulations 1 and 5
9	$\overline{\rho\epsilon} = \frac{K}{2}(\bar{r}_5 - \bar{r}_i)$	$\overline{\rho\epsilon} = \frac{K}{2}$	Combination of formulations 2 and 6

Figures 4 and 5 present the portion of the solution for the Mach 2.22 jet which is independent of any eddy viscosity assumption. In the core region, $\bar{r}_5$ is related to $\bar{r}_i$ (fig. 4) by the assumed velocity profile (eq. (A4)) and by the density-velocity relationship (eq. (A10)) applied through conservation of momentum (eq. (A3)). Similarly, in the developed region, $\bar{r}_5$ is related to U (fig. 5) by the assumed velocity profile (eq. (A5)) and by the density-velocity relationship (eq. (A11)) applied through conservation of momentum (eq. (A3)). The various eddy viscosity assumptions serve to relate $\bar{r}_5$ and thus $\bar{r}_i$ and U to the axial coordinate.

The core region solutions for a Mach 2.22 jet for the eddy viscosity formulations of table I are presented in figure 6. The jet spread $\bar{r}_5$ is plotted against $\bar{x}/\bar{x}_0$. The nondimensionalization removes any considerations of the empirical constant K. The formulations based on constant eddy viscosity (see curves 5 and 6 in fig. 6) are unrealistic, as the jet spread is known to be nearly linear in the core region and need not be considered further. The formulation based on an eddy viscosity proportional to $\bar{x}$ (see curve 3 in fig. 6) predicts the most linear spreading of the jet in the core region. The remaining formulations (see curves 1, 2, 4, and 7) predict spreading which deviates at most by 3 percent from curve 3, and all the formulations predict somewhat less spreading for all coordinates less than the potential core length. On the basis of near-linear spreading in the core region, formulations 1, 2, 4, and 3 of figure 6, when incorporated in an analysis, would be expected to produce reasonable approximations of the jet radius $\bar{r}_5$.

The developed region solutions for a Mach 2.22 jet for the eddy viscosity formulations of table I are presented in figures 7(a) and 7(b). The most rapid decay of center-line velocity and the associated effect of rapid jet spreading are predicted by formulations 1, 4, and 7. Similarly, the slowest decay of center-line velocity and the slowest jet spreading are predicted by formulations 5 and 6. No trend is evident as to whether an eddy viscosity formulation based on mass flux predicts more or less rapid mixing than does a formulation based on velocity. Final conclusions as to the most proper formulation must be determined by comparison with experiment.

PRESENTATION AND DISCUSSION OF DATA

Developed Region

As is evident in figure 8, velocity profile similarity for the Mach 2.22 jet appears well established for all axial stations from 28.9 to 127.3 nozzle radii from the exit. Profiles for stations beyond 127.3 radii are not presented because the flatness of the profiles makes determination of the axis of symmetry and thus of the jet radius r_5 very uncertain. (Experimental data for the Mach 2.22 jet are presented in tabular form in appendix B.) Scatter in the data in the jet extremes is due to the fact that small errors in experimentally determined velocities produce a relatively large uncertainty in the radial dimension. Comparison of the data with Warren's assumed profile (eq. (4)) shows good agreement, particularly for large $\bar{x}$.

Figure 9 presents the experimental velocity profiles compared with the theoretical profiles obtained by the method of Kleinstein (ref. 1) and of Warren (ref. 2) at five axial stations. The methods of obtaining the two theoretical profiles are fundamentally different. The measured center-line velocity was used to compute the Kleinstein profiles at each station. The Warren profiles were computed by using the equations in appendix A

and an average value of the empirical constant K of 0.031. The constant K was obtained by comparing theoretical $K\bar{x}$ with experimental $\bar{x}$ for a given value of U, and the value 0.031 was the average value of K obtained over the range of U from 0.9 to 0.2 at intervals of U of 0.1. (All other values of K reported herein were obtained by an identical method. It is evident that a wide range of values of K, determined by comparing $K\bar{x}$ with $\bar{x}$, is valid criteria for rejecting an eddy viscosity formulation.) The Kleinstein profiles therefore represent the best possible fit at each axial station, whereas the Warren profiles represent an average fit over the range of values of U considered. The Kleinstein profiles tend to underestimate the jet velocity spread for a substantial portion of the central region of the profile at all stations considered, but substantially overestimate the velocity spread at the jet extremes. Justification for the choice of profiles employed by Warren is evident in figures 8 and 9(c), where Warren's velocity profile can be seen to compare quite favorably with experiment. Warren's velocity profile for the developed region of the jet (eq. (A5)) is considered superior to Kleinstein's because it allows an implicit, serviceable expression for the velocity, because the fit with data in the jet extremes is more precise, and because employing a proper value of $\bar{r}_5$ as evidenced by figure 9(c) produces excellent correspondence with experimental data. Some restriction on how precise a correspondence of theoretical and experimental velocity profiles can be obtained is imposed by the relationship between $\bar{r}_5$ and U given in equation (A32). However, good agreement with theory is indicated in figure 5 which presents data from the Mach 2.22 jet for U as a function of $\bar{r}_5$.

As previously stated in the theoretical section of this report, a conclusion of reference 1 was that a plot of nondimensional center-line velocity as a function of $\bar{\rho}_a^{1/2}\bar{x}$ would be independent of Mach number and the fluid considered. The conclusion is herein shown to be invalid, as may be seen in figure 10. The data considered in reference 1 were from references 2 and 5. Data presented in figure 10 were from the same sources with the following four additions: the low-speed data of reference 6, the low-speed data of reference 7, the Mach 1.4 data of reference 8, and the Mach 2.22 jet data obtained in the present study. (The data in ref. 6 were obtained from the low-speed jet in ref. 9 and it was noted in ref. 6 that some uncertainty exists as to the test conditions of the jet in ref. 9.) A general trend of decreasing center-line velocity decay with increasing Mach number is indicated. The correlation of the Mach number data in reference 1 is thus considered inadequate, and the incomplete understanding of velocity decay in turbulent jets is exemplified.

Figures 11 and 12 present the experimentally determined center-line velocity decay and the jet radius $\bar{r}_5$, respectively, as functions of the nondimensional axial coordinate. Figures 11 and 12 also present theoretical curves for formulations 1, 4, and 7 of eddy viscosity for the developed region, as listed in table I. Each of the other formulations

listed in table I was rejected from further consideration when the value of the empirical constant was found to vary by a factor of 2 or more over the range of U considered. The range of values of K was from 0.028 to 0.038 for formulation 1, from 0.032 to 0.040 for formulation 4, and from 0.030 to 0.039 for formulation 7. Average values of K, determined as previously discussed, were used in forming the theoretical curves of figures 11 and 12 and are given in the figures. Inspection of figures 11 and 12 indicates that no one formulation for the eddy viscosity coefficient was more valid than another for either center-line velocity decay or jet spread. In fact, the difference in velocity decay and jet spread predicted by the three formulations is so slight that a choice of the best of the three formulations is considered impossible. Note that, at 140 jet radii from the jet exit, the values of the jet radius $\bar{r}_5$ predicted by the three eddy viscosity formulations vary by only 5 percent. (See fig. 12.) Similarly, for a given $\bar{x}$ the variation of the values of U predicted by the three formulations is much less than 5 percent. (See fig. 11.) It is considered doubtful that accuracy significantly greater than 5 percent can be achieved from a given experiment. Furthermore, the radically different analytical approaches employed by various authors (e.g., see refs. 1 and 2) would, for a given eddy viscosity function, be expected to produce theoretical results which differ by much more than 5 percent. The primary difference in the three formulations is in the potential core length, which ranges from 23.05 to 25.10 jet radii. However, difficulty in defining the potential core length from the experimental data makes this difference somewhat insignificant.

For the Mach 2.22 jet, comparison of the theoretical curves with the experimental data in figures 11 and 12 indicates that the velocity decay and jet spread are only fairly well predicted by theory. However, the predicted values are of sufficient accuracy for most engineering applications. Attention is directed to the fact that it is possible to make theory and experiment coincide for a limited range of values by using a different value of the empirical constant K. However, such adjustments of the empirical constant K were not made herein, as the view was taken that an adequate representation of the eddy viscosity coefficient should produce correlation of data over the entire range of values considered.

Core Region

Experimental and theoretical values of the jet radius $\bar{r}_5$ for the core region are presented in figure 13. (Experimental data for the Mach 2.22 jet are given in tabular form in appendix B.) Only the theoretical formulations which were found to be acceptable for the developed region are considered. The nondimensional axial coordinate associated with the experimental data has been corrected by adding a length to account for the initial boundary layer at the nozzle exit. This additional length was determined by plotting the

mixing width $b_{0.1} - b_{0.9}$ as a function of the axial coordinate $\bar{x}$ and extrapolating the mixing width to zero, as shown in the following sketch:

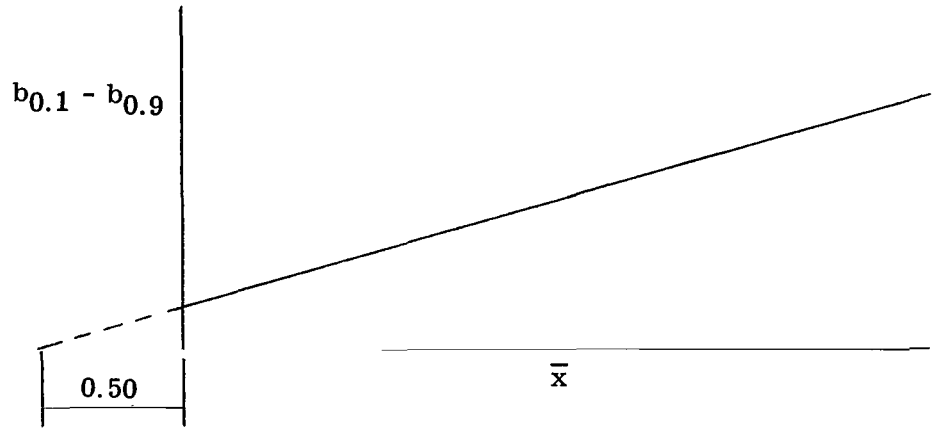

The magnitude of the correction to $\bar{x}$ was found to be 0.50. An identical method of determining the additional length was employed in reference 10. In figure 13 formulation 1 for the eddy viscosity coefficient corresponds best to the experimental data for the Mach 2.22 jet. All three formulations underestimate the jet spread within the core region. However, the predicted values of jet spreading within the core region are in fair agreement with the experimental data and are of sufficient accuracy for most engineering applications.

The velocity profiles in the core region are presented in figure 14, where $\bar{r}_{0.9}$ and $\bar{r}_{0.1}$ are the radii to $\bar{u} = 0.9$ and $\bar{u} = 0.1$, respectively. The data presented in figure 14 are moderately well correlated. Further correlation was not attempted herein, as an adequate discussion of various two-dimensional correlation methods that are commonly applied for the core region is available in reference 10.

Further inspection of figure 13 for the core region and of figures 11 and 12 for the developed region indicates that solutions which employ a representative density in the eddy viscosity formulation (such as solutions for eddy viscosity formulations 4 and 7 in table I) do not necessarily result in better correlation with experimental data than solutions which do not employ a representative density in the eddy viscosity formulation (such as solution for formulation 1 in table I). It is concluded that recent modifications of eddy viscosity functions by incorporation of a density appear unwarranted for the supersonic jet in quiescent air. In reference 11 a somewhat similar conclusion was reached for isothermal, coaxial mixing in low-speed concentric flows. Also, in reference 11 an assumption of uniform eddy viscosity was found to be sufficient for correlating the data; that is, no axial variation in eddy viscosity was required. For the supersonic jet considered herein, however, a theoretical assumption of uniform eddy viscosity, as stated in formulations 5 and 6 of table I, would not correlate the data. Formulations 5

and 6 were rejected from consideration when the previously discussed criterion for the empirical constant K was applied.

Eddy Viscosity Distributions

The experimental eddy viscosity distributions for the developed region of the Mach 2.22 jet, as computed by the method outlined in appendix C, are presented in figures 15 and 16. Equation (C12) was employed to compute the values of center-line eddy viscosity and equations (C8) and (C9) were employed to compute all other experimental eddy viscosity values reported. Values of $\overline{\rho\epsilon}$ and $\bar{\epsilon}$ are plotted as functions of the radial coordinate $\bar{r}$ for axial stations of 28.9, 47.9, 65.7, 90.9, and 127 nozzle radii from the nozzle exit. No assumption as to similarity of profiles was applied in generating the experimental eddy viscosity distributions; only the assumptions inherent in the use of the momentum equation (eq. (C2)) were involved. Since experimental scatter cannot be eliminated, graphical smoothing was performed at each intermediate step of the calculations. Axial gradients as required were determined by the use of survey data from at least four axial stations. Scatter in the data is especially noticeable at small radial coordinates and near the jet extremes. At small radial coordinates the scatter is due both to problems in determining the velocity gradient and to the fact that the shear stress and the velocity gradient approach zero simultaneously (see eq. (C9)). Consistent trends of a maximum in the eddy viscosity coefficient at a radial location near the point of maximum velocity gradient were noted during computation. For small radial coordinates the values of eddy viscosity coefficient become large and are subject to significant error for reasons discussed previously. Computations, with the exception of computations near the jet center line and near the jet extremes, were found to be repeatable within ±15 percent, as determined by a repeated computation of data at one axial station. Figures 15 and 16 indicate that neither an assumption of $\overline{\rho\epsilon}$ nor an assumption of $\bar{\epsilon}$ independent of the radial coordinate is experimentally justified throughout the flow field. Only in the extreme downstream region of flow do the assumptions appear approximately true. In short, experimentally determined distributions of the eddy viscosity coefficient do not correspond to the eddy viscosity distributions currently employed in analyses which assume $\overline{\rho\epsilon}$ and $\bar{\epsilon}$ are functions of $\bar{x}$ only. An identical conclusion was reached in reference 12 as a result of hot-wire measurements in a two-dimensional incompressible jet. In reference 13, where attention was focused upon coaxial concentric jet mixing, eddy viscosity was maximum at the center line and decreased smoothly with increasing radial dimension. Such a distribution does not agree with the eddy viscosity distributions determined in this report, apparently because of the analytical assumptions employed in reference 13.

Since the assumption of uniform $\overline{\rho\epsilon}$ or $\bar{\epsilon}$ was shown to be invalid, Prandtl's mixing length theory was investigated to determine whether an assumption of uniform mixing length might be physically justified. Figure 17 presents the radial distribution of Prandtl's mixing length for the Mach 2.22 jet for axial stations of 28.9 and 47.9 nozzle radii. In this figure the mixing length distributions for the Mach 2.22 jet are compared with a distribution from reference 14 for a low-speed jet. In reference 14, the mixing length distribution was computed from data which were obtained by the hot-wire technique. Identical trends for the Prandtl mixing length for the Mach 2.22 jet of the present report and the subsonic jet of reference 14 are evident in figure 17. It was noted in reference 14 that a complete reversal in mixing length distribution can result from slight refairing of data when obtaining velocity gradients for small radii. Such a reversal occurs for the Prandtl mixing length computed at the axial station $\bar{x} = 28.9$ for the Mach 2.22 jet. However uncertain the computations are at small radial coordinates, the distribution over the remainder of the jet (i.e., $\bar{r} \gtrsim 0.25$) is sufficient to conclude that an assumption of uniform mixing length at an axial station is not justified.

Since a correspondence is lacking between the experimental eddy viscosity distributions and the uniform eddy viscosity distributions employed in various analyses, an attempt is made to determine whether experimental and analytical distributions might be related by the use of some average or representative value. Included in figure 15 is the predicted eddy viscosity coefficient $\overline{\rho\epsilon}$, as determined from Kleinstein's analysis. No implicit form for the eddy viscosity is required for this computation; only the use of the measured center-line velocity, the assumption of $\overline{\rho\epsilon}$ as a function of $\bar{x}$ only, and the mathematic limitations of the analysis are involved. No readily useful relationship between $\overline{\rho\epsilon}$ of Kleinstein's analysis and the computed values for the Mach 2.22 jet is apparent. Also included in figure 15 is the predicted eddy viscosity coefficient $\overline{\rho\epsilon}$, which was computed by employing equation (A11) for density and Warren's formulation for ϵ. Included in figure 16 is the predicted eddy viscosity coefficient $\bar{\epsilon}$ as computed from Warren's eddy viscosity formulation (formulation 1 in table I). Again, no readily useful relationship between the computed and predicted eddy viscosity is evident. Note that a meaningful average or representative value for the coefficient was not extracted from the computed values at a station because of the sizable uncertainties at the jet center region and at the jet extremes. It is concluded that theoretical and experimental eddy viscosity distributions do not correspond and that general computational difficulties make an experimental determination of the eddy viscosity coefficient subject to large uncertainties and possible errors. Therefore, the method of validating an eddy viscosity formulation by comparing predicted values of velocity, temperature, and so forth, with experimentally determined values is recommended. This method is believed to have more promise for the solution of turbulent mixing problems within the limitations of the

eddy viscosity concept than does a direct comparison of analytical and experimental eddy viscosity values.

Attempts to compute the eddy viscosity distribution within the core region produced inconsistent results because of computational difficulties due to the rapid change of property gradients encountered. Thus, no results are presented for the core region.

Entrainment

A byproduct of the eddy viscosity computations is the amount of air entrained by the Mach 2.22 jet. Figure 18 presents the normalized mass flow of air entrained, as determined by integrations at each axial station. Uncertainties on the order of ±10 percent exist at axial stations far from the nozzle exit because of uncertainties in the zero velocity location. Figure 18 indicates that at 150 nozzle radii from the nozzle exit the total mass flow is approximately 10.7 times the jet exit flow; that is, 9.7 times the initial mass flow has been entrained.

Figure 18 also presents theoretical entrainment which was computed for the Mach 2.22 jet by using Warren's equations (eqs. (A4), (A5), (A10), and (A11)). The predicted entrainment is seen to be slightly higher than the experimental data for the Mach 2.22 jet; however, theoretical and experimental trends are in very good agreement, and predicted entrainment values are generally within the accuracy of the data. In addition, the entrainment of a low-speed jet (54 m/sec (176 ft/sec)) from reference 7 is compared with the Mach 2.22 data. It is evident that, for comparable axial lengths, the low-speed jet entrains a much larger quantity of air than the supersonic jet. This larger entrainment is at least partially due to the wider divergence of the mixing boundaries for the low-speed jet.

CONCLUSIONS

As the result of an analytical and experimental investigation of a Mach 2.22 jet in quiescent air and at design conditions, with jet total temperature equal to ambient temperture, the following conclusions were obtained:

1. Of the two analyses considered, Kleinstein's and Warren's, the latter was the more successful in correlating the Mach 2.22 jet velocity profiles within the developed region.

2. When employed in an analysis similar to Warren's, three formulations of eddy viscosity coefficient, which assume an eddy viscosity independent of the radial coordinate, were found to produce negligible differences in center-line velocity decay and jet spreading within the developed region and only small differences in jet spreading within

the core region. Predicted values of jet spreading and velocity decay within the developed region and predicted values of jet spreading within the core region were in fair agreement with experimental data for the Mach 2.22 jet and are of sufficient accuracy for most engineering applications.

3. Eddy viscosity distributions computed from the Mach 2.22 jet experimental data indicate that the assumption of an eddy viscosity independent of the radial coordinate is not justified. Furthermore, general computational difficulties make an experimental determination of the eddy viscosity coefficient subject to large uncertainties and errors.

4. Recent modifications of eddy viscosity functions by incorporation of a density appear unwarranted for the supersonic jet in quiescent air.

5. Theoretical predictions of jet entrainment, made by employing Warren's equations, were found to be in good agreement with the Mach 2.22 jet experimental data in both trend and magnitude.

Langley Research Center,
National Aeronautics and Space Administration,
Langley Station, Hampton, Va., March 25, 1966.

APPENDIX A

ANALYSIS OF THE JET BY THE USE OF VARIOUS FORMULATIONS OF EDDY VISCOSITY

General Equations

The equations employed in the analysis of a turbulent, compressible, axisymmetric jet in quiescent air and at design pressure ratio are summarized in this appendix. The analytical approach is similar to that used by Warren (ref. 2). The primary difference between the present analysis and the analysis in reference 2 is that, in the present analysis, provision for various formulations of the eddy viscosity coefficient is retained in the final equations. The coordinate system and the nomenclature employed herein for the various regions of the flow field are shown in figure 1.

A combination of the conservation-of-mass and conservation-of-momentum equations for turbulent, compressible, axisymmetric flow with negligible pressure gradient and the usual Prandtl boundary-layer approximations results in the equation

$$\frac{d}{d\bar{x}}\int_0^{\bar{r}_5}\overline{\rho u^2 r}\,d\bar{r} - \bar{u}_5\frac{d}{d\bar{x}}\int_0^{\bar{r}_5}\overline{\rho u r}\,d\bar{r} = \bar{\tau}_5\bar{r}_5 \tag{A1}$$

where

$$\bar{\tau}_5\bar{r}_5 = \bar{\rho}_5\bar{\epsilon}\,\bar{r}_5\left(\frac{\partial u}{\partial r}\right)_5 \tag{A2}$$

The apparent turbulent shear stress is represented by $\bar{\tau}_5$ and the eddy (or virtual or apparent) kinematic viscosity by $\bar{\epsilon}$. Equation (A1) is equivalent to the equation for laminar flow with the molecular laminar viscosity replaced by the eddy viscosity. Substitution of equation (A2) into equation (A1) produces equation (51) of reference 2. For eddy viscosity, assumed proportional to mass flux per unit area, of the form

$$\rho\epsilon = \frac{K}{2}(\text{radial dimension which varies as } x \text{ only})\rho u$$

$\bar{\rho}_5$ in equation (A2) is interpreted as $\bar{\rho}$ in accordance with the constant-exchange-coefficient theory. This theory, which assumes that the eddy viscosity is invariant with the radial dimension, was employed by Warren (ref. 2) and is employed herein.

A second equation which expresses conservation of momentum at each axial station is

APPENDIX A

$$\int_0^\infty \overline{\rho u^2 r}\, d\bar{r} = \frac{1}{2} \tag{A3}$$

Equations (A1), (A2), and (A3) are the fundamental equations employed herein and in reference 2. Application of these three equations requires relating the velocity profile to the radial coordinate and relating the density to the velocity. For the core region the velocity profile is assumed to have the form

$$\bar{u} = \exp\left(-0.6932\, \frac{\bar{r}^2 - \bar{r}_i^2}{\bar{r}_5^2 - \bar{r}_i^2}\right) \tag{A4}$$

where, for $\bar{r} < \bar{r}_i$, $\bar{u}$ is defined as unity. Equation (A4) is identical to equation (48) of reference 2. A criticism of this velocity profile is its discontinuity at the edge of the potential core.

For the developed region downstream of the core region, the velocity profile is assumed to have the form

$$\bar{u} = U \exp\left(-0.6932\, \frac{\bar{r}^2}{\bar{r}_5^2}\right) \tag{A5}$$

equation (A5) is identical to equation (49) of reference 2.

The density is related to the velocity by employing the following form of Crocco's energy integral:

$$T_t = T_a + \left(T_{t,1} - T_a\right)\bar{u} \tag{A6}$$

By using the isentropic relationship between total temperature and velocity and an assumption of uniform static pressure, the density is related to the velocity (for identical ambient and jet gases) as follows:

$$\frac{\bar{\rho}}{\bar{\rho}_a} = \frac{1}{1 + \left(\frac{T_{t,1}}{T_a} - 1\right)\bar{u} - \frac{\frac{\gamma - 1}{2} M_1^2 \frac{T_{t,1}}{T_a}}{1 + \frac{\gamma - 1}{2} M_1^2}\bar{u}^2} \tag{A7}$$

For convenience, c is defined as

$$c = \bar{\rho}_a - 1 \tag{A8}$$

and $\tilde{d}$ is defined as

$$\tilde{d} = \frac{\frac{\gamma - 1}{2} M_1^2 \frac{T_{t,1}}{T_a}}{1 + \frac{\gamma - 1}{2} M_1^2} \tag{A9}$$

By substituting c and $\tilde{d}$ into equation (A7) for the core region, the following equation is obtained:

$$\frac{\bar{\rho}}{\bar{\rho}_a} = \frac{1}{1 + (c + \tilde{d})\bar{u} - \tilde{d}\bar{u}^2} \tag{A10}$$

For the developed region it is more convenient to nondimensionalize the velocity with respect to the center-line velocity U. The following equation for the developed region is obtained:

$$\frac{\bar{\rho}}{\bar{\rho}_a} = \frac{1}{1 + (c + \tilde{d})\frac{\bar{u}}{U}U - \tilde{d}\left(\frac{\bar{u}}{U}\right)^2 U^2} \tag{A11}$$

Equations (A10) and (A11) are identical to equations employed in reference 2. For the particular case of jet total temperature equal to ambient static temperature, $c = -\tilde{d}$ simplifies the solution.

General Solution for the Core Region

The relationship between the variables $\bar{r}_i$ and $\bar{r}_5$ and the relationship of these variables to the axial coordinate are required for the general solution in the core region. Eddy viscosity relationships are inserted subsequently when particular solutions are desired.

By inserting equation (A10) into equation (A3) and expanding the integral, the following relationship between $\bar{r}_5$ and $\bar{r}_i$ is obtained:

$$\int_0^{\bar{r}_i} \frac{\bar{\rho}_a \bar{u}^2 \bar{r}\, d\bar{r}}{1 + (c + \tilde{d})\bar{u} - \tilde{d}\bar{u}^2} + \int_{\bar{r}_i}^{\infty} \frac{\bar{\rho}_a \bar{u}^2 \bar{r}\, d\bar{r}}{1 + (c + \tilde{d})\bar{u} - \tilde{d}\bar{u}^2} = \frac{1}{2} \tag{A12}$$

For $0 \leqq r \leqq r_i$, $\bar{u} = 1$ allows immediate evaluation of the first integral on the left of equation (A12). The second term is integrated by converting the variable of integration from $\bar{r}$ to $\bar{u}$. From equation (A4) the following equation is obtained:

APPENDIX A

$$\bar{r}\, d\bar{r} = \frac{-\bar{r}_5^{\,2} + \bar{r}_i^{\,2}}{1.3864} \frac{d\bar{u}}{\bar{u}} \tag{A13}$$

Substituting equation (A13) into the second integral of equation (A12), performing the integration, and combining terms yield the following expression:

$$\left(1 - 2\bar{\rho}_a A\right)\bar{r}_i^{\,2} + 2\bar{\rho}_a A \bar{r}_5^{\,2} = 1.0 \tag{A14}$$

The following definitions were used:

$$A = \frac{1}{1.3864(\gamma - 1)M_1^{\,2}\bar{\rho}_a}\left(\frac{c + \tilde{d}}{H} \ln \frac{c + \tilde{d} + H + 2}{c + \tilde{d} - H + 2} - \ln \bar{\rho}_a\right) \tag{A15}$$

$$H = \sqrt{4\tilde{d} + \left(c + \tilde{d}\right)^2} \tag{A16}$$

Equation (A14) gives the desired relationship between $\bar{r}_5$ and $\bar{r}_i$ for the core region and is identical to equation (55) of reference 2. Attention is directed to the fact that the relationship in equation (A14) is independent of any eddy viscosity assumption, as none has been employed in its derivation.

For the core region it remains to relate $\bar{r}_5$, and thus $\bar{r}_i$ (through eq. (A14)), to the axial coordinate. By noting that $\bar{u}_5 = 1/2$ and by expanding the integrals, equation (A1) is rewritten as

$$\frac{d}{d\bar{x}} \int_0^{\bar{r}_i} \overline{\rho u^2 r}\, d\bar{r} + \frac{d}{d\bar{x}} \int_{\bar{r}_i}^{\bar{r}_5} \overline{\rho u^2 r}\, d\bar{r} - \frac{1}{2}\frac{d}{d\bar{x}} \int_0^{\bar{r}_i} \overline{\rho u r}\, d\bar{r} - \frac{1}{2}\frac{d}{d\bar{x}} \int_{\bar{r}_i}^{\bar{r}_5} \overline{\rho u r}\, d\bar{r} = \bar{\tau}_5 \bar{r}_5 \tag{A17}$$

Since $\bar{u} = 1$ and $\bar{\rho} = 1$ within the core region, for $0 \leq \bar{r} \leq \bar{r}_i$, the first and third terms of equation (A17) can be readily integrated. The remaining two terms are converted to the variable of integration $\bar{u}$ by use of equation (A13), and the density is substituted from equation (A10). The resulting equation is

$$\frac{1}{4}\frac{d\bar{r}_i^{\,2}}{d\bar{x}} - \frac{\bar{\rho}_a}{1.3864}\frac{d}{d\bar{x}}\left[\left(\bar{r}_5^{\,2} - \bar{r}_i^{\,2}\right)\int_{\bar{u}=1}^{\bar{u}=1/2} \frac{\bar{u}\, d\bar{u}}{1 + \left(c + \tilde{d}\right)\bar{u} - \tilde{d}\bar{u}^2}\right]$$

$$+ \frac{\bar{\rho}_a}{2(1.3864)}\frac{d}{d\bar{x}}\left[\left(\bar{r}_5^{\,2} - \bar{r}_i^{\,2}\right)\int_{\bar{u}=1}^{\bar{u}=1/2} \frac{d\bar{u}}{1 + \left(c + \tilde{d}\right)\bar{u} - \tilde{d}\bar{u}^2}\right] = \bar{\tau}_5 \bar{r}_5 \tag{A18}$$

APPENDIX A

When integration is performed and terms are combined, equation (A18) becomes

$$\frac{1}{4}\frac{d\bar{r}_i^2}{d\bar{x}} - \frac{\bar{\rho}_a}{1.3864}\frac{d}{d\bar{x}}\left[\left(\bar{r}_5^2 - \bar{r}_i^2\right)\left(\frac{1}{2\tilde{d}}\ln\frac{1+c}{1+\frac{c}{2}+\frac{\tilde{d}}{4}} + \frac{c+\tilde{d}}{2\tilde{d}H}\ln\frac{\frac{c-H}{c+H}}{\frac{c-\tilde{d}-H}{c-\tilde{d}+H}}\right)\right]$$

$$+\frac{\bar{\rho}_a}{2(1.3864)}\frac{d}{d\bar{x}}\left[\left(\bar{r}_5^2 - \bar{r}_i^2\right)\frac{1}{H}\ln\frac{\frac{c-H}{c+H}}{\frac{c-\tilde{d}-H}{c-\tilde{d}+H}}\right] = \bar{\tau}_5\bar{r}_5 \qquad \text{(A19)}$$

The following equations are obtained from the definitions of c, $\tilde{d}$, and H:

$$\frac{1+\frac{c}{2}+\frac{\tilde{d}}{4}}{1+c} = \frac{1}{2\bar{\rho}_a} + \frac{1}{2} + \frac{\gamma-1}{8}M_1^2 \qquad \text{(A20)}$$

$$\frac{\frac{c-H}{c+H}}{\frac{c-\tilde{d}-H}{c-\tilde{d}+H}} = \frac{3c+H+4+\tilde{d}}{3c-H+4+\tilde{d}} \qquad \text{(A21)}$$

The following terms are defined for convenience:

$$B = \frac{1}{1.3864(\gamma-1)M_1^2\bar{\rho}_a}\left[\ln\left(\frac{1}{2\bar{\rho}_a} + \frac{1}{2} + \frac{\gamma-1}{8}M_1^2\right) + \frac{c+\tilde{d}}{H}\ln\frac{3c+H+4+\tilde{d}}{3c-H+4+\tilde{d}}\right] \qquad \text{(A22)}$$

$$D = \frac{1}{1.3864H}\ln\frac{3c+H+4+\tilde{d}}{3c-H+4+\tilde{d}} \qquad \text{(A23)}$$

Equations (A20), (A21), (A22), and (A23) are then substituted into equation (A19) and the terms are rearranged to obtain

$$\left(\frac{1}{4} - \bar{\rho}_a B + \frac{\bar{\rho}_a D}{2}\right)\frac{d\bar{r}_i^2}{d\bar{x}} + \left(\bar{\rho}_a B - \bar{\rho}_a\frac{D}{2}\right)\frac{d\bar{r}_5^2}{d\bar{x}} = \bar{\tau}_5\bar{r}_5 \qquad \text{(A24)}$$

By obtaining the derivative $\frac{d\bar{r}_i^2}{d\bar{x}}$ in terms of $\frac{d\bar{r}_5}{d\bar{x}}$ from equation (A14), the shear

stress $\bar{\tau}_5$ from equation (A2), the velocity gradient from equation (A4), and $\bar{r}_i^2$ in terms of $\bar{r}_5^2$ from equation (A14), the final equation is written as

$$\frac{2\bar{\rho}_a\left(B - \frac{D}{2} - \frac{A}{2}\right)\left(1 - \bar{r}_5^2\right)}{0.6932\left(1 - 2\bar{\rho}_a A\right)^2 \overline{\rho\epsilon}\,\bar{r}_5}\, d\bar{r}_5 = d\bar{x} \tag{A25}$$

Equation (A25) permits the axial coordinate $\bar{x}$ (actually $K\bar{x}$, where K is an empirical constant) to be computed for a given eddy viscosity formulation. As previously noted for the eddy viscosity coefficient expressed as $\overline{\rho\epsilon}$ rather than $\bar{\epsilon}$, $\bar{\rho}_5$ in equation (A25) requires interpretation as $\bar{\rho}$ to be consistent with the constant-exchange-coefficient theory employed herein. Limits of integration are from 1 to $\bar{r}_5$ and from 0 to $\bar{x}$, but the integrals have not been inserted so as not to preclude an eddy viscosity formulation which contains $\bar{x}$. The potential core length $\bar{x}_o$ is obtained from the solution of equation (A25) for $\bar{r}_5$, determined from equation (A14) for $\bar{r}_i = 0$. Equations (A14) and (A25) are the general equations for the core region.

General Solution for the Developed Region

The solution for the developed region differs from that for the core region only in the necessity of including the center-line jet velocity U, which varies with the axial coordinate $\bar{x}$. First $\bar{r}_5$ is related to U, and then U is related to $\bar{x}$.

Employing conservation of momentum in the form of equation (A3) changing the variable of integration from $\bar{r}$ to $\bar{u}/U$ by use of equation (A5), and employing the density-velocity relationship of equation (A11) yield

$$\frac{-\bar{\rho}_a U^2 \bar{r}_5^2}{1.3864} \int_1^0 \frac{\frac{\bar{u}}{U}}{1 + \left(c + \tilde{d}\right)\frac{\bar{u}}{U}U - \tilde{d}\left(\frac{\bar{u}}{U}\right)^2 U^2}\, d\frac{\bar{u}}{U} = \frac{1}{2} \tag{A26}$$

Integrating equation (A26) yields

$$\frac{-\bar{\rho}_a \bar{r}_5^2}{2(1.3864)\tilde{d}}\left\{\ln\left[1 + \left(c + \tilde{d}\right)U - \tilde{d}U^2\right] - \frac{c + \tilde{d}}{H}\ln\frac{c + \tilde{d} + H}{c + \tilde{d} - H} + \frac{c + \tilde{d}}{H}\ln\frac{-2\tilde{d}U + c + \tilde{d} - H}{-2\tilde{d}U + c + \tilde{d} + H}\right\} = \frac{1}{2} \tag{A27}$$

The following definitions apply:

$$\delta = 1 + \left(c + \tilde{d}\right)U - \tilde{d}U^2 \tag{A28}$$

$$\alpha = \tilde{d} + H + c + \frac{2}{U} \tag{A29}$$

$$\beta = \tilde{d} - H + c + \frac{2}{U} \tag{A30}$$

$$G = \frac{1}{1.3864(\gamma - 1)M_1^2\bar{\rho}_a} \tag{A31}$$

Combining terms in equation (A27) and factoring produce the following final equation:

$$\bar{\rho}_a\bar{r}_5^2 G\left(\frac{c + \tilde{d}}{H} \ln\frac{\alpha}{\beta} - \ln\delta\right) = \frac{1}{2} \tag{A32}$$

Equation (A32) relates U to $\bar{r}_5$ for the developed region through the inclusion of U in the definitions of δ, α, and β. Attention is directed to the fact that the relationship in equation (A32) is independent of any eddy viscosity assumption, as none has been employed in its derivation. Equation (A32) is identical to equation (58) of reference 2.

It remains to relate U, and thus $\bar{r}_5$ (through eq. (A32)), to the axial coordinate. Integrating equation (A1) for the developed region in which the velocities are nondimensionalized with respect to U, changing the variable of integration from $\bar{r}$ to $\bar{u}/U$ by employing equation (A5), and substituting for the density from equation (A11) yield the following equation:

$$\frac{d}{d\bar{x}}\left[\frac{-\bar{\rho}_a\bar{r}_5^2}{2\tilde{d}(1.3864)} \ln\frac{1 + (c + \tilde{d})U - \tilde{d}U^2}{1 + (c + \tilde{d})\frac{U}{2} - \frac{\tilde{d}}{4}U^2}\right] + \frac{d}{d\bar{x}}\left[\frac{-\bar{\rho}_a\bar{r}_5^2}{2\tilde{d}(1.3864)} \frac{c + \tilde{d}}{H} \ln\frac{\frac{-\tilde{d}U + c + \tilde{d} - H}{-\tilde{d}U + c + \tilde{d} + H}}{\frac{-2\tilde{d}U + c + \tilde{d} - H}{-2\tilde{d}U + c + \tilde{d} + H}}\right]$$

$$+ \frac{U}{2}\frac{d}{d\bar{x}}\left(\frac{\bar{\rho}_a\bar{r}_5^2}{1.3864H} \ln\frac{\frac{-\tilde{d}U + c + \tilde{d} - H}{-\tilde{d}U + c + \tilde{d} + H}}{\frac{-2\tilde{d}U + c + \tilde{d} - H}{-2\tilde{d}U + c + \tilde{d} + H}}\right) = \bar{\tau}_5\bar{r}_5 \tag{A33}$$

The following definitions are given:

$$\theta = 1 + \frac{c + \tilde{d}}{2}U - \frac{\tilde{d}}{4}U^2 \tag{A34}$$

$$\varphi = -2\tilde{d}U + 3\tilde{d} - H + 3c + \frac{4}{U} \tag{A35}$$

$$\epsilon_2 = -2\tilde{d}U + 3\tilde{d} + H + 3c + \frac{4}{U} \tag{A36}$$

$$G = \frac{1}{1.3864(\gamma - 1)M_1^2\bar{\rho}_a} \tag{A37}$$

$$V = G\left(\frac{c + \tilde{d}}{H} \ln \frac{\epsilon_2}{\varphi} + \ln \frac{\theta}{\delta}\right) \tag{A38}$$

$$W = \frac{1}{1.3864H} \ln \frac{\epsilon_2}{\varphi} \tag{A39}$$

(Note that ϵ_2 in equation (A36) is ϵ in ref. 2. The symbol was changed herein to prevent confusion with the eddy viscosity.) After simplification of equation (A33) and substitution of equations (A34), (A35), (A36), (A37), (A38), and (A39), the following equation is obtained:

$$\frac{d}{d\bar{x}}\left(\bar{\rho}_a \bar{r}_5^2 V\right) - \frac{U}{2} \frac{d}{d\bar{x}}\left(\bar{\rho}_a \bar{r}_5^2 W\right) = \bar{\tau}_5 \bar{r}_5 \tag{A40}$$

Warren's analysis has shown that an implicit solution of equation (A40) is not generally possible; thus, it is desirable to express equation (A40) in the form $f(U)\, dU = d\bar{x}$, where $f(U)$ is a function of U. From the definition of V,

$$\frac{dV}{d\bar{x}} = G\left[\frac{2\left(c + \tilde{d}\right)}{\epsilon_2 \varphi}\left(2\tilde{d} + \frac{4}{U^2}\right) + \frac{c + \tilde{d} - \tilde{d}U}{2\theta} - \frac{c + \tilde{d} - 2\tilde{d}U}{\delta}\right]\frac{dU}{d\bar{x}} \tag{A41}$$

where the identity $\epsilon_2 - \varphi = 2H$ was employed. From the definition of W,

$$\frac{dW}{d\bar{x}} = \frac{2\left(2\tilde{d} + \frac{4}{U^2}\right)}{1.3864\varphi\epsilon_2} \frac{dU}{d\bar{x}} \tag{A42}$$

and, from equation (A32),

$$\frac{d\bar{r}_5}{d\bar{x}} = \frac{\frac{-4\left(c + \tilde{d}\right)\bar{r}_5}{\alpha\beta U^2} + \frac{\bar{r}_5}{\delta}\left(c + \tilde{d} - 2\tilde{d}U\right)}{2\left(\frac{c + \tilde{d}}{H} \ln \frac{\alpha}{\beta} - \ln \delta\right)} \tag{A43}$$

where the following identity was employed:

$$\frac{1}{\alpha U^2} - \frac{1}{\beta U^2} = \frac{-2H}{\alpha\beta U^2} \tag{A44}$$

APPENDIX A

The shear stress $\bar{\tau}_5$ from equation (A2) and the velocity gradient from equation (A5) are substituted along with equations (A41), (A42), and (A43), into equation (A40) to yield, after terms are combined,

$$-\frac{1}{1.3864GU\bar{\rho}_5\bar{\epsilon}}\left(\frac{c+\tilde{d}}{H}\ln\frac{\alpha}{\beta}-\ln\delta\right)\left\{G\left[(c+\tilde{d})\left(\frac{4\tilde{d}+\frac{8}{U^2}}{\epsilon_2\varphi}-\frac{1-\frac{\tilde{d}U^2}{2}}{2\delta\theta}\right)+\frac{3\tilde{d}U}{2\delta\theta}\right]\right.$$

$$\left.+\left(V-\frac{U}{2}W\right)\left[\frac{(c+\tilde{d})\left(\frac{4\delta+\alpha\beta U^2}{\delta\alpha\beta U^2}\right)-\frac{2\tilde{d}U}{\delta}}{\frac{c+\tilde{d}}{H}\ln\frac{\alpha}{\beta}-\ln\delta}\right]-\frac{\left(2\tilde{d}+\frac{4}{U^2}\right)U}{1.3864\varphi\epsilon_2}\right\}dU=d\bar{x} \qquad \text{(A45)}$$

Equation (A45) gives the desired relationship between U and $\bar{x}$ for the developed region. Limits of integration proceed from 1 to U and from $\bar{x}$ to $\bar{x}_o$, where $\bar{x}_o$ defines the potential core length obtained from the core region solution. The integrals have not been inserted into equation (A45) so as not to preclude the case of $\bar{\epsilon}$ containing an $\bar{x}$. As in the core region solution when the eddy viscosity coefficient is experessed as $\overline{\rho\epsilon}$ rather than $\bar{\epsilon}$, $\bar{\rho}_5$ in equation (A45) requires interpretation as $\bar{\rho}$ to be consistent with the constant-exchange-coefficient theory. Attention is directed to the fact that the solution relates U to $K\bar{x}-K\bar{x}_o$ and an experimental determination of K is always a necessity. Equations (A32) and (A45) are the general equations for the developed region.

Particular Solutions for the Core Region

1. For the core region the form of the eddy viscosity coefficient employed by Warren in reference 2 is

$$\bar{\epsilon}=\frac{K}{2}\left(\bar{r}_5-\bar{r}_i\right) \qquad \text{(A46)}$$

Expressing $\bar{r}_i$ in equation (A46) in terms of $\bar{r}_5$ by the use of equation (A14), substituting the result into equation (A25), and performing the integration yield the solution

$$\frac{2F\left(\frac{A}{2}+\frac{D}{2}-B\right)}{\left(1-2\bar{\rho}_aA\right)}\left[\bar{r}_5-2+\sqrt{\frac{1-2\bar{\rho}_aA\bar{r}_5^2}{1-2\bar{\rho}_aA}}+\frac{1}{\sqrt{1-2\bar{\rho}_aA}}\ln\frac{\bar{r}_5\left(1+\sqrt{1-2\bar{\rho}_aA}\right)}{1+\sqrt{1-2\bar{\rho}_aA\bar{r}_5^2}}\right]=K\bar{x} \qquad \text{(A47)}$$

where

$$F=\frac{1+\bar{\rho}_a\left(1+\frac{\gamma-1}{4}M_1^2\right)}{0.6932} \qquad \text{(A47a)}$$

which, by use of the definitions of c, $\tilde{d}$, and $\bar{\rho}_5$, is expressed as

$$F = \frac{2\bar{\rho}_a}{0.6932\bar{\rho}_5} \tag{A47b}$$

Equation (A47) is equivalent to equation (57) of reference 2, with the constants rearranged. Inherent in the solution of equation (A47) is the restriction that the terms $1 - 2\bar{\rho}_a A$ and $1 - 2\bar{\rho}_a A\bar{r}_5^2$ remain positive. The restriction may be removed by a reintegration of equation (A25) which yields

$$\frac{2F\left(\frac{A}{2} - \frac{D}{2} - B\right)}{\left(1 - 2\bar{\rho}_a A\right)}\left(\bar{r}_5 - 2 + \frac{\sqrt{2\bar{\rho}_a A\bar{r}_5^2 - 1} - \arccos\frac{1}{\sqrt{2\bar{\rho}_a A\bar{r}_5^2}} + \arccos\frac{1}{\sqrt{2\bar{\rho}_a A}}}{\sqrt{1 - 2\bar{\rho}_a A}}\right) = K\bar{x} \tag{A48}$$

Equation (A48) gives the relationship between $\bar{r}_5$ and $K\bar{x}$ for the core region for positive $2\bar{\rho}_a A\bar{r}_5^2 - 1$ and positive $2\bar{\rho}_a A - 1$. General specification as to when equation (A48) or equation (A47) applies is not readily definable due to the complex nature of the variable A, but the restrictions of equation (A47) were violated during computations for a hot subsonic jet.

2. For the core region when the mixing is assumed mass-flux-per-unit-area controlled rather than velocity controlled, the eddy viscosity is assumed to have the form

$$\overline{\rho\epsilon} = \frac{K}{2}\left(\bar{r}_5 - \bar{r}_i\right) \tag{A49}$$

This solution differs from the Warren solution only in the interpretation of the factor $\bar{\rho}_5$ as $\bar{\rho}$. Since $\bar{\rho}_5$ is a constant, the following solution may be immediately written from equation (A47) and from equation (A10), in which the substitution $\bar{u} = 1/2$ yields $\bar{\rho}_5$:

$$\frac{2F\left(\frac{A}{2} + \frac{D}{2} - B\right)\bar{\rho}_a}{\left(1 - 2\bar{\rho}_a A\right)\left(1 + \frac{c}{2} + \frac{\tilde{d}}{4}\right)}\left[\bar{r}_5 - 2 + \sqrt{\frac{1 - 2\bar{\rho}_a A\bar{r}_5^2}{1 - 2\bar{\rho}_a A}} + \frac{1}{\sqrt{1 - 2\bar{\rho}_a A}}\ln\frac{\bar{r}_5\left(1 + \sqrt{1 - 2\bar{\rho}_a A}\right)}{1 + \sqrt{1 - 2\bar{\rho}_a A\bar{r}_5^2}}\right] = K\bar{x} \tag{A50}$$

3. A solution is determined for the core region when the eddy viscosity is assumed to have the form

$$\overline{\rho\epsilon} = \frac{K_2}{2}\bar{x} \tag{A51}$$

Eddy viscosity of this form was suggested in reference 3. The subscript 2 on K is a reminder that K for the core region is not necessarily equal to K for the developed region. Substituting equation (A51) into equation (A25) and integrating produce the solution

$$\frac{4\bar{\rho}_a\left(B - \frac{D}{2} - \frac{A}{2}\right)\left(\ln \bar{r}_5^2 - \bar{r}_5^2 + 1\right)}{0.6932\left(1 - 2\bar{\rho}_a A\right)^2} = K_2\bar{x}^2 \tag{A52}$$

The relationship between K_2 for the core region and the empirical constant for the developed region may be obtained by equating the expression for the core region eddy viscosity to a particular expression for the developed region eddy viscosity at the end of the potential core.

4. A solution is determined for the core region when the eddy viscosity has the form

$$\overline{\rho\epsilon} = \frac{K}{2}\left(\bar{r}_5 - \bar{r}_i\right)\bar{\rho}_a \tag{A53}$$

which was suggested in reference 4. This form differs only by the constant factor $\bar{\rho}_a$ from formulation 2 given in equation (A49). The following solution can thus be immediately written from equation (A50):

$$\frac{2F\left(\frac{A}{2} + \frac{D}{2} - B\right)}{\left(1 - 2\bar{\rho}_a A\right)\left(1 + \frac{c}{2} + \frac{d}{4}\right)}\left[\bar{r}_5 - 2 + \sqrt{\frac{1 - 2\bar{\rho}_a A\bar{r}_5^2}{1 - 2\bar{\rho}_a A}} + \frac{1}{\sqrt{1 - 2\bar{\rho}_a A}} \ln \frac{\bar{r}_5\left(1 + \sqrt{1 - 2\bar{\rho}_a A}\right)}{1 + \sqrt{1 - 2\bar{\rho}_a A\bar{r}_5^2}}\right] = K\bar{x} \tag{A54}$$

5. The trivial form of uniform eddy kinematic viscosity is

$$\bar{\epsilon} = \frac{K}{2} \tag{A55}$$

Substituting equation (A55), along with $\bar{\rho}_5$ from equation (A10), into equation (A25) and integrating yield

$$\frac{F\left(B - \frac{D}{2} - \frac{A}{2}\right)}{\left(1 - 2\bar{\rho}_a A\right)^2}\left(\ln \bar{r}_5^2 - \bar{r}_5^2 - 1\right) = K\bar{x} \tag{A56}$$

which is the desired relationship between $\bar{r}_5$ and $\bar{x}$.

6. For the simple case of $\overline{\rho\epsilon}$ equal to a constant, the eddy viscosity is

$$\overline{\rho\epsilon} = \frac{K}{2} \tag{A57}$$

Substituting equation (A57) into equation (A25) and integrating yield

$$\frac{2\bar{\rho}_a\left(B - \frac{D}{2} - \frac{A}{2}\right)}{0.6932\left(1 - 2\bar{\rho}_a A\right)^2}\left(\ln \bar{r}_5^2 - \bar{r}_5^2 - 1\right) = K\bar{x} \tag{A58}$$

which is the desired final equation.

7. A solution is determined for the core region when the eddy viscosity is assumed to have the form

$$\overline{\rho\epsilon} = \frac{K}{2}\left(\bar{y}_5 - \bar{r}_i\right) \tag{A59}$$

The radial distance $\bar{y}_5$ and the potential core radius $\bar{r}_i$ must be expressed in terms of $\bar{r}_5$ before integration of equation (A25) can be performed. From equation (A10)

$$\overline{\rho u} = \frac{\bar{\rho}_a \bar{u}}{1 + \left(c + \tilde{d}\right)\bar{u} - \tilde{d}\bar{u}^2} \tag{A60}$$

Then $\bar{u}_{y_5}$ may be solved from equation (A60) by substituting $\overline{\rho u} = 1/2$. The result is

$$\bar{u}_{y_5} = \frac{-\bar{\rho}_a + \frac{c + \tilde{d}}{2}\sqrt{\left(\bar{\rho}_a - \frac{c + \tilde{d}}{2}\right)^2 + \tilde{d}}}{\tilde{d}} \tag{A61}$$

The solution of equation (A4) for the parameter $\bar{y}_5$ (note $\bar{r} = \bar{y}_5$ when $\bar{u} = \bar{u}_{y_5}$) is

$$\bar{y}_5 = \sqrt{\frac{1 + \frac{\ln \bar{u}_{y_5}}{0.6932} - \left(\frac{\ln \bar{u}_{y_5}}{0.6932} + 2\bar{\rho}_a A\right)\bar{r}_5^2}{1 - 2\bar{\rho}_a A}} \tag{A62}$$

In this solution of equation (A4) $\bar{r}_i$ was eliminated by the use of equation (A14). The result of substituting equations (A59), (A62), (A14) for $\bar{r}_i$, and (A10) for $\bar{\rho}_5$ into equation (A25) and integrating is

$$\frac{4\bar{\rho}_a\left(B - \frac{D}{2} - \frac{A}{2}\right)}{\ln \bar{u}_{y_5}\left(1 - 2\bar{\rho}_a A\right)^{3/2}}\left[\sqrt{1 + \frac{\ln \bar{u}_{y_5}}{0.6932} - \left(\frac{\ln \bar{u}_{y_5}}{0.6932} + 2\bar{\rho}_a A\right)\bar{r}_5^2}\right.$$

$$- \left(1 + \frac{\ln \bar{u}_{y_5}}{0.6932}\right)^{1/2} \operatorname{arc\,tanh} \sqrt{\frac{1 + \frac{\ln \bar{u}_{y_5}}{0.6932} - \left(\frac{\ln \bar{u}_{y_5}}{0.6932} + 2\bar{\rho}_a A\right)\bar{r}_5^2}{1 + \frac{\ln \bar{u}_{y_5}}{0.6932}}}$$

$$+ \sqrt{1 - 2\bar{\rho}_a A\bar{r}_5^2} - \operatorname{arc\,tanh} \sqrt{1 - 2\bar{\rho}_a A\bar{r}_5^2} - 2\sqrt{1 - 2\bar{\rho}_a A}$$

$$\left. + \left(1 + \frac{\ln \bar{u}_{y_5}}{0.6932}\right)^{1/2} \operatorname{arc\,tanh} \sqrt{\frac{1 - 2\bar{\rho}_a A}{1 + \frac{\ln \bar{u}_{y_5}}{0.6932}}} + \operatorname{arc\,tanh} \sqrt{1 - 2\bar{\rho}_a A}\right] = K\bar{x} \qquad \text{(A63)}$$

Particular Solutions for the Developed Region

1. For the developed region the form of the eddy viscosity coefficient employed by Warren in reference 2 is

$$\bar{\epsilon} = \frac{K}{2}\bar{r}_5 U \qquad \text{(A64)}$$

The solution may be obtained by substituting $\bar{u}/U = 1/2$ into equation (A11) to obtain $\bar{\rho}_5$ which, together with equation (A32) solved for $\bar{r}_5$ and $\bar{\epsilon}$ from equation (A64), permits numerical integration of equation (A45). The solution relates U to $K\bar{x} - K\bar{x}_o$. The relationship between $\bar{r}_5$ and U for all eddy viscosity formulations is obtained from equation (A32).

2. The expression for the eddy viscosity, if the assumption is made that the mixing is mass-flux controlled with a representative width based on velocity, has the form

$$\overline{\rho\epsilon} = \frac{K}{2}\bar{r}_5\bar{\rho}_{\text{¢}} U \qquad \text{(A65)}$$

By obtaining $\bar{r}_5$ from equation (A32) and $\bar{\rho}_{\text{¢}}$ from equation (A11) for $\bar{u}/U = 1$, and by employing equation (A65), numerical integration of equation (A45) can be performed to produce the solution which relates U to $K\bar{x} = K\bar{x}_o$.

3. The expression for the eddy viscosity when the mixing is assumed mass-flux controlled has the form

$$\overline{\rho\epsilon} = \frac{K}{2}\bar{y}_5\rho_{\ell}U \tag{A66}$$

Substitution of equation (A66) into equation (A45) to numerically integrate requires that $\bar{y}_5$ and $\bar{\rho}_{\ell}$ be related to U. Thus $\bar{\rho}_{\ell}$ is related to U by using equation (A11) for $\bar{u}/U = 1.0$, and $\bar{y}_5$ is related to U by first using equation (A11) to form the expression

$$\frac{\overline{\rho u}}{\bar{\rho}_{\ell}U} = \left[\frac{1 + (c + \tilde{d})U - \tilde{d}U^2}{1 + (c + \tilde{d})\frac{\bar{u}}{U}U - \tilde{d}\left(\frac{\bar{u}}{U}\right)^2U^2}\right]\frac{\bar{u}}{U} \tag{A67}$$

and then solving equation (A67) for $(\bar{u}/U)_{\bar{y}_5}$ where $\frac{\overline{\rho u}}{\bar{\rho}_{\ell}U} = 1/2$. The resulting equation is

$$\left(\frac{\bar{u}}{U}\right)_{\bar{y}_5} = \frac{-\left[2\delta - (c + \tilde{d})U\right] + \sqrt{\left[2\delta - (c + \tilde{d})U\right]^2 + 4\tilde{d}U^2}}{2\tilde{d}U^2} \tag{A68}$$

It is possible to relate $\bar{y}_5$ to U by employing equation (A5) where $\frac{\bar{u}}{U} = \left(\frac{\bar{u}}{U}\right)_{\bar{y}_5}$ defines $\bar{r} = \bar{y}_5$. Substitution of equations (A66), (A68), and (A5) into equation (A45) permits numerical integration for the solution.

4. The eddy viscosity is assumed to have the form

$$\overline{\rho\epsilon} = \frac{K}{2}\bar{\rho}_a\bar{r}_5U \tag{A69}$$

which was suggested in reference 4. The solution requires numerical integration of equation (A45) through the use of equations (A69) and (A32).

5. Under the assumption of uniform eddy kinematic viscosity, the formulation is

$$\bar{\epsilon} = \frac{K}{2} \tag{A70}$$

The solution is obtained by substituting equation (A11) for $\bar{\rho}_5$ and equation (A70) into equation (A45) and performing the numerical integration.

6. The solution for the case of uniform eddy viscosity expressed as

$$\overline{\rho\epsilon} = \frac{K}{2} \tag{A71}$$

may be obtained by substituting equation (A71) into equation (A45) and numerically integrating.

APPENDIX B

TABULATION OF VELOCITY PROFILES*

(a) Core region

$\bar{r}$	$\bar{u}$	$\overline{\rho u}$	$\overline{\rho u r}$	$\overline{\rho u^2 r}$
$\bar{x} = 0$; $\bar{r}_5 = 0.9964$				
0.0662	1.0020	0.9940	0.0658	0.0660
.1457	1.0010	1.0010	.1459	.1462
.2120	1.0030	1.0000	.2120	.2127
.2380	1.0030	1.0010	.2383	.2389
.3310	1.0030	1.0010	.3312	.3322
.4170	1.0030	1.0010	.4173	.4185
.5300	.9970	1.0030	.5320	.5305
.6420	.9910	1.0070	.6470	.6410
.7180	.9910	1.0070	.7230	.7165
.7350	.9970	1.0020	.7370	.7350
.8610	.9970	1.0020	.8630	.8610
.9140	.9970	1.0020	.9160	.9140
.9200	.9940	.9970	.9170	.9120
.9269	.9991	.9978	.9249	.9241
.9335	.9698	.9167	.8557	.8299
.9400	.9533	.8755	.8230	.7846
.9434	.9359	.8344	.7872	.7367
.9533	.9169	.7926	.7556	.6928
.9567	.8956	.7502	.7177	.6428
.9599	.8476	.6642	.6376	.5404
.9666	.8200	.6204	.5997	.4918
.9698	.7886	.5751	.5577	.4398
.9732	.7534	.5288	.5146	.3877
.9766	.7336	.5047	.4929	.3616
.9865	.6650	.4297	.4239	.2819
.9897	.6195	.3859	.3819	.2366
.9964	.5278	.3089	.3078	.1625
.9976	.2975	.1570	.1566	.0466
1.0000	0	0	0	0

*For data conversion purposes the following representative values of pertinent parameters are given: $T_{t,1} = 292^{\circ}$ K (525° R); $u_1 = 538$ m/sec (1765 ft/sec); $r_1 = 1.279$ centimeters (0.5035 in.); $\rho_1 = 2.404$ kg/m^3 $\left(0.1501 \text{ lbm/ft}^3\right)$.

APPENDIX B

TABULATION OF VELOCITY PROFILES – Continued

(a) Core region – Continued

$\bar{r}$	$\bar{u}$	$\overline{\rho u}$	$\overline{\rho u r}$	$\overline{\rho u^2 r}$
		$\bar{x} = 2.01$; $\bar{r}_5 = 1.065$		
0.9136	1.0116	1.0352	0.9458	0.9568
.9170	1.0060	1.0183	.9338	.9394
.9235	.9991	.9978	.9215	.9207
.9301	.9847	.9569	.8900	.8764
.9335	.9698	.9167	.8557	.8299
.9400	.9533	.8755	.8230	.7846
.9468	.9359	.8344	.7900	.7394
.9533	.9169	.7926	.7556	.6928
.9567	.8956	.7502	.7177	.6428
.9666	.8727	.7075	.6839	.5968
.9797	.8476	.6642	.6507	.5515
.9831	.8200	.6204	.6099	.5001
.9897	.7886	.5751	.5692	.4489
.9930	.7715	.5520	.5481	.4229
.9964	.7534	.5288	.5269	.3970
1.0064	.7336	.5047	.5079	.3726
1.0129	.7128	.4805	.4867	.3469
1.0195	.6898	.4554	.4643	.3203
1.0262	.6650	.4297	.4410	.2933
1.0328	.6432	.4082	.4216	.2712
1.0393	.6195	.3859	.4011	.2485
1.0441	.5928	.3621	.3781	.2241
1.0493	.5628	.3368	.3534	.1989
1.0592	.5278	.3089	.3272	.1727
1.0592	.5077	.2937	.3111	.1579
1.0659	.4860	.2776	.2959	.1438
1.0725	.4613	.2602	.2791	.1287
1.0824	.4337	.2413	.2612	.1133
1.0858	.4026	.2209	.2399	.0966
1.0924	.3851	.2097	.2291	.0882
1.0957	.3663	.1980	.2169	.0794
1.0989	.3456	.1853	.2036	.0704
1.1088	.3235	.1721	.1908	.0617
1.1122	.2975	.1570	.1746	.0519
1.1188	.2688	.1407	.1574	.0423
1.1287	.2355	.1222	.1379	.0325
1.1321	.1938	.0996	.1128	.0219
1.1519	.1385	.0705	.0813	.0112
1.1652	.0988	.0501	.0584	.0058
1.1784	.0698	.0353	.0416	.0029

APPENDIX B

TABULATION OF VELOCITY PROFILES – Continued

(a) Core region – Continued

$\bar{r}$	$\bar{u}$	$\overline{\rho u}$	$\overline{\rho u r}$	$\overline{\rho u^2 r}$
		$\bar{x} = 4.01$; $\bar{r}_5 = 1.116$		
0.8276	0.9987	0.9959	0.8242	0.8231
.8673	.9847	.9569	.8299	.8172
.8872	.9698	.9167	.8133	.7887
.9003	.9533	.8755	.7882	.7514
.9136	.9359	.8344	.7623	.7134
.9269	.9169	.7926	.7347	.6736
.9400	.8956	.7502	.7052	.6316
.9468	.8727	.7075	.6699	.5846
.9533	.8476	.6642	.6332	.5367
.9698	.8200	.6204	.6017	.4934
.9865	.7886	.5751	.5673	.4474
.9996	.7715	.5520	.5518	.4257
1.0064	.7534	.5288	.5322	.4010
1.0095	.7336	.5047	.5095	.3738
1.0195	.7128	.4805	.4899	.3492
1.0328	.6898	.4554	.4703	.3244
1.0461	.6650	.4297	.4495	.2989
1.0560	.6432	.4082	.4311	.2773
1.0626	.6195	.3859	.4101	.2541
1.0759	.5928	.3621	.3896	.2310
1.0858	.5628	.3368	.3657	.2058
1.1057	.5278	.3089	.3416	.1803
1.1122	.5077	.2937	.3267	.1659
1.1221	.4860	.2776	.3115	.1514
1.1321	.4613	.2602	.2946	.1359
1.1420	.4337	.2413	.2756	.1195
1.1519	.4026	.2209	.2545	.1025
1.1652	.3851	.2097	.2443	.0941
1.1718	.3663	.1980	.2320	.0850
1.1784	.3456	.1853	.2184	.0755
1.1917	.3235	.1721	.2051	.0664
1.2050	.2975	.1570	.1892	.0563
1.2181	.2688	.1407	.1714	.0461
1.2379	.2355	.1222	.1513	.0356
1.2578	.1938	.0996	.1253	.0243
1.2910	.1385	.0705	.0911	.0126
1.3108	.0988	.0501	.0657	.0065
1.3174	.0698	.0353	.0465	.0032

APPENDIX B

TABULATION OF VELOCITY PROFILES – Continued

(a) Core region – Continued

$\bar{r}$	$\bar{u}$	$\overline{\rho u}$	$\overline{\rho u r}$	$\overline{\rho u^2 r}$
		$\bar{x} = 6.02$; $\bar{r}_5 = 1.170$		
0.4634	1.0086	1.0252	0.4751	0.4792
.5660	1.0060	1.0183	.5764	.5799
.6455	1.0035	1.0104	.6522	.6545
.7215	.9991	.9978	.7199	.7193
.7944	.9847	.9569	.7602	.7486
.8342	.9698	.9167	.7647	.7416
.8606	.9533	.8755	.7535	.7183
.8739	.9359	.8344	.7292	.6825
.8904	.9169	.7926	.7057	.6471
.9136	.8956	.7502	.6854	.6138
.9301	.8727	.7075	.6580	.5742
.9468	.8476	.6642	.6289	.5331
.9599	.8200	.6204	.5955	.4883
.9831	.7886	.5751	.5654	.4459
.9996	.7715	.5520	.5518	.4257
1.0064	.7534	.5288	.5322	.4010
1.0195	.7336	.5047	.5145	.3774
1.0393	.7128	.4805	.4994	.3560
1.0526	.6898	.4554	.4794	.3307
1.0659	.6650	.4297	.4580	.3046
1.0790	.6432	.4082	.4404	.2833
1.0957	.6195	.3859	.4228	.2619
1.1122	.5928	.3621	.4027	.2387
1.1355	.5628	.3368	.3824	.2152
1.1519	.5278	.3089	.3558	.1878
1.1652	.5077	.2937	.3422	.1737
1.1784	.4860	.2776	.3271	.1590
1.1917	.4613	.2602	.3101	.1430
1.2115	.4337	.2413	.2923	.1268
1.2248	.4026	.2209	.2706	.1089
1.2379	.3851	.2097	.2596	.1000
1.2578	.3663	.1980	.2490	.0912
1.2711	.3456	.1853	.2355	.0814
1.2844	.3235	.1721	.2210	.0715
1.2975	.2975	.1570	.2037	.0606
1.3241	.2688	.1407	.1863	.0486
1.3440	.2355	.1222	.1642	.0387
1.3837	.1938	.0996	.1379	.0267
1.4167	.1385	.0705	.0999	.0138
1.4564	.0988	.0501	.0730	.0072
1.4828	.0698	.0353	.0523	.0036

APPENDIX B

TABULATION OF VELOCITY PROFILES – Continued

(a) Core region – Continued

$\bar{r}$	$\bar{u}$	$\overline{\rho u}$	$\overline{\rho u r}$	$\overline{\rho u^2 r}$
		$\bar{x} = 8.02$; $\bar{r}_5 = 1.208$		
0.6157	0.9968	0.9902	0.6097	0.6077
.6620	.9939	.9824	.6503	.6463
.7084	.9900	.9705	.6875	.6806
.7315	.9847	.9569	.7000	.6893
.7879	.9698	.9167	.7223	.7005
.8143	.9533	.8755	.7129	.6796
.8342	.9359	.8344	.6961	.6515
.8606	.9169	.7926	.6821	.6254
.8739	.8956	.7502	.6556	.5872
.8937	.8727	.7075	.6323	.5518
.9136	.8476	.6642	.6068	.5143
.9468	.8200	.6204	.5874	.4817
.9732	.7886	.5751	.5597	.4414
.9865	.7715	.5520	.5445	.4201
.9996	.7534	.5288	.5286	.3982
1.0228	.7336	.5047	.5162	.3787
1.0393	.7128	.4805	.4994	.3560
1.0592	.6898	.4554	.4824	.3328
1.0725	.6650	.4297	.4609	.3065
1.0924	.6432	.4082	.4459	.2868
1.1088	.6195	.3859	.4279	.2651
1.1386	.5928	.3621	.4123	.2444
1.1519	.5628	.3368	.3880	.2184
1.1851	.5278	.3089	.3661	.1932
1.1982	.5077	.2937	.3519	.1787
1.2115	.4860	.2776	.3363	.1634
1.2379	.4613	.2602	.3221	.1486
1.2578	.4337	.2413	.3035	.1316
1.2910	.4026	.2209	.2852	.1148
1.3009	.3851	.2097	.2728	.1051
1.3241	.3663	.1980	.2622	.0960
1.3372	.3456	.1853	.2478	.0856
1.3571	.3235	.1721	.2336	.0756
1.3823	.2975	.1570	.2170	.0646
1.3968	.2688	.1407	.1965	.0528
1.4234	.2355	.1222	.1739	.0410
1.4763	.1938	.0996	.1471	.0285
1.5426	.1385	.0705	.1088	.0151
1.5954	.0988	.0501	.0799	.0079
1.6320	.0698	.0353	.0576	.0040

APPENDIX B

TABULATION OF VELOCITY PROFILES – Continued

(a) Core region – Continued

$\bar{r}$	$\bar{u}$	$\overline{\rho u}$	$\overline{\rho u r}$	$\overline{\rho u^2 r}$
		$\bar{x} = 11.03$; $\bar{r}_5 = 1.254$		
0.4236	1.0068	1.0203	0.4322	0.4351
.4965	1.0035	1.0104	.5017	.5035
.6091	.9926	.9782	.5958	.5914
.5660	.9991	.9978	.5648	.5643
.6520	.9847	.9569	.6239	.6144
.6985	.9698	.9167	.6403	.6210
.7215	.9533	.8755	.6317	.6022
.7482	.9359	.8344	.6243	.5843
.7811	.9169	.7926	.6191	.5677
.8077	.8956	.7502	.6059	.5426
.8475	.8727	.7075	.5996	.5233
.8773	.8476	.6642	.5827	.4939
.9136	.8200	.6204	.5668	.4648
.9400	.7886	.5751	.5406	.4263
.9633	.7715	.5520	.5317	.4102
.9831	.7534	.5288	.5199	.3917
.9996	.7336	.5047	.5045	.3701
1.0228	.7128	.4805	.4915	.3503
1.0427	.6898	.4554	.4748	.3275
1.0691	.6650	.4297	.4594	.3055
1.0924	.6432	.4082	.4459	.2868
1.1188	.6195	.3859	.4317	.2674
1.1519	.5928	.3621	.4171	.2473
1.1851	.5628	.3368	.3991	.2246
1.2314	.5278	.3089	.3804	.2008
1.2447	.5077	.2937	.3656	.1856
1.2711	.4860	.2776	.3529	.1715
1.2975	.4613	.2602	.3376	.1557
1.3241	.4337	.2413	.3195	.1386
1.3539	.4026	.2209	.2991	.1204
1.3803	.3851	.2097	.2894	.1114
1.3968	.3663	.1980	.2766	.1013
1.4201	.3456	.1853	.2631	.0909
1.4499	.3235	.1721	.2495	.0807
1.4828	.2975	.1570	.2328	.0693
1.5227	.2688	.1407	.2142	.0576
1.5492	.2355	.1222	.1893	.0446
1.6286	.1938	.0996	.1623	.0314
1.7245	.1385	.0705	.1216	.0168
1.8272	.0988	.0501	.0915	.0090
1.8868	.0698	.0353	.0666	.0046

APPENDIX B

TABULATION OF VELOCITY PROFILES – Continued

(a) Core region – Concluded

$\bar{r}$	$\bar{u}$	$\overline{\rho u}$	$\overline{\rho u r}$	$\overline{\rho u^2 r}$
		$\bar{x} = 16.90$; $\bar{r}_5 = 1.390$		
0	0.9918	0.9758	0	0
.2516	.9910	.9738	.2450	.2428
.3112	.9900	.9705	.3020	.2990
.3839	.9847	.9569	.3674	.3618
.4832	.9698	.9167	.4429	.4295
.5527	.9533	.8755	.4839	.4613
.6091	.9359	.8344	.5082	.4756
.6620	.9169	.7926	.5247	.4811
.7150	.8956	.7502	.5364	.4804
.7547	.8727	.7075	.5340	.4660
.8077	.8476	.6642	.5365	.4547
.8606	.8200	.6204	.5339	.4378
.9269	.7886	.5751	.5331	.4204
.9533	.7715	.5520	.5262	.4060
.9797	.7534	.5288	.5181	.3903
1.0064	.7336	.5047	.5079	.3726
1.0461	.7128	.4805	.5027	.3583
1.0858	.6898	.4554	.4945	.3411
1.1255	.6650	.4297	.4836	.3216
1.1652	.6432	.4082	.4756	.3059
1.1982	.6195	.3859	.4624	.2865
1.2379	.5928	.3621	.4482	.2657
1.2777	.5628	.3368	.4303	.2422
1.3372	.5278	.3089	.4131	.2180
1.3823	.5077	.2937	.4060	.2061
1.4036	.4860	.2776	.3896	.1893
1.4499	.4613	.2602	.3773	.1740
1.4896	.4337	.2413	.3594	.1559
1.5358	.4026	.2209	.3393	.1366
1.5690	.3851	.2097	.3290	.1267
1.6087	.3663	.1980	.3185	.1167
1.6419	.3456	.1853	.3042	.1051
1.6882	.3235	.1721	.2905	.0940
1.7345	.2975	.1570	.2723	.0810
1.7940	.2688	.1407	.2524	.0678
1.8669	.2355	.1222	.2281	.0537
1.9464	.1938	.0996	.1939	.0376
2.0755	.1385	.0705	.1464	.0203
2.1714	.0988	.0501	.1088	.0108
2.2377	.0698	.0353	.0790	.0055

APPENDIX B

TABULATION OF VELOCITY PROFILES – Continued

(b) Developed region

$\bar{r}$	$\bar{u}$	$\bar{u}/U$	$\overline{\rho u}$	$\overline{\rho u r}$	$\overline{\rho u^2 r}$
		$\bar{x} = 22.92$; $\bar{r}_5 = 1.469$			
0	0.9832	1.0000	0.9522	0	0
.0662	.9824	.9990	.9500	.0629	.0618
.1456	.9774	.9940	.9368	.1364	.1333
.2185	.9698	.9860	.9167	.2003	.1943
.3178	.9533	.9695	.8755	.2782	.2652
.4038	.9359	.9515	.8344	.3369	.3153
.4701	.9169	.9325	.7926	.3726	.3416
.5329	.8956	.9110	.7502	.3998	.3581
.5958	.8727	.8880	.7075	.4215	.3678
.6620	.8476	.8620	.6642	.4397	.3727
.7283	.8200	.8345	.6204	.4518	.3705
.8010	.7886	.8025	.5751	.4607	.3633
.8407	.7715	.7850	.5520	.4640	.3580
.8739	.7534	.7665	.5288	.4621	.3481
.9136	.7336	.7463	.5047	.4611	.3383
.9533	.7128	.7255	.4805	.4581	.3265
.9996	.6898	.7018	.4554	.4552	.3140
1.0530	.6650	.6765	.4297	.4525	.3009
1.1090	.6432	.6543	.4082	.4527	.2912
1.1720	.6195	.6300	.3859	.4523	.2802
1.2380	.5928	.6035	.3621	.4483	.2658
1.3108	.5628	.5725	.3368	.4415	.2485
1.3943	.5278	.5365	.3089	.4307	.2273
1.4360	.5077	.5163	.2937	.4218	.2141
1.4830	.4860	.4943	.2776	.4117	.2001
1.5426	.4613	.4693	.2604	.4014	.1852
1.5954	.4337	.4410	.2413	.3850	.1670
1.6618	.4026	.4095	.2209	.3671	.1478
1.7080	.3851	.3919	.2097	.3582	.1379
1.7543	.3663	.3727	.1980	.3474	.1273
1.8008	.3456	.3515	.1853	.3337	.1153
1.8604	.3235	.3290	.1721	.3202	.1036
1.9331	.2975	.3027	.1570	.3035	.0903
2.0258	.2688	.2732	.1407	.2850	.0766
2.1317	.2355	.2396	.1222	.2605	.0614
2.2642	.1938	.1971	.0996	.2256	.0437
2.5025	.1385	.1409	.0705	.1765	.0244
2.6878	.0988	.1006	.0501	.1347	.0133
2.8203	.0698	.0710	.0353	.0995	.0069

APPENDIX B

TABULATION OF VELOCITY PROFILES – Continued

(b) Developed region – Continued

$\bar{r}$	$\bar{u}$	$\bar{u}/U$	$\overline{\rho u}$	$\overline{\rho u r}$	$\overline{\rho u^2 r}$
		$\bar{x} = 24.93$; $\bar{r}_5 = 1.512$			
0	0.9577	1.0	0.8857	0	0
.0993	.9557	.9979	.8804	.0874	.0836
.1324	.9533	.9954	.8755	.1159	.1105
.2250	.9453	.9871	.8555	.1925	.1820
.2781	.9359	.9772	.8344	.2320	.2171
.3839	.9169	.9574	.7926	.3043	.2790
.4634	.8956	.9352	.7502	.3476	.3113
.5297	.8727	.9112	.7075	.3748	.3271
.6091	.8476	.8850	.6642	.4046	.3429
.6886	.8200	.8562	.6204	.4272	.3503
.7547	.7886	.8234	.5751	.4340	.3423
.7944	.7715	.8056	.5520	.4385	.3383
.8375	.7534	.7867	.5288	.4429	.3337
.8872	.7336	.7660	.5047	.4478	.3285
.9335	.7128	.7443	.4805	.4485	.3197
.9865	.6898	.7203	.4554	.4493	.3099
1.0461	.6650	.6944	.4297	.4495	.2989
1.1057	.6432	.6716	.4082	.4513	.2903
1.1652	.6195	.6469	.3859	.4497	.2786
1.2314	.5928	.6190	.3621	.4459	.2643
1.3108	.5628	.5877	.3368	.4415	.2485
1.3903	.5278	.5511	.3089	.4295	.2267
1.4365	.5077	.5301	.2937	.4219	.2142
1.4961	.4860	.5075	.2776	.4153	.2018
1.5492	.4613	.4817	.2602	.4031	.1860
1.6286	.4337	.4529	.2413	.3930	.1704
1.7080	.4026	.4204	.2209	.3773	.1519
1.7577	.3851	.4021	.2097	.3686	.1419
1.8139	.3663	.3825	.1980	.3592	.1316
1.8769	.3456	.3609	.1853	.3478	.1202
1.9331	.3235	.3378	.1721	.3327	.1076
2.0193	.2975	.3106	.1570	.3170	.0943
2.1152	.2688	.2807	.1407	.2976	.0800
2.2278	.2355	.2459	.1222	.2722	.0641
2.3899	.1938	.2024	.0996	.2381	.0461
2.6350	.1385	.1446	.0705	.1859	.0258
2.7740	.0988	.1032	.0501	.1390	.0137
2.8634	.0698	.0729	.0353	.1010	.0070

APPENDIX B

TABULATION OF VELOCITY PROFILES – Continued

(b) Developed region – Continued

$\bar{r}$	$\bar{u}$	$\bar{u}/U$	$\overline{\rho u}$	$\overline{\rho u r}$	$\overline{\rho u^2 r}$
$\bar{x} = 26.93$; $\bar{r}_5 = 1.497$					
0	0.9413	1.0000	0.8469	0	0
.1192	.9359	.9943	.8344	.0995	.0931
.1953	.9265	.9843	.8136	.1589	.1472
.2647	.9169	.9741	.7926	.2098	.1924
.3641	.8956	.9515	.7502	.2731	.2446
.4502	.8727	.9271	.7075	.3185	.2780
.5297	.8476	.9005	.6642	.3518	.2982
.6222	.8200	.8711	.6204	.3860	.3165
.7084	.7886	.8378	.5751	.4074	.3213
.7547	.7715	.8196	.5520	.4166	.3214
.8010	.7534	.8004	.5288	.4236	.3191
.8540	.7336	.7793	.5047	.4310	.3162
.9003	.7128	.7573	.4805	.4326	.3084
.9533	.6898	.7328	.4554	.4341	.2994
1.0064	.6650	.7065	.4297	.4325	.2876
1.0592	.6432	.6833	.4082	.4324	.2781
1.1221	.6195	.6581	.3859	.4330	.2682
1.1917	.5928	.6298	.3621	.4315	.2558
1.2578	.5628	.5979	.3368	.4236	.2384
1.3539	.5278	.5607	.3089	.4182	.2207
1.4036	.5077	.5394	.2937	.4122	.2093
1.4564	.4860	.5163	.2776	.4043	.1965
1.5227	.4613	.4901	.2602	.3962	.1828
1.6022	.4337	.4607	.2413	.3866	.1677
1.6816	.4026	.4277	.2209	.3715	.1496
1.7478	.3581	.4091	.2097	.3665	.1411
1.8272	.3663	.3891	.1980	.3618	.1325
1.8933	.3456	.3672	.1853	.3508	.1212
1.9728	.3235	.3437	.1721	.3395	.1098
2.0590	.2975	.3161	.1570	.3233	.0962
2.1714	.2688	.2856	.1407	.3055	.0821
2.3039	.2355	.2502	.1222	.2815	.0663
2.4562	.1938	.2059	.0996	.2447	.0474
2.6679	.1385	.1471	.0705	.1882	.0261
2.8268	.0988	.1050	.0501	.1416	.0140
2.9394	.0698	.0741	.0353	.1037	.0072

APPENDIX B

TABULATION OF VELOCITY PROFILES – Continued

(b) Developed region – Continued

$\bar{r}$	$\bar{u}$	$\bar{u}/U$	$\overline{\rho u}$	$\overline{\rho u r}$	$\overline{\rho u^2 r}$
$\bar{x} = 28.93$; $\bar{r}_5 = 1.625$					
0	0.9077	1.0000	0.7742	0	0
.1225	.9049	.9969	.7679	.0941	.0851
.2218	.8956	.9867	.7502	.1664	.1490
.3078	.8846	.9746	.7291	.2244	.1985
.3774	.8727	.9614	.7075	.2670	.2330
.4800	.8476	.9338	.6642	.3188	.2702
.5660	.8200	.9034	.6204	.3511	.2879
.6489	.7886	.8688	.5751	.3732	.2943
.6951	.7715	.8500	.5520	.3837	.2960
.7414	.7534	.8300	.5288	.3921	.2954
.8044	.7336	.8082	.5047	.4060	.2978
.8606	.7128	.7853	.4805	.4135	.2947
.9269	.6898	.7599	.4554	.4221	.2912
.9964	.6650	.7326	.4297	.4282	.2848
1.0592	.6432	.7086	.4082	.4324	.2781
1.1255	.6195	.6825	.3859	.4343	.2690
1.2050	.5928	.6531	.3621	.4363	.2586
1.2975	.5628	.6200	.3368	.4370	.2459
1.3968	.5278	.5815	.3089	.4315	.2277
1.4632	.5077	.5593	.2937	.4297	.2182
1.5293	.4860	.5354	.2776	.4245	.2063
1.6022	.4613	.5082	.2602	.4169	.1923
1.7047	.4337	.4778	.2413	.4113	.1784
1.8139	.4026	.4435	.2209	.4007	.1613
1.8802	.3851	.4243	.2097	.3943	.1518
1.9597	.3663	.4035	.1980	.3880	.1421
2.0324	.3456	.3807	.1853	.3766	.1302
2.1186	.3235	.3564	.1721	.3646	.1179
2.2111	.2975	.3278	.1570	.3471	.1033
2.3303	.2688	.2961	.1407	.3279	.0881
2.4628	.2355	.2594	.1222	.3010	.0709
2.6316	.1938	.2135	.0996	.2622	.0508
2.8367	.1385	.1526	.0705	.2001	.0277
3.0453	.0988	.1089	.0501	.1526	.0151
3.2109	.0698	.0769	.0353	.1133	.0079

APPENDIX B

TABULATION OF VELOCITY PROFILES – Continued

(b) Developed region – Continued

$\bar{r}$	$\bar{u}$	$\bar{u}/U$	$\overline{\rho u}$	$\overline{\rho u r}$	$\overline{\rho u^2 r}$
		$\bar{x} = 30.92$; $\bar{r}_5 = 1.635$			
0	0.8800	1.0000	0.7205	0	0
.1059	.8776	.9970	.7161	.0758	.0666
.1721	.8727	.9910	.7075	.1218	.1063
.2781	.8606	.9780	.6861	.1908	.1642
.3476	.8476	.9630	.6642	.2309	.1957
.4602	.8200	.9320	.6204	.2855	.2341
.5660	.7886	.8960	.5751	.3255	.2567
.6123	.7715	.8763	.5520	.3380	.2608
.6753	.7534	.8560	.5288	.3571	.2690
.7448	.7336	.8335	.5047	.3759	.2758
.8077	.7128	.8100	.4805	.3881	.2766
.8804	.6898	.7840	.4554	.4009	.2765
.9567	.6650	.7560	.4297	.4111	.2734
1.0195	.6432	.7306	.4082	.4162	.2677
1.0824	.6195	.7040	.3859	.4177	.2588
1.1652	.5928	.6740	.3621	.4219	.2501
1.2578	.5628	.6400	.3368	.4236	.2384
1.3605	.5278	.5995	.3089	.4203	.2218
1.4167	.5077	.5770	.2937	.4161	.2113
1.4862	.4860	.5520	.2776	.4126	.2005
1.5690	.4613	.5240	.2602	.4083	.1883
1.6550	.4337	.4930	.2413	.3994	.1732
1.7742	.4026	.4573	.2209	.3919	.1578
1.8306	.3851	.4378	.2097	.3839	.1478
1.9132	.3663	.4163	.1980	.3788	.1388
1.9728	.3456	.3927	.1853	.3656	.1264
2.0655	.3235	.3677	.1721	.3555	.1150
2.1648	.2975	.3381	.1570	.3399	.1011
2.2775	.2688	.3054	.1407	.3204	.0861
2.4131	.2355	.2677	.1222	.2949	.0694
2.6083	.1938	.2203	.0996	.2599	.0504
2.9527	.1385	.1574	.0705	.2083	.0288
3.1778	.0988	.1123	.0501	.1592	.0157
3.3466	.0698	.0792	.0353	.1181	.0082

APPENDIX B

TABULATION OF VELOCITY PROFILES – Continued

(b) Developed region – Continued

$\bar{r}$	$\bar{u}$	$\bar{u}/U$	$\overline{\rho u}$	$\overline{\rho u r}$	$\overline{\rho u^2 r}$
$\bar{x} = 43.93$; $\bar{r}_5 = 2.245$					
0	0.6640	1.0000	0.4310	0	0
.2483	.6575	.9900	.4240	.1053	.0692
.3428	.6530	.9830	.4200	.1440	.0940
.4221	.6479	.9760	.4150	.1752	.1135
.5018	.6420	.9665	.4090	.2052	.1317
.6110	.6310	.9520	.3990	.2438	.1538
.6902	.6190	.9320	.3870	.2671	.1653
.7800	.6070	.9140	.3760	.2933	.1780
.8590	.5930	.8930	.3650	.3135	.1859
.9465	.5780	.8700	.3520	.3332	.1926
1.0420	.5627	.8475	.3390	.3532	.1987
1.1400	.5457	.8220	.3250	.3705	.2022
1.2410	.5280	.7950	.3110	.3860	.2038
1.3450	.5075	.7640	.2950	.3968	.2014
1.4550	.4852	.7310	.2790	.4059	.1969
1.5630	.4613	.6950	.2620	.4095	.1889
1.7030	.4333	.6525	.2430	.4138	.1793
1.8570	.4023	.6060	.2220	.4123	.1659
2.0500	.3660	.5510	.1990	.4080	.1493
2.3000	.3233	.4870	.1730	.3979	.1286
2.4620	.2975	.4480	.1580	.3890	.1157
2.6510	.2689	.4048	.1420	.3764	.1012
2.8900	.2350	.3540	.1230	.3555	.0835
3.2080	.1930	.2908	.1000	.3208	.0619
3.4460	.1637	.2465	.0843	.2905	.0476
3.6630	.1389	.2090	.0713	.2612	.0363
3.9980	.1080	.1625	.0552	.2207	.0238
4.2700	.0871	.1311	.0444	.1896	.0165
4.6370	.0636	.0958	.0324	.1502	.0096
$\bar{x} = 45.94$; $\bar{r}_5 = 2.347$					
0	0.6360	1.0000	0.4037	0	0
.2037	.6330	.9955	.4015	.0818	.0518
.2680	.6310	.9920	.3990	.1069	.0674
.3425	.6255	.9830	.3937	.1348	.0843
.4070	.6190	.9730	.3877	.1578	.0977
.5390	.6070	.9545	.3766	.2030	.1232
.6602	.5930	.9330	.3645	.2406	.1427
.7743	.5780	.9080	.3518	.2724	.1574
.8985	.5627	.8845	.3386	.3042	.1712
1.0100	.5457	.8570	.3251	.3284	.1792
1.1320	.5280	.8295	.3108	.3518	.1858
1.2570	.5075	.7970	.2952	.3711	.1883

APPENDIX B

TABULATION OF VELOCITY PROFILES – Continued

(b) Developed region – Continued

$\bar{r}$	$\bar{u}$	$\bar{u}/U$	$\overline{\rho u}$	$\overline{\rho u r}$	$\overline{\rho u^2 r}$
		$\bar{x} = 45.94$; $\bar{r}_5 = 2.347$ – Concluded			
1.3850	0.4852	0.7623	0.2790	0.3864	0.1875
1.5300	.4613	.7250	.2619	.4007	.1848
1.6790	.4333	.6810	.2426	.4073	.1765
1.8520	.4023	.6323	.2222	.4115	.1655
2.0550	.3660	.5753	.1993	.4096	.1499
2.3130	.3233	.5080	.1732	.4006	.1295
2.4910	.2975	.4673	.1581	.3938	.1172
2.7050	.2689	.4225	.1416	.3830	.1030
2.9700	.2350	.3692	.1228	.3647	.0857
3.2900	.1930	.3033	.1000	.3288	.0635
3.5500	.1637	.2573	.0843	.2991	.0490
3.7830	.1389	.2183	.0713	.2697	.0375
4.1200	.1080	.1697	.0552	.2275	.0246
4.3400	.0871	.1369	.0444	.1929	.0168
4.6800	.0636	.1000	.0324	.1519	.0097
		$\bar{x} = 47.94$; $\bar{r}_5 = 2.505$			
0	0.6083	1.0000	0.3783	0	0
.1886	.6070	.9980	.3766	.0710	.0431
.2730	.6040	.9940	.3741	.1021	.0617
.3278	.6020	.9900	.3700	.1213	.0730
.4420	.5930	.9760	.3645	.1611	.0955
.6257	.5780	.9505	.3518	.2201	.1272
.7600	.5627	.9260	.3386	.2573	.1448
.8967	.5457	.8975	.3251	.2915	.1591
1.0330	.5280	.8680	.3108	.3211	.1695
1.1620	.5075	.8340	.2952	.3430	.1741
1.3110	.4852	.7980	.2790	.3658	.1775
1.4700	.4613	.7590	.2619	.3850	.1776
1.6580	.4333	.7127	.2426	.4022	.1743
1.8620	.4023	.6618	.2222	.4137	.1664
2.1000	.3660	.6020	.1993	.4185	.1532
2.3690	.3233	.5317	.1732	.4103	.1326
2.5480	.2975	.4893	.1581	.4028	.1198
2.7600	.2689	.4420	.1416	.3908	.1051
3.0350	.2350	.3865	.1228	.3727	.0876
3.3650	.1930	.3173	.1000	.3363	.0649
3.6550	.1637	.2692	.0843	.3080	.0504
3.9030	.1389	.2283	.0713	.2782	.0386
4.2630	.1080	.1776	.0552	.2354	.0254
4.5580	.0871	.1432	.0444	.2026	.0176
4.9840	.0636	.1046	.0324	.1614	.0103

APPENDIX B

TABULATION OF VELOCITY PROFILES – Continued

(b) Developed region – Continued

	$\bar{r}$	$\bar{u}$	$\bar{u}/U$	$\overline{\rho u}$	$\overline{\rho u r}$	$\overline{\rho u^2 r}$
			$\bar{x} = 49.95$; $\bar{r}_5 = 2.865$			
	0	0.5800	1.0000	0.3536	0	0
	.1738	.5780	.9966	.3518	.0611	.0353
	.2980	.5743	.9902	.3485	.1039	.0597
	.3792	.5702	.9831	.3451	.1309	.0746
	.4587	.5670	.9776	.3424	.1571	.0891
	.5142	.5627	.9702	.3386	.1741	.0980
	.6850	.5457	.9409	.3251	.2227	.1215
	.8640	.5280	.9103	.3108	.2685	.1418
	1.0470	.5075	.8750	.2952	.3091	.1569
	1.2310	.4852	.8366	.2790	.3434	.1666
	1.4150	.4613	.7953	.2619	.3706	.1710
	1.6190	.4333	.7471	.2426	.3928	.1702
	1.8520	.4023	.6936	.2222	.4115	.1655
	2.1140	.3660	.6310	.1993	.4213	.1542
	2.4320	.3233	.5574	.1732	.4212	.1362
	2.6300	.2975	.5129	.1581	.4158	.1237
	2.8730	.2689	.4636	.1416	.4068	.1094
	3.1520	.2350	.4052	.1228	.3871	.0910
	3.5000	.1930	.3328	.1000	.3498	.0675
	3.7820	.1637	.2822	.0843	.3187	.0522
	4.0050	.1389	.2395	.0713	.2855	.0397
	4.3580	.1080	.1862	.0552	.2406	.0260
	4.6350	.0871	.1502	.0444	.2060	.0179
	5.1330	.0636	.1097	.0324	.1663	.0106
			$\bar{x} = 51.96$; $\bar{r}_5 = 2.755$			
	0	0.5575	1.0000	0.3345	0	0
	.1589	.5542	.9950	.3320	.0528	.0292
	.2979	.5501	.9875	.3288	.0980	.0539
	.3942	.5457	.9790	.3251	.1282	.0700
	.5660	.5366	.9630	.3178	.1799	.0965
	.6953	.5280	.9475	.3108	.2161	.1141
	.9185	.5075	.9100	.2952	.2711	.1376
	1.1020	.4852	.8710	.2790	.3075	.1492
	1.2920	.4613	.8280	.2619	.3384	.1561
	1.5100	.4333	.7780	.2426	.3663	.1587
	1.7470	.4023	.7220	.2222	.3882	.1562

APPENDIX B

TABULATION OF VELOCITY PROFILES – Continued

(b) Developed region – Continued

$\bar{r}$	$\bar{u}$	$\bar{u}/U$	$\overline{\rho u}$	$\overline{\rho u r}$	$\overline{\rho u^2 r}$
		$\bar{x}$ = 51.96; $\bar{r}_5$ = 2.755 – Concluded			
2.0370	0.3660	0.6570	0.1993	0.4060	0.1486
2.3720	.3233	.5800	.1732	.4108	.1328
2.6010	.2975	.5340	.1581	.4112	.1223
2.8400	.2689	.4825	.1416	.4021	.1081
3.1280	.2350	.4219	.1228	.3841	.0903
3.5230	.1930	.3463	.1000	.3521	.0680
3.8180	.1637	.2950	.0843	.3217	.0527
4.0720	.1389	.2493	.0713	.2903	.0403
4.4700	.1080	.1937	.0552	.2468	.0266
4.7910	.0871	.1563	.0444	.2129	.0185
5.2950	.0636	.1142	.0324	.1715	.0109
		$\bar{x}$ = 61.65; $\bar{r}_5$ = 3.495			
0	0.4525	1.0000	0.2547	0	0
.4370	.4493	.9930	.2526	.1104	.0496
.5960	.4470	.9880	.2510	.1496	.0669
.6757	.4442	.9820	.2492	.1684	.0748
.7750	.4388	.9700	.2457	.1904	.0836
.9735	.4233	.9355	.2352	.2290	.0969
1.1920	.4072	.9000	.2247	.2678	.1090
1.4100	.3895	.8605	.2133	.3008	.1172
1.6690	.3702	.8180	.2012	.3358	.1243
1.9270	.3500	.7730	.1890	.3642	.1275
2.2150	.3268	.7220	.1749	.3874	.1266
2.5330	.3009	.6645	.1597	.4045	.1217
2.9100	.2715	.6000	.1429	.4158	.1129
3.3480	.2371	.5240	.1238	.4145	.0983
3.6150	.2177	.4810	.1132	.4092	.0891
3.9220	.1951	.4313	.1010	.3961	.0773
4.2900	.1701	.3760	.0876	.3760	.0640
4.7700	.1389	.3069	.0712	.3398	.0472
4.9850	.1243	.2749	.0636	.3172	.0394
5.2220	.1083	.2393	.0553	.2889	.0313
5.5820	.0884	.1954	.0451	.2516	.0222
5.7800	.0774	.1710	.0395	.2281	.0176
6.0800	.0623	.1376	.0317	.1928	.0120
6.5180	.0394	.0871	.0200	.1306	.0052

APPENDIX B

TABULATION OF VELOCITY PROFILES – Continued

(b) Developed region – Continued

$\bar{r}$	$\bar{u}$	$\bar{u}/U$	$\overline{\rho u}$	$\overline{\rho u r}$	$\overline{\rho u^2 r}$
		$\bar{x} = 65.7$; $\bar{r}_5 = 3.823$			
0	0.4165	1.0000	0.2307	0	0
.4410	.4130	.9910	.2284	.1007	.0416
.6755	.4072	.9770	.2247	.1518	.0618
.9540	.3990	.9580	.2195	.2094	.0836
1.1710	.3895	.9350	.2133	.2498	.0973
1.5090	.3702	.8890	.2012	.3036	.1124
1.8370	.3500	.8400	.1890	.3472	.1215
2.1500	.3268	.7840	.1749	.3760	.1229
2.5120	.3009	.7220	.1597	.4012	.1207
2.9200	.2715	.6520	.1429	.4173	.1133
3.4170	.2371	.5695	.1238	.4230	.1003
3.6940	.2177	.5222	.1132	.4182	.0910
4.0120	.1951	.4683	.1010	.4052	.0790
4.4000	.1701	.4083	.0876	.3857	.0656
4.8650	.1389	.3333	.0712	.3466	.0481
5.1030	.1243	.2985	.0636	.3247	.0404
5.4000	.1083	.2600	.0553	.2988	.0324
5.8000	.0884	.2123	.0451	.2615	.0231
6.0500	.0774	.1859	.0395	.2387	.0185
6.3600	.0623	.1495	.0317	.2017	.0126
6.8550	.0394	.0946	.0200	.1373	.0054
		$\bar{x} = 69.73$; $\bar{r}_5 = 4.077$			
0	0.3830	1.0000	0.2093	0	0
.3970	.3810	.9940	.2081	.0826	.0315
.6950	.3745	.9780	.2039	.1417	.0531
.8440	.3702	.9660	.2012	.1698	.0629
1.1520	.3605	.9410	.1955	.2252	.0812
1.3810	.3500	.9140	.1890	.2610	.0914
1.8370	.3268	.8530	.1749	.3213	.1050
2.2830	.3009	.7850	.1597	.3646	.1097
2.7900	.2715	.7085	.1429	.3987	.1082
3.3570	.2371	.6195	.1238	.4156	.0985

APPENDIX B

TABULATION OF VELOCITY PROFILES – Continued

(b) Developed region – Continued

$\bar{r}$	$\bar{u}$	$\bar{u}/U$	$\overline{\rho u}$	$\overline{\rho u r}$	$\overline{\rho u^2 r}$
		$\bar{x} = 69.73$; $\bar{r}_5 = 4.077$ – Concluded			
3.6530	0.2177	0.5680	0.1132	0.4135	0.0900
4.0000	.1951	.5095	.1010	.4040	.0788
4.4300	.1701	.4440	.0876	.3883	.0660
4.9870	.1389	.3625	.0712	.3553	.0495
5.3020	.1243	.3247	.0636	.3374	.0419
5.6600	.1083	.2828	.0553	.3132	.0339
6.1170	.0884	.2310	.0451	.2758	.0244
6.4170	.0774	.2021	.0395	.2532	.0196
6.7700	.0623	.1626	.0317	.2147	.0134
7.2800	.0394	.1028	.0200	.1458	.0057
		$\bar{x} = 73.80$; $\bar{r}_5 = 4.40$			
0	0.3568	1.0000	0.1931	0	0
.4765	.3543	.9940	.1915	.0912	.0323
.7940	.3500	.9810	.1890	.1501	.0525
.9930	.3450	.9670	.1859	.1846	.0637
1.2410	.3389	.9500	.1822	.2261	.0766
1.5690	.3268	.9160	.1749	.2744	.0897
2.1050	.3009	.8430	.1597	.3362	.1012
2.3620	.2870	.8040	.1517	.3583	.1028
2.6200	.2715	.7615	.1429	.3744	.1016
2.9000	.2554	.7160	.1340	.3886	.0992
3.2270	.2371	.6653	.1238	.3995	.0947
3.6140	.2177	.6100	.1132	.4091	.0891
4.0500	.1951	.5473	.1010	.4091	.0798
4.5980	.1701	.4770	.0876	.4030	.0686
5.2730	.1389	.3892	.0712	.3756	.0522
5.6200	.1243	.3488	.0636	.3576	.0444
6.0000	.1083	.3038	.0553	.3320	.0360
6.5020	.0884	.2480	.0451	.2931	.0259
6.8100	.0774	.2170	.0395	.2687	.0208
7.2470	.0623	.1746	.0317	.2298	.0143
7.9030	.0394	.1105	.0200	.1583	.0062

APPENDIX B

TABULATION OF VELOCITY PROFILES – Continued

(b) Developed region – Continued

$\bar{r}$	$\bar{u}$	$\bar{u}/U$	$\overline{\rho u}$	$\overline{\rho u r}$	$\overline{\rho u^2 r}$
		$\bar{x} = 86.9$; $\bar{r}_5 = 5.540$			
0	0.2899	1.0000	0.1522	0	0
.6356	.2878	.9928	.1509	.0959	.0276
.8441	.2872	.9907	.1505	.1270	.0365
1.0710	.2859	.9862	.1498	.1605	.0459
1.2120	.2770	.9555	.1448	.1756	.0486
1.4500	.2731	.9420	.1426	.2067	.0565
1.6880	.2670	.9210	.1392	.2350	.0628
1.9270	.2601	.8972	.1354	.2609	.0679
2.1550	.2530	.8727	.1314	.2832	.0716
2.3690	.2459	.8482	.1276	.3023	.0743
2.6020	.2389	.8241	.1237	.3219	.0769
2.8400	.2311	.7972	.1195	.3394	.0784
3.0980	.2236	.7713	.1154	.3575	.0799
3.3570	.2149	.7413	.1107	.3716	.0799
3.6350	.2069	.7137	.1064	.3868	.0800
3.9030	.1973	.6806	.1013	.3954	.0780
4.2110	.1880	.6485	.0963	.4056	.0762
4.5480	.1775	.6123	.0908	.4128	.0733
4.9060	.1661	.5730	.0848	.4159	.0691
5.2630	.1540	.5312	.0784	.4129	.0636
5.6410	.1408	.4857	.0716	.4040	.0569
6.0770	.1267	.4373	.0643	.3908	.0495
6.3360	.1178	.4063	.0598	.3786	.0446
6.5940	.1098	.3788	.0556	.3667	.0403
6.9310	.1011	.3487	.0512	.3546	.0358
7.3780	.0908	.3132	.0459	.3387	.0308
7.8350	.0814	.2808	.0412	.3224	.0262
8.3160	.0714	.2463	.0361	.2999	.0214
8.6590	.0576	.1985	.0290	.2515	.0145
9.1760	.0518	.1787	.0261	.2396	.0124
9.4140	.0428	.1475	.0216	.2029	.0087
10.2680	.0350	.1206	.0176	.1810	.0063

APPENDIX B

TABULATION OF VELOCITY PROFILES – Continued

(b) Developed region – Continued

$\bar{r}$	$\bar{u}$	$\bar{u}/U$	$\overline{\rho u}$	$\overline{\rho u r}$	$\overline{\rho u^2 r}$
		$\bar{x}$ = 90.86; $\bar{r}_5$ = 5.95			
0	0.2712	1.0000	0.1415	0	0
.3376	.2707	.9982	.1413	.0477	.0129
.5760	.2691	.9923	.1404	.0809	.0218
.8937	.2670	.9845	.1392	.1244	.0332
1.1820	.2633	.9709	.1372	.1622	.0427
1.4100	.2601	.9591	.1354	.1909	.0496
1.7680	.2530	.9329	.1314	.2323	.0588
2.0660	.2459	.9067	.1276	.2636	.0648
2.3630	.2389	.8809	.1237	.2923	.0698
2.6670	.2311	.8521	.1195	.3187	.0736
2.9490	.2236	.8245	.1154	.3403	.0761
3.2270	.2149	.7924	.1107	.3572	.0768
3.5150	.2069	.7629	.1064	.3740	.0774
3.8230	.1973	.7275	.1013	.3873	.0764
4.1510	.1880	.6932	.0963	.3999	.0752
4.4990	.1775	.6545	.0908	.4084	.0725
4.8760	.1661	.6125	.0848	.4134	.0687
5.3030	.1540	.5678	.0784	.4160	.0641
5.7500	.1408	.5192	.0716	.4118	.0580
6.2760	.1267	.4670	.0643	.4035	.0511
6.5540	.1178	.4344	.0598	.3917	.0461
6.8620	.1098	.4049	.0556	.3816	.0419
7.2100	.1011	.3728	.0512	.3689	.0373
7.5770	.0908	.3348	.0459	.3478	.0316
7.9440	.0814	.3001	.0412	.3269	.0266
8.3520	.0714	.2633	.0361	.3012	.0215
8.8380	.0576	.2122	.0290	.2567	.0148
9.1460	.0518	.1910	.0261	.2388	.0124
9.5930	.0428	.1576	.0216	.2067	.0088
10.2480	.0350	.1289	.0176	.1807	.0063
10.7850	.0246	.0908	.0124	.1337	.0033
		$\bar{x}$ = 94.88; $\bar{r}_5$ = 6.26			
0	0.2569	1.0000	0.1336	0	0
.8540	.2541	.9891	.1321	.1128	.0287
1.0030	.2530	.9848	.1314	.1318	.0334
1.2910	.2502	.9739	.1300	.1678	.0420
1.4800	.2459	.9572	.1276	.1888	.0464
1.8160	.2389	.9299	.1237	.2246	.0537
2.1450	.2311	.8996	.1195	.2563	.0592
2.4920	.2236	.8704	.1154	.2876	.0643
2.8400	.2149	.8365	.1107	.3144	.0676
3.1900	.2069	.8054	.1064	.3394	.0702
3.5450	.1973	.7680	.1013	.3591	.0708
3.9230	.1880	.7318	.0963	.3779	.0710

APPENDIX B

TABULATION OF VELOCITY PROFILES – Continued

(b) Developed region – Continued

$\bar{r}$	$\bar{u}$	$\bar{u}/U$	$\overline{\rho u}$	$\overline{\rho u r}$	$\overline{\rho u^2 r}$
$\bar{x} = 94.88$; $\bar{r}_5 = 6.26$ – Concluded					
4.3100	0.1775	0.6909	0.0908	0.3912	0.0694
4.7470	.1661	.6466	.0848	.4025	.0669
5.2150	.1540	.5995	.0784	.4091	.0630
5.7400	.1408	.5481	.0716	.4110	0579
6.3400	.1267	.4930	.0643	.4077	.0517
6.6750	.1178	.4585	.0598	.3989	.0470
7.0130	.1098	.4274	.0556	.3900	.0428
7.4000	.1011	.3935	.0512	.3786	.0383
7.8250	.0908	.3534	.0459	.3592	.0326
8.2230	.0814	.3169	.0412	.3384	.0276
8.6800	.0714	.2779	.0361	.3130	.0224
9.2800	.0576	.2240	.0290	.2695	.0155
9.6820	.0518	.2016	.0261	.2528	.0131
10.1890	.0428	.1664	.0216	.2196	.0094
10.8640	.0350	.1361	.0176	.1915	.0067
11.3700	.0246	.0958	.0124	.1410	.0035
$\bar{x} = 98.89$; $\bar{r}_5 = 6.57$					
0	0.2450	1.0000	0.1270	0	0
.8838	.2430	.9918	.1260	.1114	.0271
1.3900	.2389	.9751	.1237	.1719	.0411
1.6880	.2357	.9620	.1220	.2059	.0485
1.8770	.2311	.9433	.1195	.2243	.0518
2.2700	.2236	.9127	.1154	.2620	.0586
2.6810	.2149	.8771	.1107	.2968	.0638
3.0980	.2069	.8445	.1064	.3296	.0682
3.5150	.1973	.8053	.1013	.3561	.0703
3.9320	.1880	.7673	.0963	.3788	.0712
4.3890	.1775	.7245	.0908	.3984	.0707
4.8460	.1661	.6780	.0848	.4108	.0682
5.3030	.1540	.6286	.0784	.4160	.0641
5.8190	.1408	.5747	.0716	.4167	.0587
6.4150	.1267	.5170	.0643	.4125	.0523
6.7630	.1178	.4808	.0598	.4042	.0476
7.1500	.1098	.4482	.0556	.3976	.0437
7.5770	.1011	.4127	.0512	.3876	.0392
8.0440	.0908	.3706	.0459	.3692	.0335
8.5000	.0814	.3322	.0412	.3498	.0285
9.0270	.0714	.2914	.0361	.3255	.0232
9.6920	.0576	.2349	.0290	.2815	.0162
10.1490	.0518	.2114	.0261	.2650	.0137
10.7450	.0428	.1745	.0216	.2316	.0099
11.6680	.0350	.1427	.0176	.2057	.0072
12.4930	.0246	.1005	.0124	.1549	.0038

APPENDIX B

TABULATION OF VELOCITY PROFILES – Continued

(b) Developed region – Continued

$\bar{r}$	$\bar{u}$	$\bar{u}/U$	$\overline{\rho u}$	$\overline{\rho u r}$	$\overline{\rho u^2 r}$
$\bar{x} = 115.3$; $\bar{r}_5 = 8.12$					
0	0.1963	1.0000	0.1017	0	0
.5760	.1951	.9940	.1010	.0582	.0114
1.1917	.1927	.9815	.0997	.1189	.0229
1.6485	.1899	.9590	.0982	.1619	.0307
2.4230	.1831	.9325	.0946	.2292	.0420
3.3366	.1731	.8820	.0893	.2979	.0516
3.7339	.1677	.8540	.0864	.3227	.0541
4.1708	.1621	.8260	.0834	.3480	.0564
4.5482	.1563	.7963	.0804	.3656	.0571
4.9057	.1505	.7665	.0773	.3793	.0571
5.2433	.1442	.7350	.0740	.3882	.0560
5.5611	.1375	.7003	.0705	.3922	.0539
5.9186	.1306	.6650	.0669	.3961	.0517
6.3357	.1232	.6280	.0631	.3996	.0492
6.8520	.1155	.5883	.0591	.4048	.0468
7.4081	.1073	.5465	.0548	.4062	.0436
8.1231	.0978	.4983	.0499	.4056	.0397
8.7786	.0877	.4469	.0447	.3926	.0344
9.2155	.0807	.4110	.0411	.3792	.0306
9.5333	.0756	.3852	.0385	.3674	.0278
10.0298	.0680	.3464	.0346	.3476	.0237
10.3674	.0617	.3141	.0314	.3256	.0201
10.9434	.0522	.2659	.0265	.2905	.0152
11.6187	.0395	.2010	.0201	.2331	.0092
11.9100	.0344	.1750	.0175	.2080	.0072
12.2300	.0274	.1394	.0139	.1702	.0047
12.6400	.0210	.1070	.0107	.1349	.0028
$\bar{x} = 121.3$; $\bar{r}_5 = 8.38$					
0	0.1857	1.0000	0.0960	0	0
.8739	.1841	.9914	.0951	.0831	.0153
1.2210	.1825	.9828	.0942	.1151	.0210
1.6290	.1807	.9731	.0933	.1520	.0275
2.0560	.1773	.9548	.0915	.1881	.0334
2.7860	.1720	.9262	.0887	.2470	.0425
3.0590	.1664	.8961	.0857	.2621	.0436
3.5350	.1603	.8632	.0825	.2915	.0467
4.0220	.1547	.8331	.0795	.3198	.0495
4.5180	.1475	.7943	.0757	.3422	.0505
5.0250	.1407	.7577	.0722	.3627	.0510
5.5410	.1337	.7200	.0685	.3797	.0508

APPENDIX B

TABULATION OF VELOCITY PROFILES – Continued

(b) Developed region – Continued

$\bar{r}$	$\bar{u}$	$\bar{u}/U$	$\overline{\rho u}$	$\overline{\rho u r}$	$\overline{\rho u^2 r}$
$\bar{x} = 121.3$; $\bar{r}_5 = 8.38$ – Concluded					
6.0970	0.1252	0.6742	0.0641	0.3908	0.0489
6.6930	.1172	.6311	.0600	.4012	.0470
7.2990	.1092	.5880	.0558	.4073	.0445
7.9640	.0994	.5353	.0508	.4042	.0402
8.6790	.0898	.4836	.0458	.3976	.0357
9.4940	.0772	.4159	.0394	.3736	.0288
10.0600	.0688	.3708	.0351	.3528	.0243
10.4770	.0622	.3349	.0317	.3318	.0206
11.0130	.0574	.3088	.0261	.3215	.0184
11.7680	.0490	.2639	.0249	.2933	.0144
12.5520	.0406	.2186	.0206	.2590	.0105
13.1000	.0355	.1910	.0180	.2361	.0084
13.6850	.0290	.1563	.0148	.2019	.0059
14.4300	.0213	.1146	.0108	.1560	.0033
$\bar{x} = 127.3$; $\bar{r}_5 = 8.77$					
0	0.1738	1.0000	0.0896	0	0
.4568	.1731	.9960	.0893	.0408	.0071
.9930	.1710	.9839	.0882	.0875	.0150
1.5690	.1677	.9649	.0866	.1359	.0228
2.3436	.1621	.9327	.0835	.1956	.0317
3.0785	.1563	.8993	.0804	.2475	.0387
3.7537	.1505	.8659	.0773	.2903	.0437
4.4091	.1442	.8297	.0740	.3264	.0471
5.0050	.1375	.7911	.0705	.3530	.0485
5.6008	.1306	.7514	.0669	.3748	.0490
6.1370	.1232	.7089	.0631	.3870	.0477
6.7527	.1155	.6646	.0591	.3989	.0461
7.3088	.1073	.6174	.0548	.4007	.0430
7.9841	.0978	.5628	.0499	.3987	.0390
8.7190	.0877	.5045	.0447	.3899	.0342
9.1956	.0807	.4644	.0411	.3783	.0305
9.5333	.0756	.4353	.0385	.3674	.0278
10.1291	.0680	.3915	.0347	.3510	.0239
10.6058	.0617	.3549	.0314	.3331	.0206
11.7200	.0522	.3002	.0265	.3111	.0162
12.9100	.0395	.2270	.0201	.2590	.0102
13.3900	.0344	.1978	.0175	.2340	.0080
13.9200	.0274	.1575	.0139	.1937	.0053
14.2000	.0210	.1208	.0107	.1515	.0032

APPENDIX B

TABULATION OF VELOCITY PROFILES – Continued

(b) Developed region – Continued

$\bar{r}$	$\bar{u}$	$\bar{u}/U$	$\overline{\rho u}$	$\overline{\rho u r}$	$\overline{\rho u^2 r}$
		$\bar{x} = 133.6$; $\bar{r}_5 = 9.51$			
0	0.1620	1.0000	0.0834	0	0
.7547	.1614	.9960	.0831	.0627	.0101
1.3704	.1597	.9860	.0822	.1126	.0180
2.1251	.1562	.9645	.0804	.1708	.0267
2.9990	.1502	.9270	.0772	.2315	.0348
3.7736	.1439	.8880	.0739	.2788	.0401
4.4687	.1375	.8490	.0705	.3151	.0433
4.7865	.1347	.8320	.0691	.3306	.0445
5.0447	.1318	.8140	.0676	.3408	.0449
5.3227	.1291	.7970	.0662	.3521	.0455
5.6008	.1262	.7790	.0646	.3620	.0457
5.8590	.1231	.7600	.0630	.3692	.0454
6.1370	.1201	.7415	.0615	.3772	.0453
6.4548	.1170	.7220	.0599	.3864	.0452
6.7329	.1137	.7020	.0582	.3915	.0445
7.0308	.1103	.6810	.0564	.3964	.0437
7.3287	.1069	.6600	.0546	.4003	.0428
7.6663	.1031	.6370	.0526	.4037	.0416
7.9643	.0997	.6150	.0509	.4054	.0404
8.2820	.0959	.5920	.0489	.4054	.0389
8.6395	.0918	.5670	.0468	.4047	.0372
8.9772	.0874	.5395	.0446	.4001	.0350
9.3545	.0830	.5120	.0423	.3957	.0328
9.7517	.0782	.4830	.0399	.3889	.0304
10.1490	.0732	.4520	.0373	.3785	.0277
10.6058	.0678	.4184	.0345	.3663	.0248
11.0626	.0621	.3833	.0316	.3499	.0217
11.6187	.0552	.3408	.0281	.3261	.0180
12.2600	.0482	.2973	.0245	.3006	.0145
12.9300	.0393	.2427	.0200	.2583	.0102
13.3300	.0342	.2112	.0174	.2320	.0079
13.7500	.0279	.1720	.0142	.1949	.0054
14.2800	.0209	.1290	.0106	.1518	.0032

APPENDIX B

TABULATION OF VELOCITY PROFILES – Concluded

(b) Developed region – Concluded

$\bar{r}$	$\bar{u}$	$\bar{u}/U$	$\overline{\rho u}$	$\overline{\rho u r}$	$\overline{\rho u^2 r}$
		$\bar{x} = 149.5$; $\bar{r}_5 = 10.72$			
0	0.1454	1.0000	0.0750	0	0
1.2020	.1451	.9979	.0748	.0899	.0130
1.6580	.1444	.9931	.0745	.1235	.0178
2.2240	.1411	.9704	.0728	.1619	.0228
2.7610	.1379	.9484	.0711	.1963	.0271
3.2370	.1359	.9347	.0700	.2266	.0308
3.6740	.1322	.9092	.0681	.2502	.0331
4.0710	.1298	.8927	.0668	.2719	.0353
4.4690	.1266	.8707	.0652	.2914	.0369
4.8660	.1227	.8439	.0631	.3070	.0377
5.2530	.1201	.8260	.0618	.3246	.0390
5.6500	.1162	.7992	.0598	.3379	.0393
6.0580	.1138	.7827	.0585	.3544	.0403
6.4950	.1096	.7538	.0563	.3657	.0401
6.9120	.1068	.7345	.0548	.3788	.0405
7.3780	.1040	.7153	.0534	.3940	.0410
7.8650	.0973	.6692	.0499	.3925	.0382
8.3320	.0948	.6523	.0486	.4049	.0384
8.8080	.0900	.6190	.0462	.4069	.0366
9.2850	.0848	.5836	.0435	.4039	.0343
9.8210	.0812	.5588	.0416	.4086	.0332
10.3870	.0755	.5193	.0387	.4020	.0304
10.9830	.0691	.4752	.0354	.3888	.0269
11.8770	.0646	.4442	.0331	.3931	.0254
12.3930	.0576	.3958	.0294	.3644	.0210
13.3070	.0498	.3425	.0255	.3393	.0169
14.3790	.0401	.2758	.0205	.2948	.0118
15.8690	.0304	.2091	.0155	.2460	.0075

APPENDIX C

METHOD OF COMPUTING EDDY VISCOSITY DISTRIBUTIONS FROM EXPERIMENTAL DATA

For axisymmetric, turbulent, compressible flow, the conservation-of-mass equation is

$$\frac{\partial(\rho u r)}{\partial x} + \frac{\partial(\rho v r)}{\partial r} = 0 \tag{C1}$$

and the conservation-of-momentum equation is

$$\rho u \frac{\partial u}{\partial x} + \rho v \frac{\partial u}{\partial r} = \frac{1}{r} \frac{\partial}{\partial r}\left(\rho \epsilon r \frac{\partial u}{\partial r}\right) \tag{C2}$$

The assumptions inherent in equation (C2) are only the usual Prandtl boundary-layer approximations with negligible pressure gradient. A particular combination of equations (C1) and (C2) of interest herein is

$$\frac{\partial\left(\rho u^2 r\right)}{\partial x} + \frac{\partial(\rho v u r)}{\partial r} = \frac{\partial}{\partial r}\left(\rho \epsilon r \frac{\partial u}{\partial r}\right) \tag{C3}$$

Equation (C3) is now integrated from the center line to r_s, r_s being the radial distance to the surface of a stream tube. The result is the following expression:

$$\int_0^{r_s} \frac{\partial\left(\rho u^2 r\right) dr}{\partial x} + (\rho v u r)_{r_s} = \left(\rho \epsilon r \frac{\partial u}{\partial r}\right)_{r_s} + f(x) \tag{C4}$$

The subscript r_s indicates evaluation on the stream-tube surface, and $f(x)$ is a function of x, which from a consideration of center-line values must be zero. By applying Leibnitz's rule, for interchanging the order of integration and differentiation, to the integral in equation (C4), the following equation is obtained:

$$\frac{d}{dx}\int_0^{r_s}\left(\rho u^2 r\right) dr - \left(\rho u^2 r\right)_{r_s} \frac{dr_s}{dx} + (\rho v u r)_{r_s} = \left(\rho \epsilon r \frac{\partial u}{\partial r}\right)_{r_s} \tag{C5}$$

Since r_s is on a stream-tube surface, the derivative $\frac{dr_s}{dx}$ may be expressed, by employing the concept of a stream function, as

$$\frac{dr_s}{dx} = \frac{v}{u} \tag{C6}$$

Thus, the sum of the second and third terms on the left of equation (C5) is zero. By defining the turbulent shear stress τ as

$$\tau = \rho\epsilon \frac{\partial u}{\partial r} \tag{C7}$$

and solving equation (C5) for the turbulent shear stress, the following equation is obtained:

$$\tau_{r_s} = \frac{1}{r_s} \frac{d}{dx} \int_0^{r_s} \rho u^2 r \, dr \tag{C8}$$

Equation (C8) states that the shear stress at a point on a stream-tube surface varies directly as the axial gradient of momentum of the fluid within the stream tube and inversely as the radial distance to the stream-tube surface. Thus, experimental evaluation of the shear stress τ_{r_s} requires first the determination of stream tubes, that is, surfaces which contain equal mass flow rates, and second the determination of the axial gradient of momentum within the stream tubes. The eddy viscosity coefficient distribution at a given axial station x and at a given radial distance r_s may then be computed from the following equation:

$$(\rho\epsilon)_{r_s} = \frac{\tau_{r_s}}{\left(\frac{du}{dr}\right)_{r_s}} \tag{C9}$$

Computational problems arise near the center line as r_s becomes small, since the velocity gradient and the shear stress approach zero simultaneously. Furthermore, the center-line value of the eddy viscosity coefficient is not necessarily zero or readily computable, since an expression for the center-line coefficient involves the second radial derivative of the velocity. An expression for the center-line coefficient of eddy viscosity, which is taken from reference 13, is

$$(\rho\epsilon)_{\text{℄}} = \left(\frac{\rho u \frac{\partial u}{\partial x}}{2 \frac{\partial^2 u}{\partial r^2}} \right)_{\text{℄}} \tag{C10}$$

Direct evaluation of equation (C10) from experimental data was not undertaken herein, but equation (C10) was applied through the use of an assumed form for the velocity profile.

APPENDIX C

For the downstream region of a jet exhausting to still air, the following form for the velocity profile was assumed in reference 2:

$$u = u_{\text{℄}} \exp\left(-0.6932 \frac{r^2}{r_5^2}\right) \tag{C11}$$

Use of equation (C11) in equation (C10) results in the following equation for the centerline distribution of the coefficient of eddy viscosity:

$$(\rho\epsilon)_{\text{℄}} = \frac{-\left(\rho r_5^2 \frac{\partial u}{\partial x}\right)_{\text{℄}}}{2.7728} \tag{C12}$$

REFERENCES

1. Kleinstein, Gdalia: On the Mixing of Laminar and Turbulent Axially Symmetric Compressible Flows. PIBAL Rept. No. 756 (Contract No. AF 33(616)-7661), Polytech. Inst. Brooklyn, Feb. 1963.

2. Warren, Walter R., Jr.: An Analytical and Experimental Study of Compressible Free Jets. Publ. No.: 23,885, Univ. Microfilms, Inc., 1957.

3. Shoemaker, Charles J.: Performance of Seven Semicircular Lift-Producing Nozzles. NASA TN D-2731, 1965.

4. Alpinieri, Louis J.: An Experimental Investigation of the Turbulent Mixing on Non-Homogeneous Coaxial Jets. PIBAL Rept. No. 789 (Contract No. AF 49(638)-217), Polytech. Inst. Brooklyn, Aug. 1963.

5. Corrsin, Stanley; and Uberoi, Mahinder S.: Further Experiments on the Flow and Heat Transfer in a Heated Turbulent Air Jet. NACA Rept. 998, 1950.

6. Szablewski, W.: The Diffusion of a Hot Air Jet in Air in Motion. Part II. The Flow Field in the Transition Zone. NACA TM 1288, 1950.

7. Faris, George Naim: Some Entrainment Properties of a Turbulent Axi-Symmetric Jet. Res. Rept. No. 39 (Contract NONR 978(03)), Aerophys. Dept., Mississippi State Univ., Jan. 15, 1963.

8. Johannesen, N. H.: Further Results on the Mixing of Free Axially-Symmetrical Jets of Mach Number 1.40. R. & M. No. 3292, British A.R.C., 1962.

9. Ruden, P.: Turbulente Ausbreitungsvorgange im Freistrahl. Die Naturwissenschaften, Bd. 21, Heft. 21/23, May 1933, pp. 375-378.

10. Maydew, R. C.; and Reed, J. F.: Turbulent Mixing of Axisymmetric Compressible Jets (in the Half-Jet Region) With Quiescent Air. SC-4764(RR), Sandia Corp. (Albuquerque, N. Mex.), Mar. 1963.

11. Ragsdale, Robert G.; and Edwards, Oliver J.: Data Comparisons and Photographic Observations of Coaxial Mixing of Dissimilar Gases at Nearly Equal Stream Velocities. NASA TN D-3131, 1965.

12. Liepmann, Hans Wolfgang; and Laufer, John: Investigations of Free Turbulent Mixing. NACA TN 1257, 1947.

13. Zakkay, Victor; Krause, Egon; and Woo, Stephen D. L.: Turbulent Transport Properties for Axisymmetric Heterogeneous Mixing. ARL 64-103, U.S. Air Force, June 1964.

14. Corrsin, Stanley: Investigation of Flow in an Axialy Symmetrical Heated Jet of Air. NACA WR W-94, 1943. (Formerly NACA ACR 3L23, 1943.)

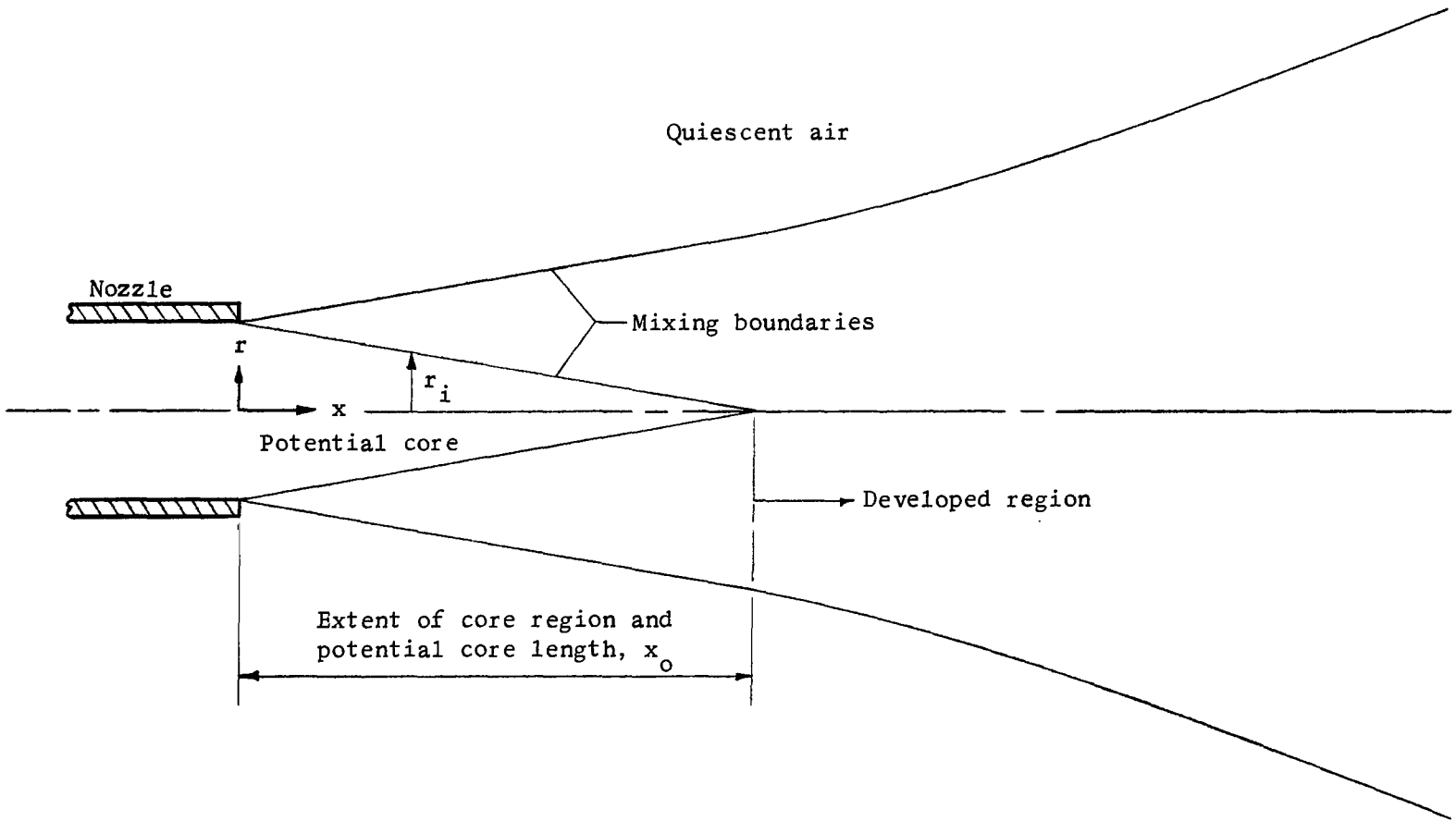

Figure 1.- Flow-field schematic.

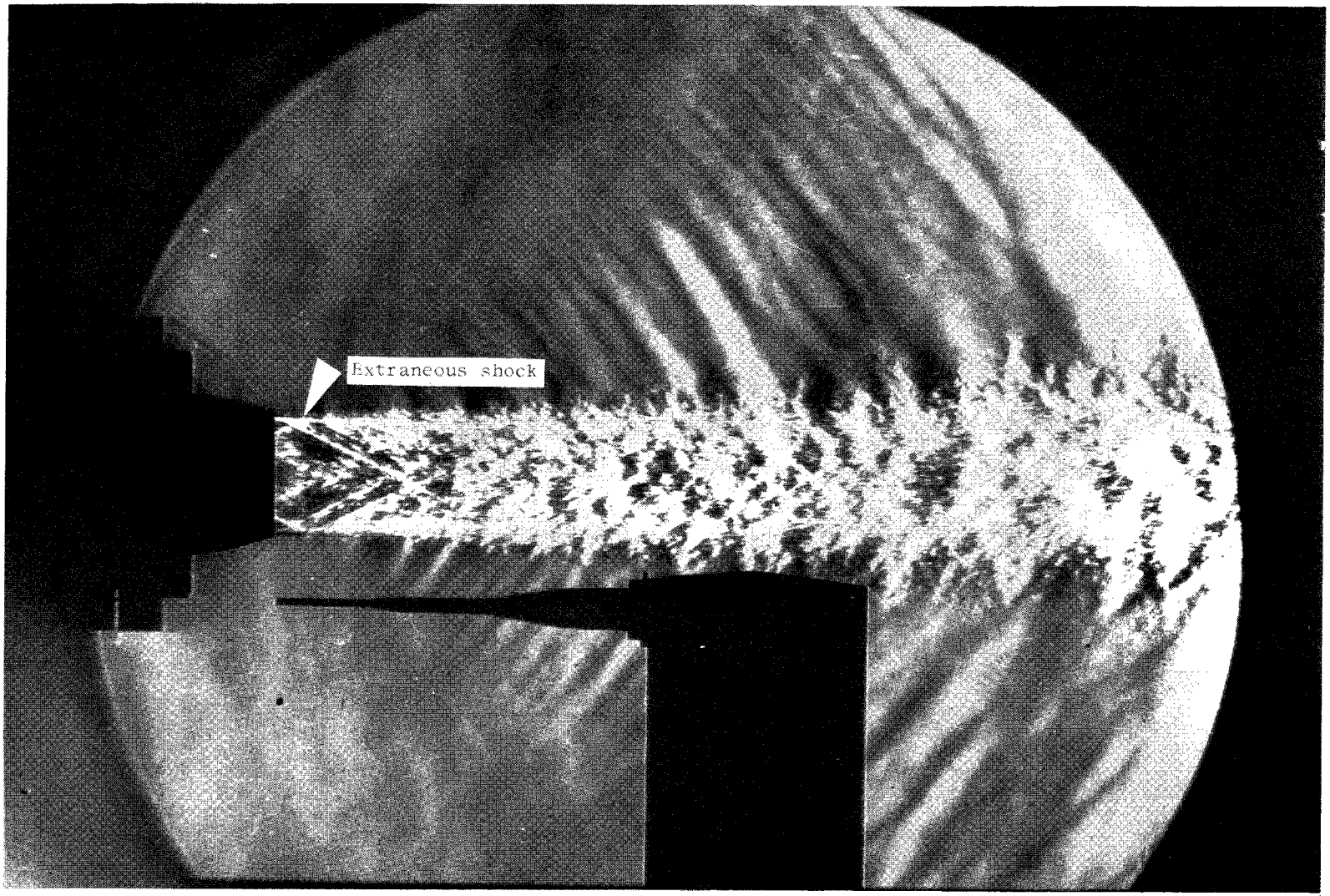

Figure 2.- Schlieren of Mach 2.22 jet. (Knife edge is normal to flow.)

L-66-1139

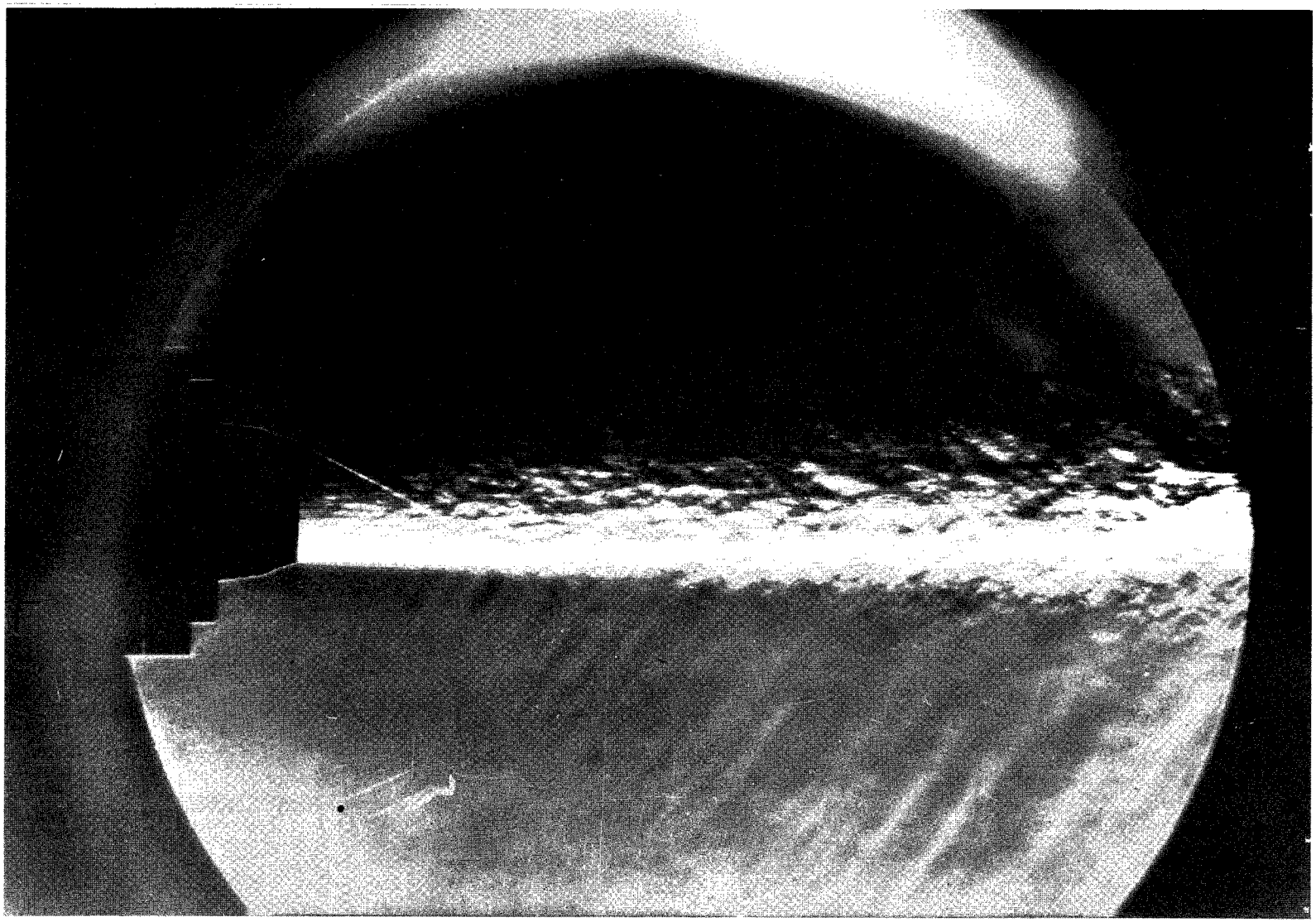

Figure 3.- Schlieren of Mach 2.22 jet. (Knife edge is tangential to flow.) L-66-1140

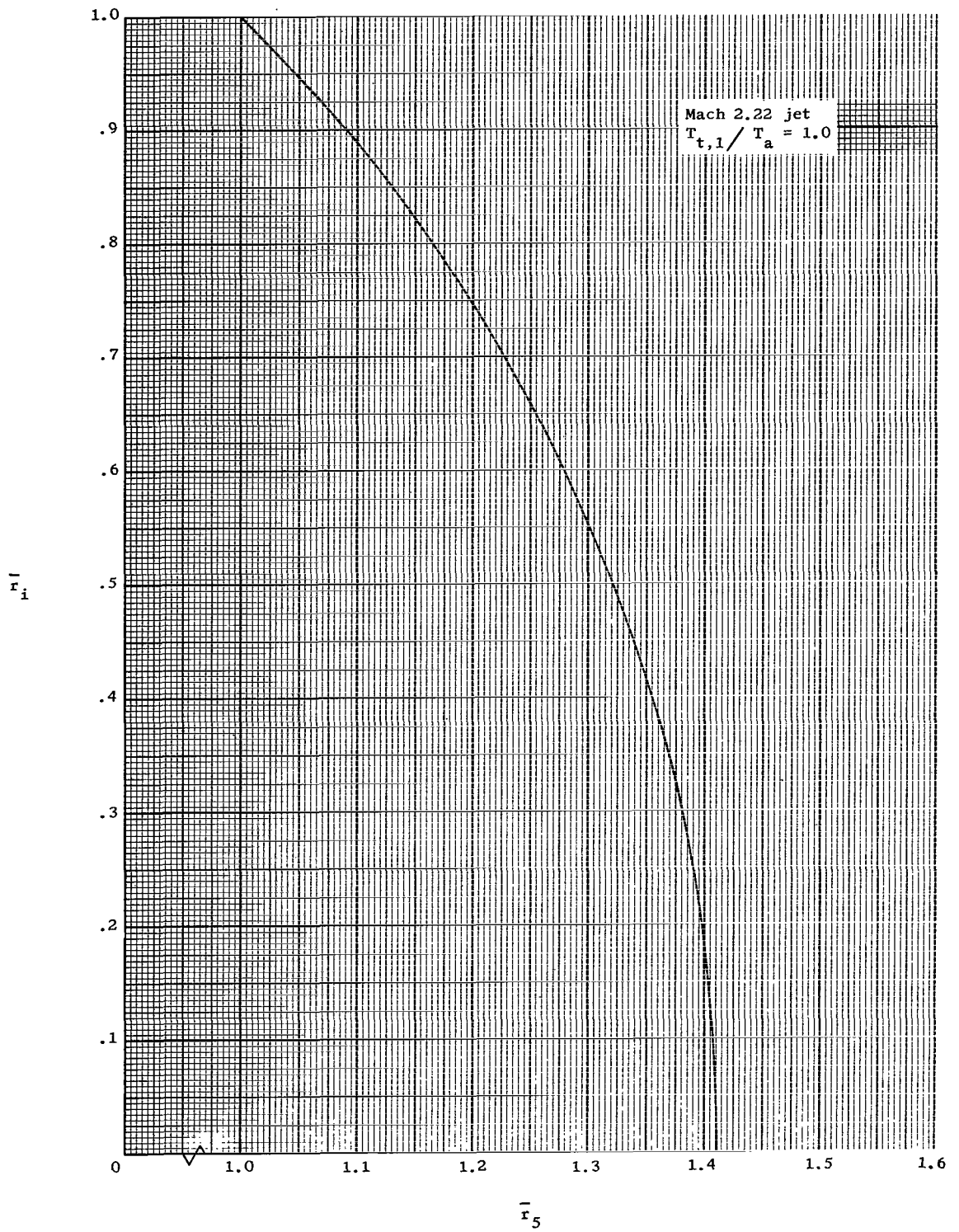

Figure 4.- Radius of potential core $\bar{r}_i$ as a function of jet radius $\bar{r}_5$.

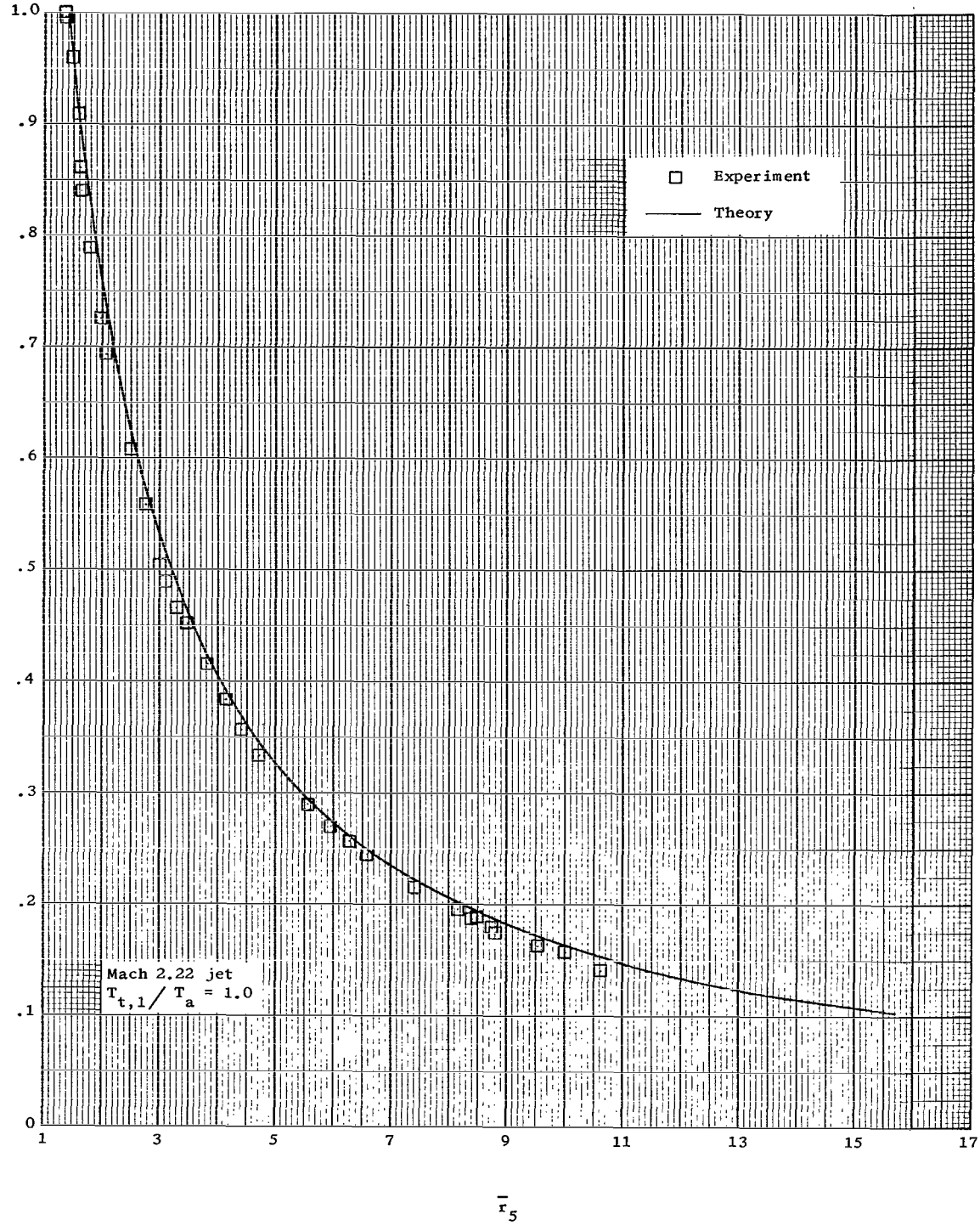

Figure 5.- Center-line velocity as a function of jet radius $\bar{r}_5$.

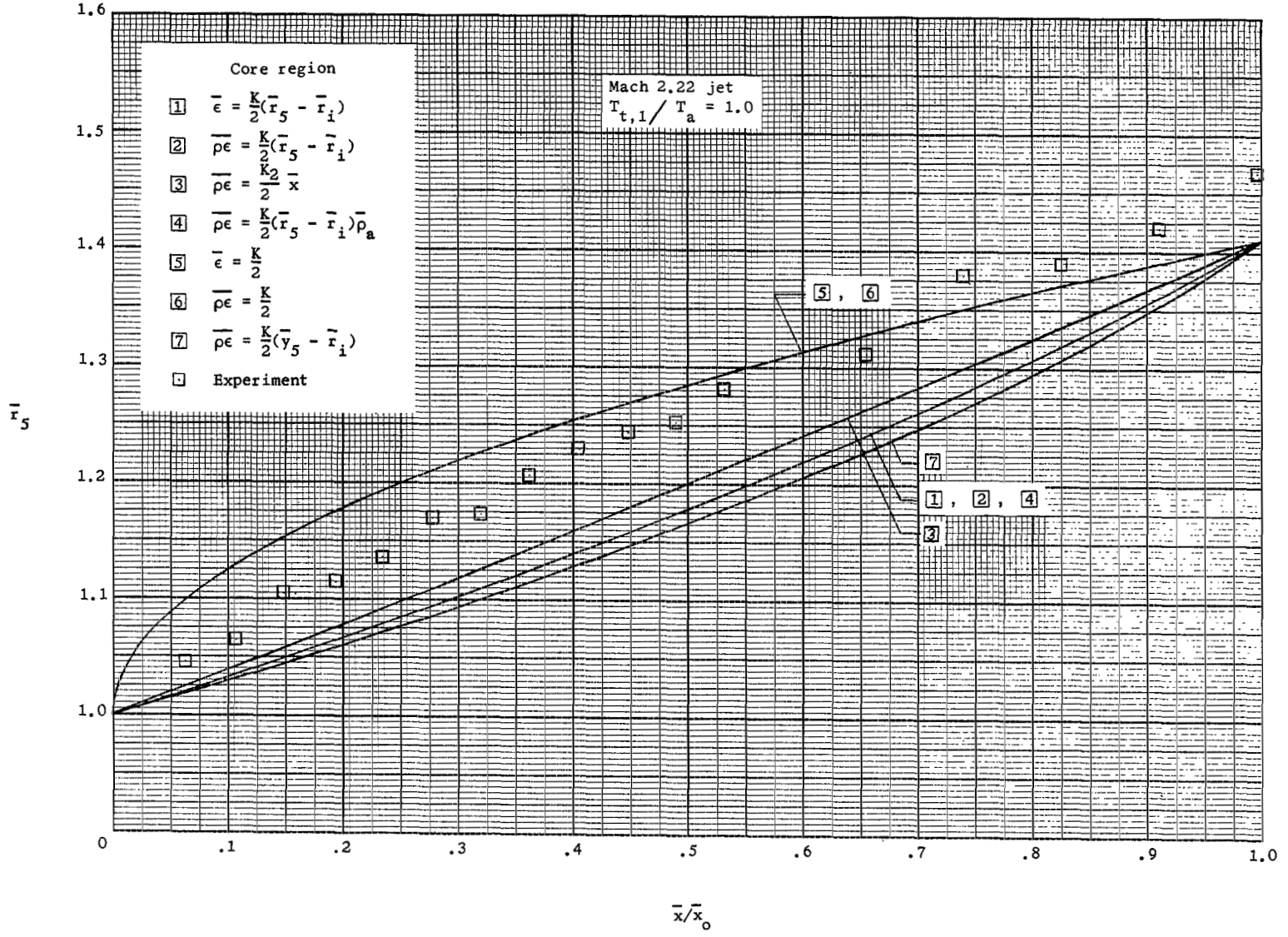

Figure 6.- Core region jet radius $\bar{r}_5$ as a function of $\bar{x}/\bar{x}_0$ for various eddy viscosity formulations.

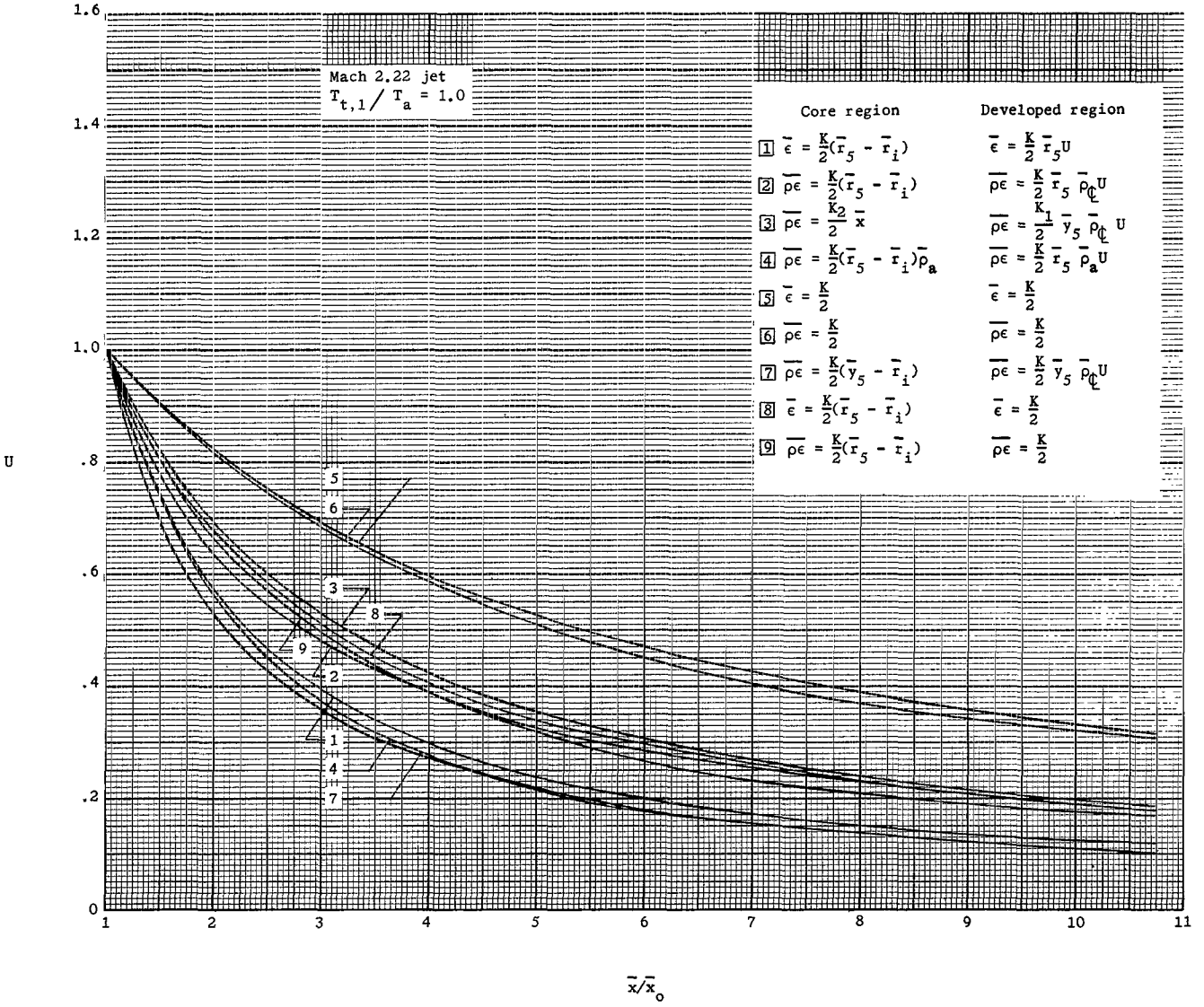

(a) Center-line velocity as a function of $\bar{x}/\bar{x}_o$.

Figure 7.- Developed region solutions for various eddy viscosity formulations.

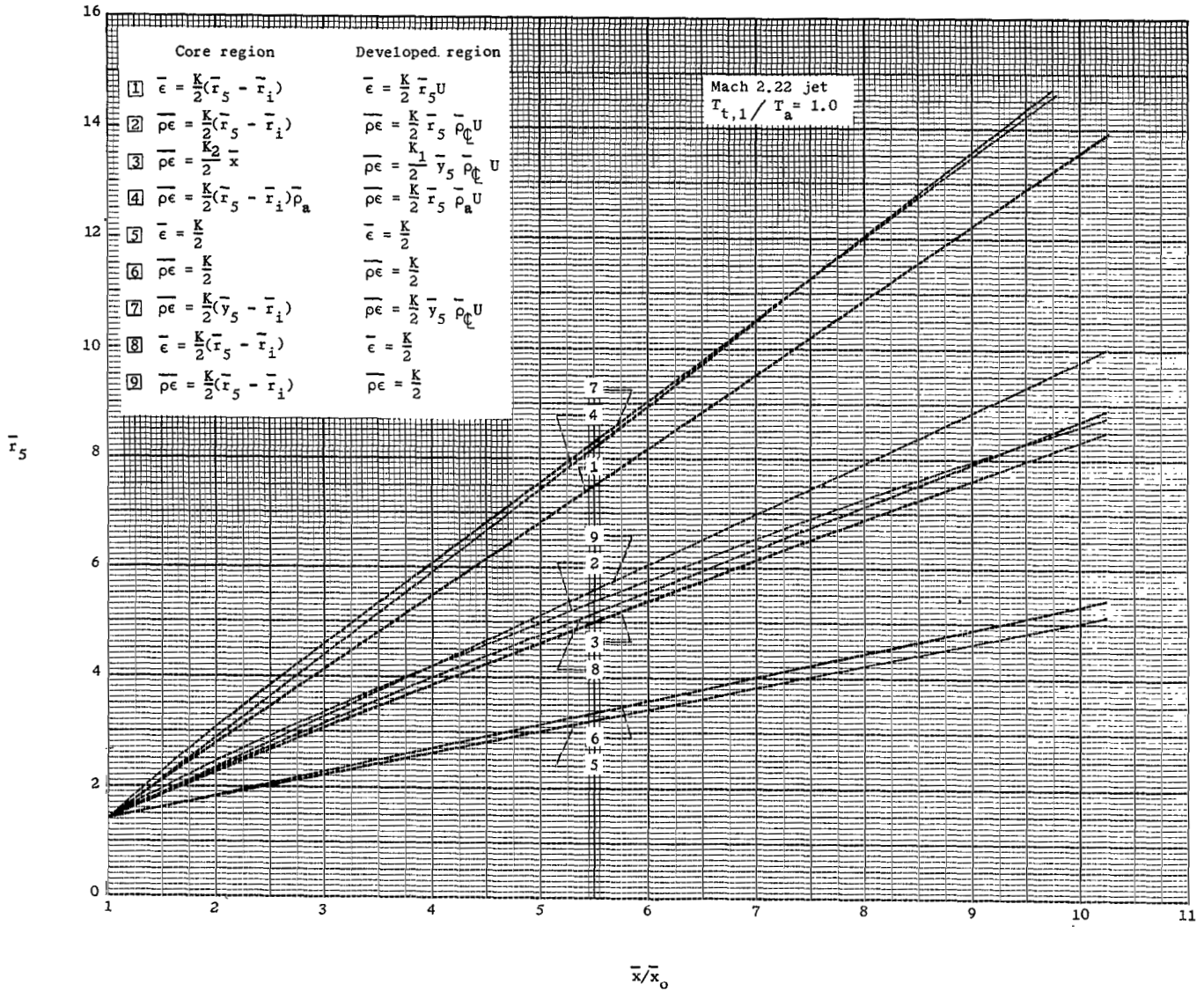

(b) Jet radius $\bar{r}_5$ as a function of $\bar{x}/\bar{x}_o$.

Figure 7.- Concluded.

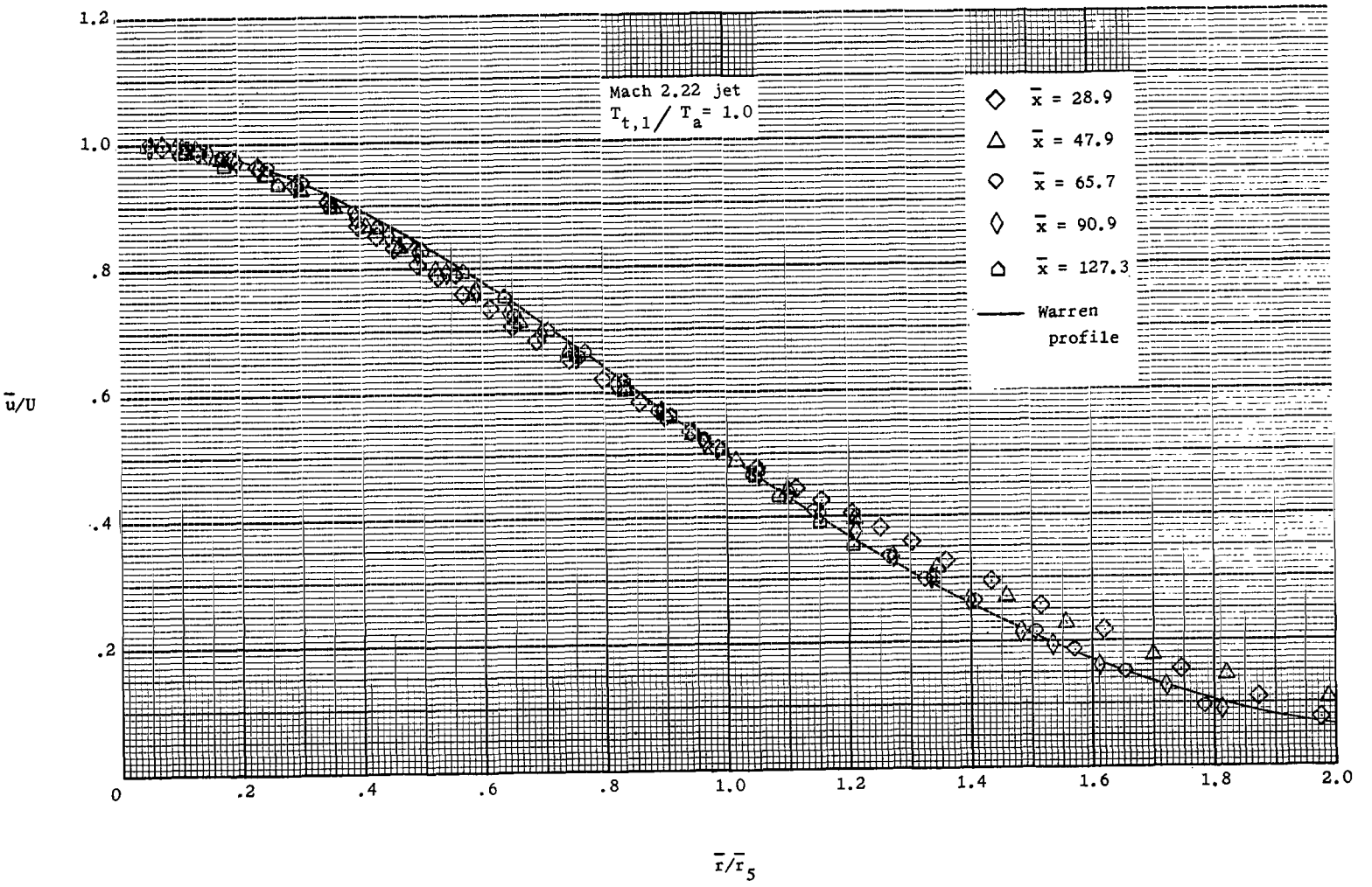

Figure 8.- Similarity plot.

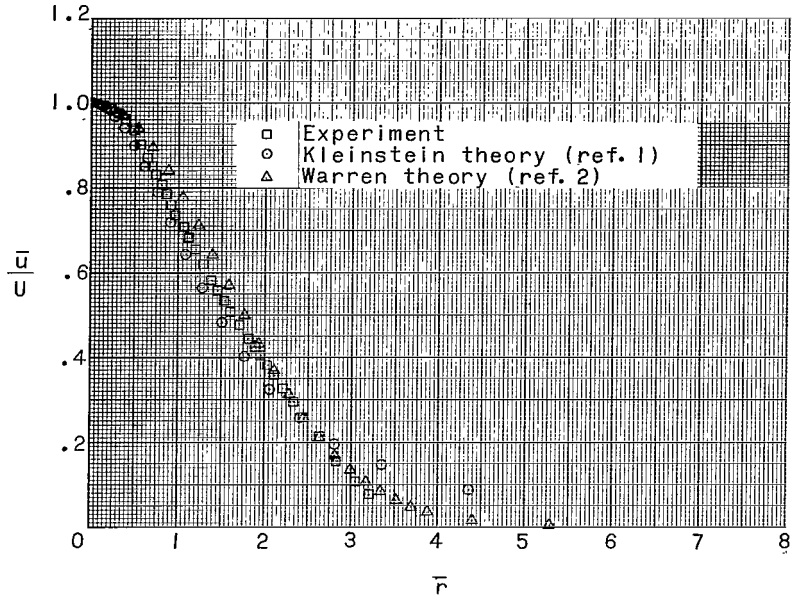

(a) $\bar{x} = 28.9$.

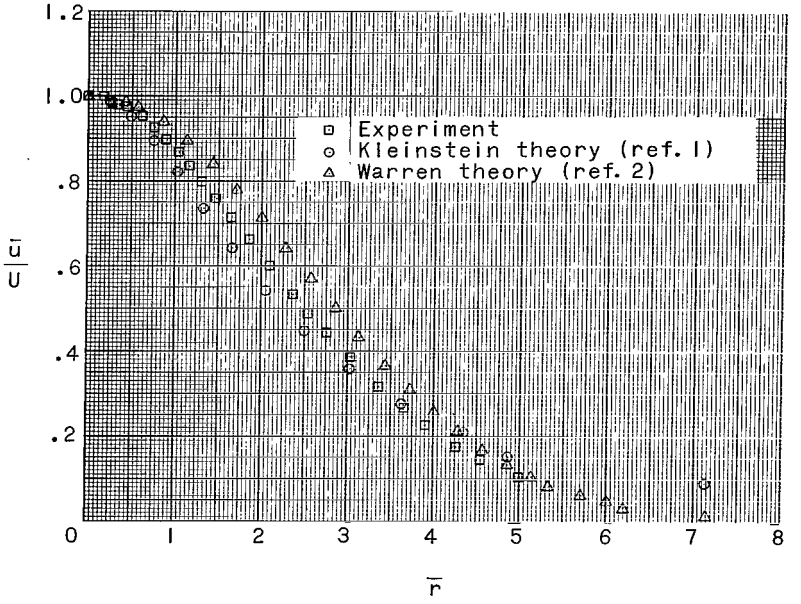

(b) $\bar{x} = 47.9$.

Figure 9.- Theoretical and experimental velocity profiles for Mach 2.22 jet.

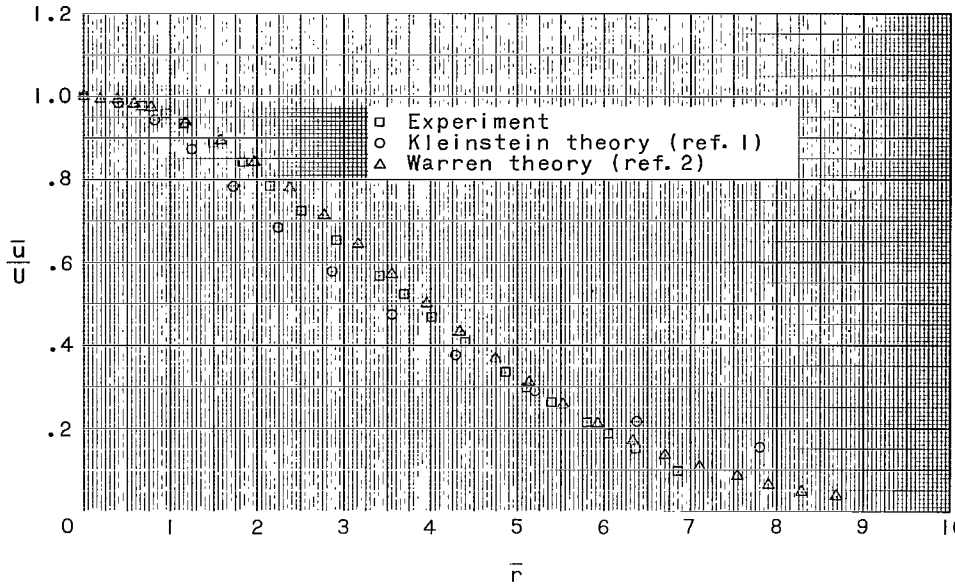

(c) $\bar{x}$ = 65.7.

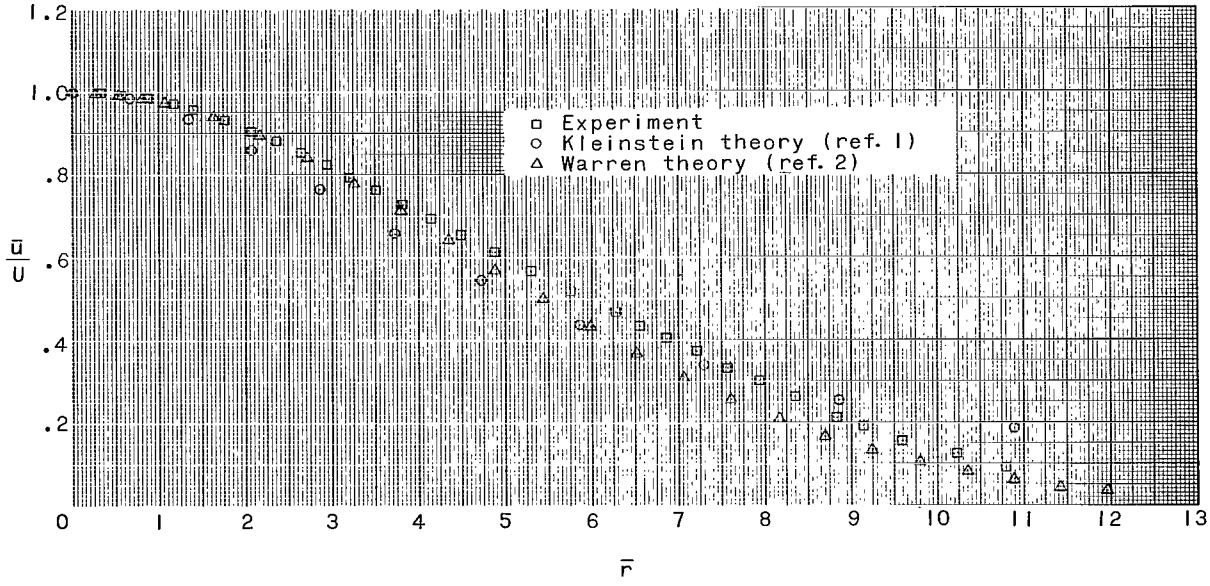

(d) $\bar{x}$ = 90.9.

Figure 9.- Continued.

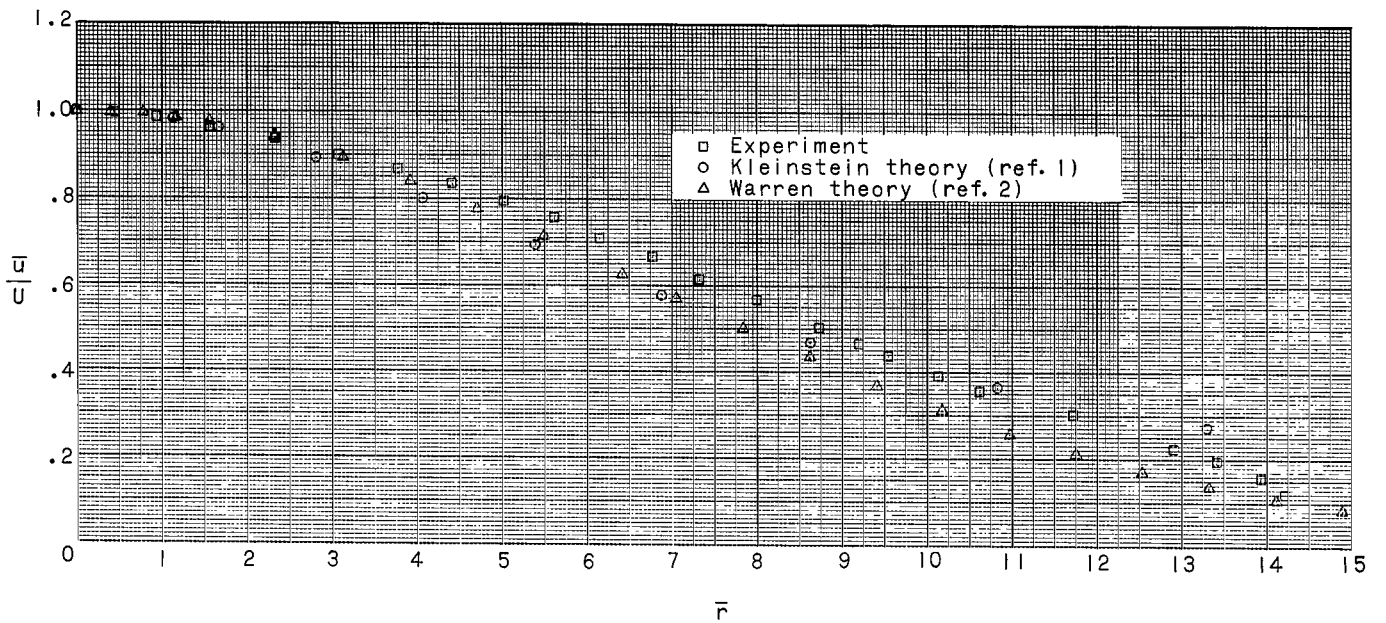

(e) $\bar{x} = 127.3$.

Figure 9.- Concluded.

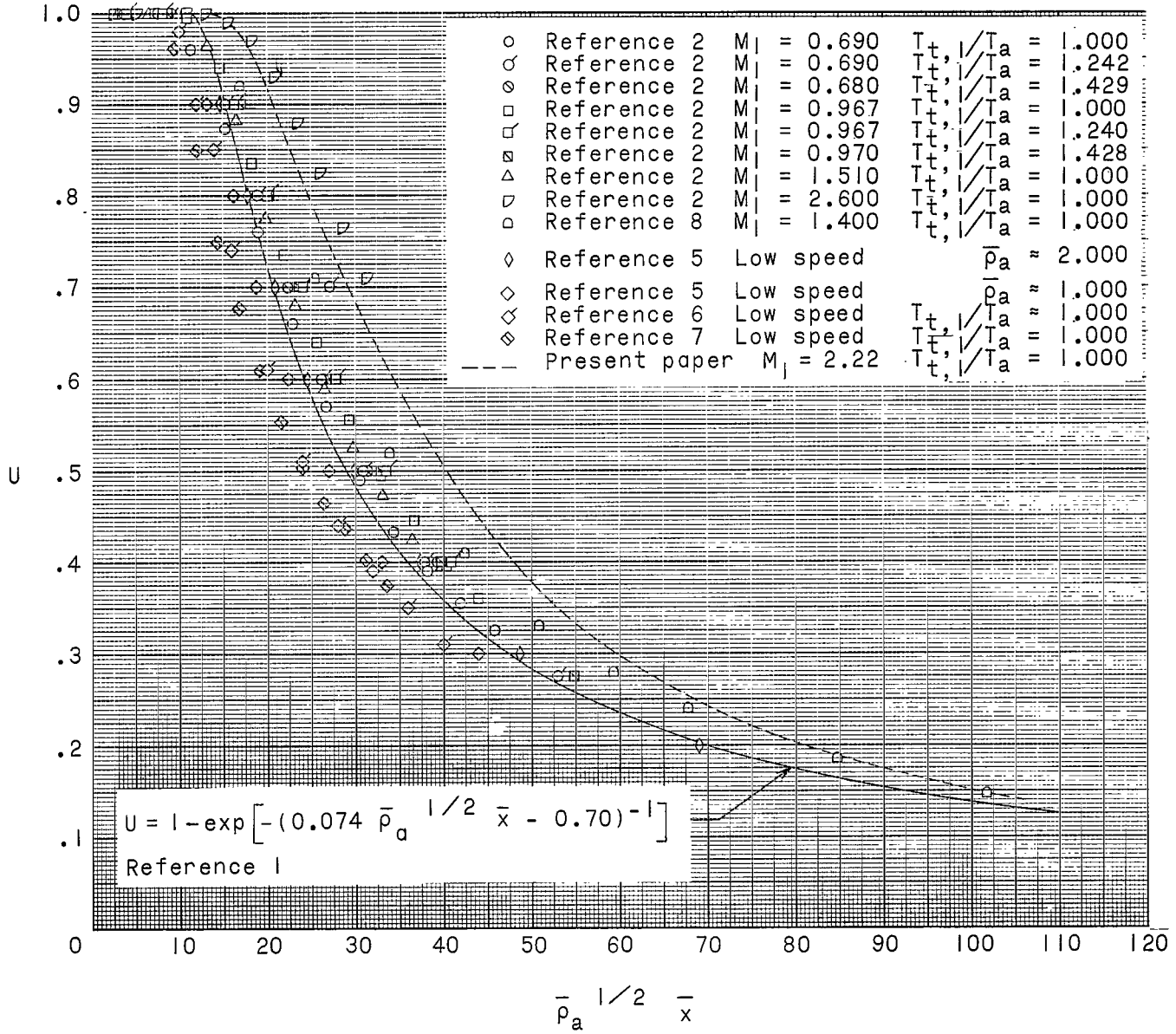

Figure 10.- Data from various sources for center-line velocity as a function of $\bar{\rho}_a^{1/2}\bar{x}$.

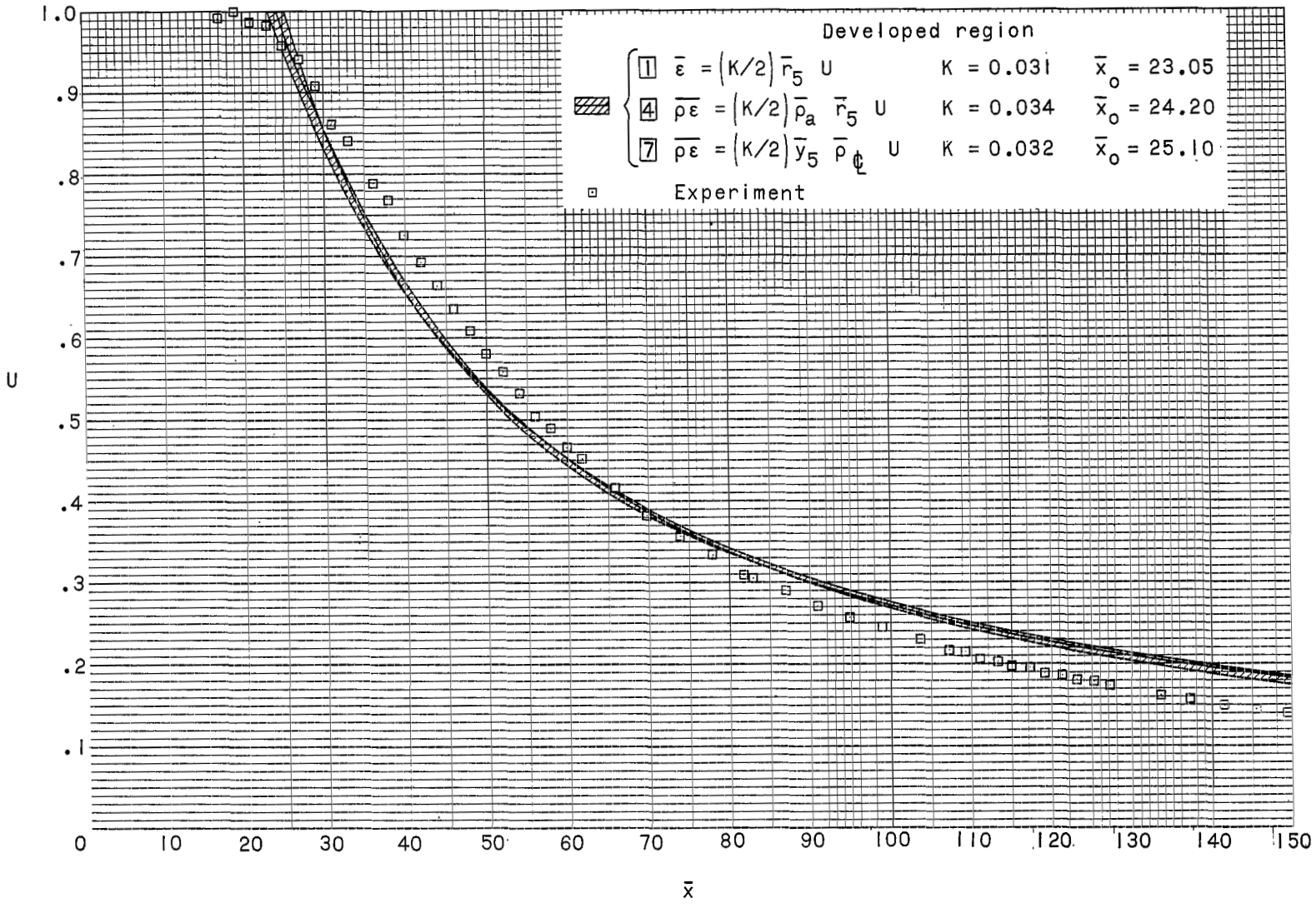

Figure 11.- Developed region center-line velocity as a function of $\bar{x}$. Mach 2.22 jet.

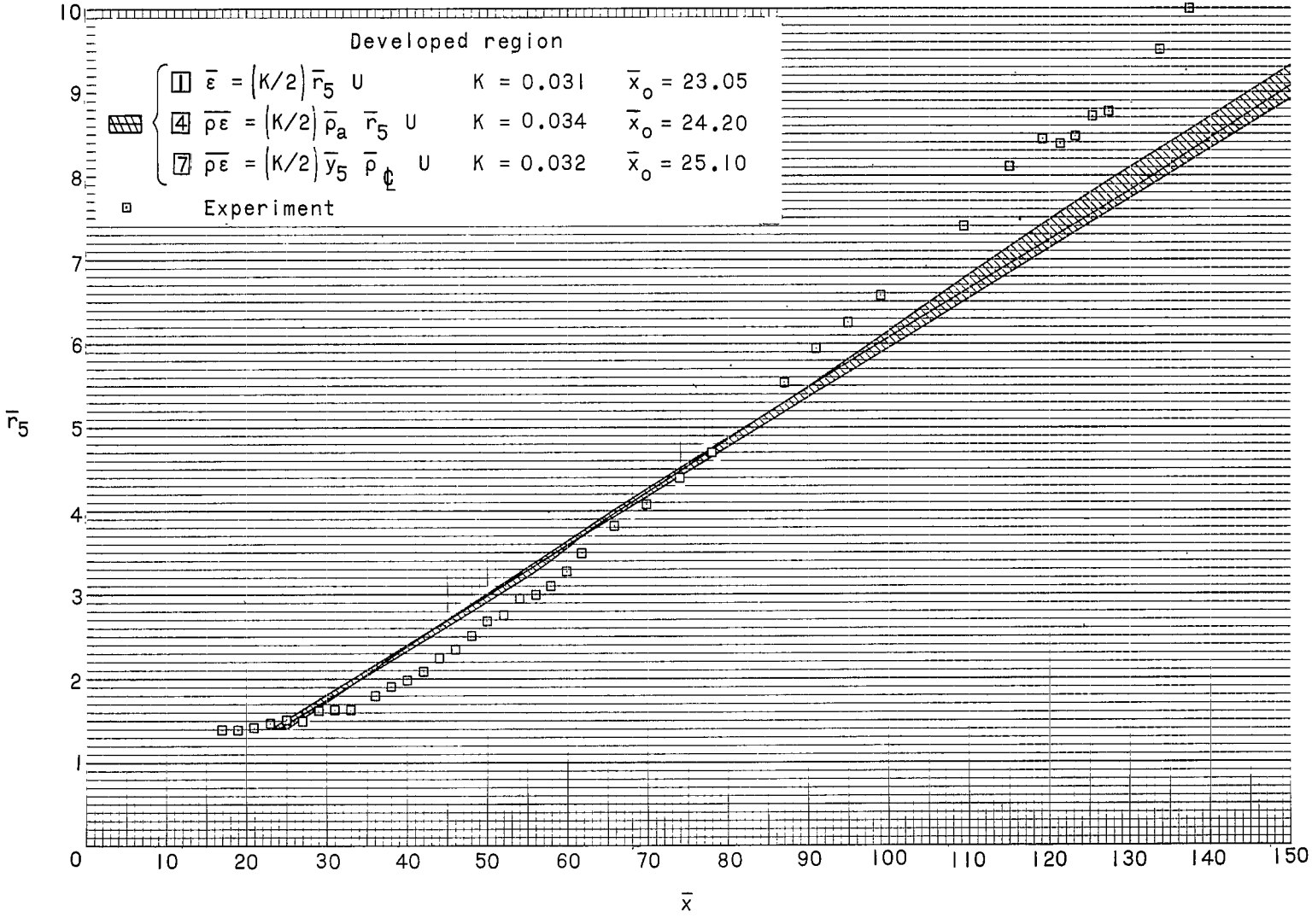

Figure 12.- Developed region jet radius $\bar{r}_5$ as a function of $\bar{x}$. Mach 2.22 jet.

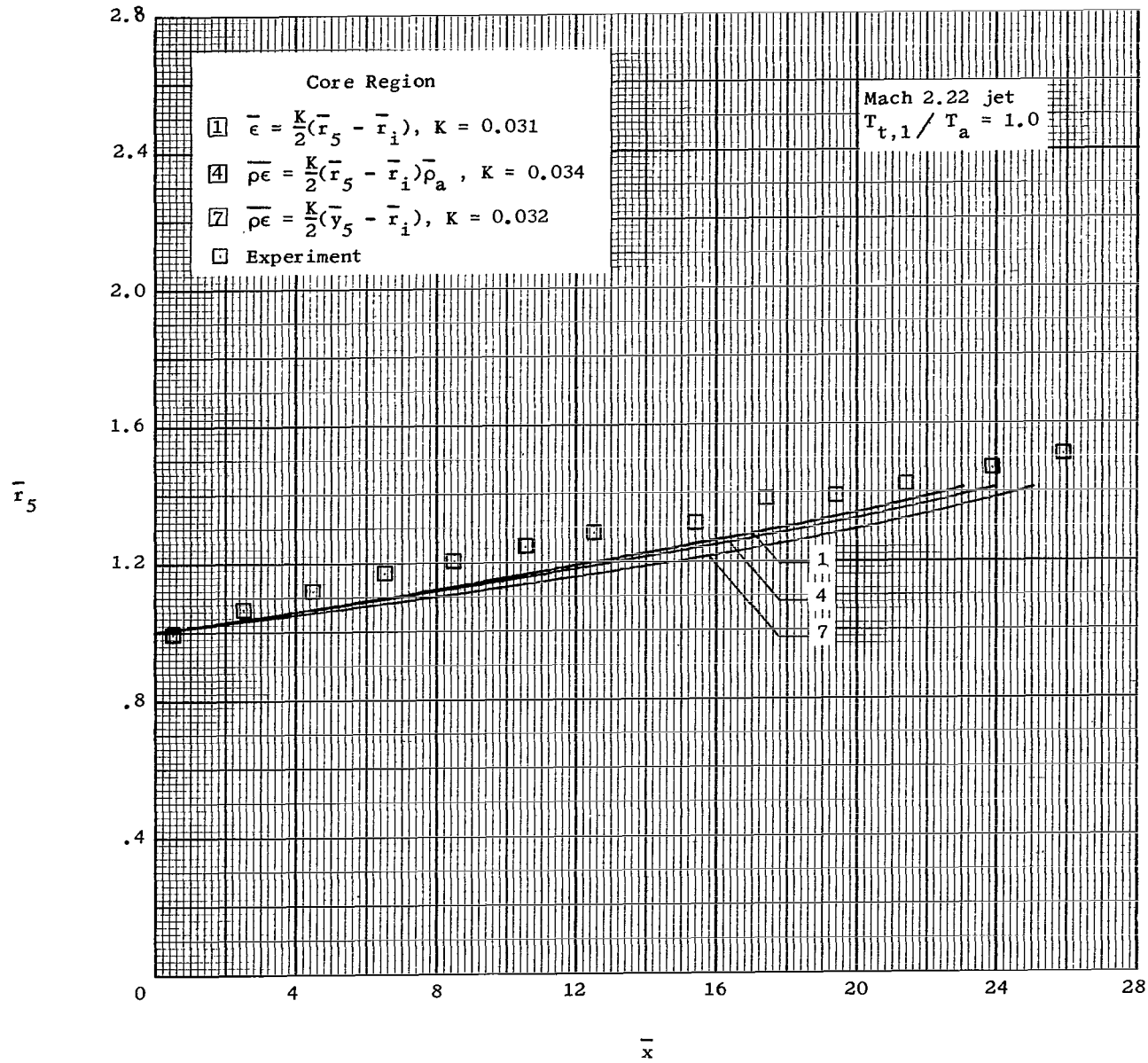

Figure 13.- Core region jet radius $\bar{r}_5$ as a function of $\bar{x}$.

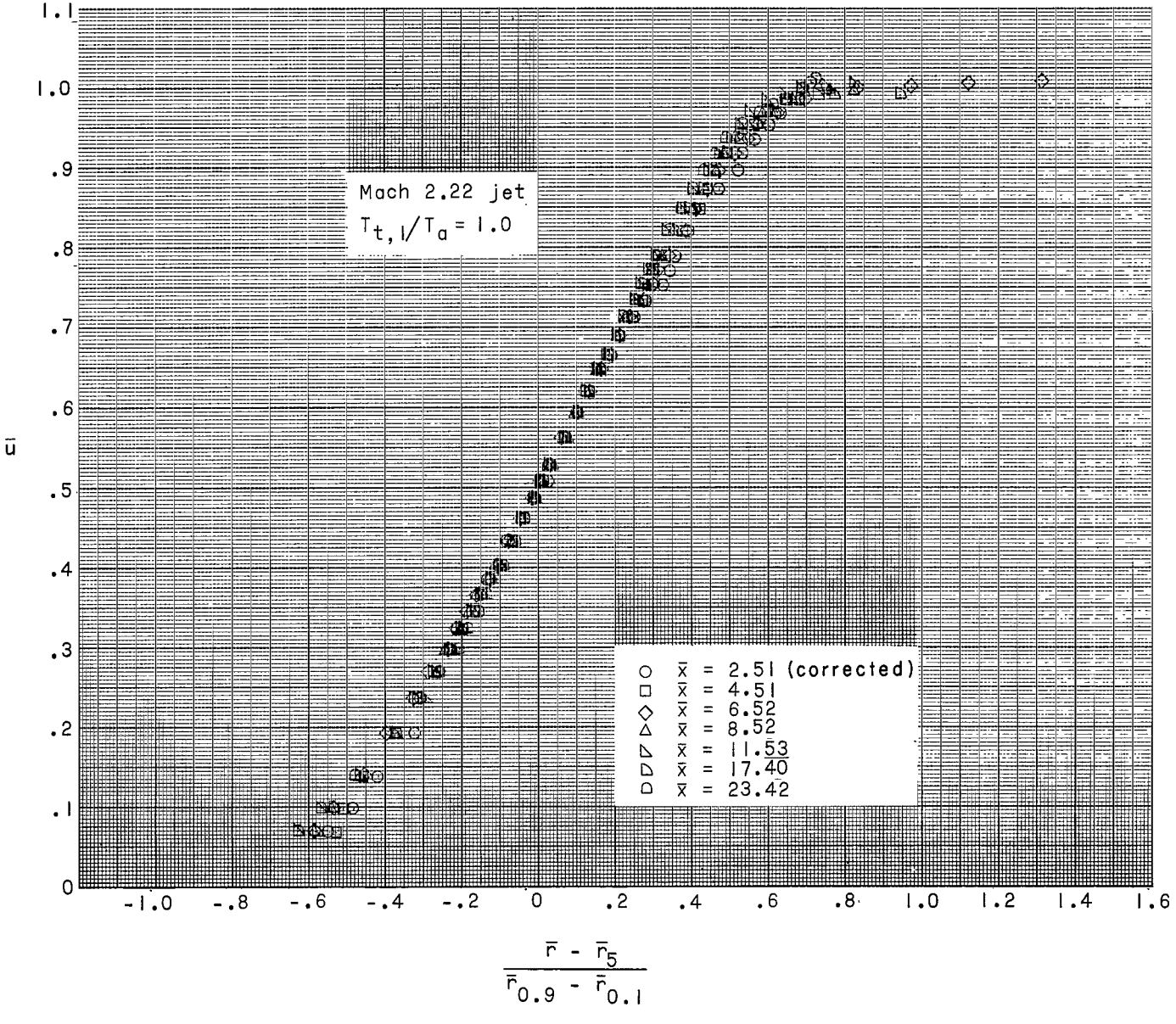

Figure 14.- Core region velocity profile correlation.

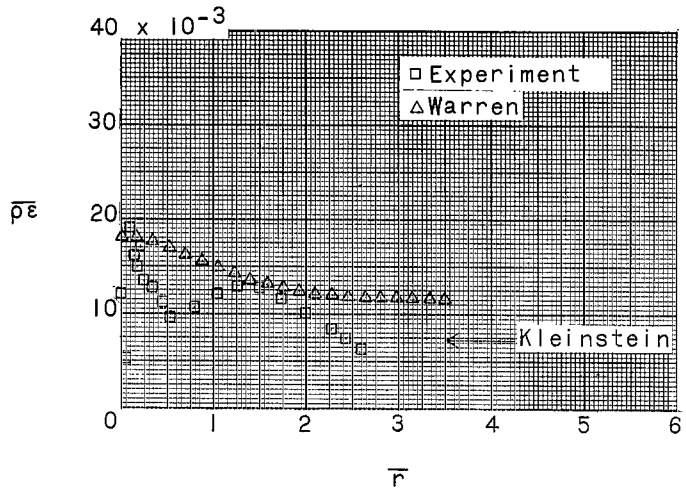

(a) $\bar{x}$ = 28.9.

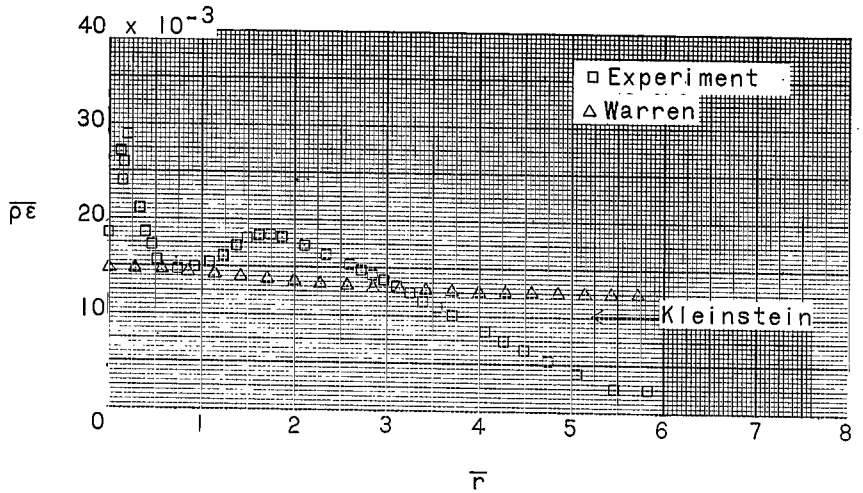

(b) $\bar{x}$ = 47.9.

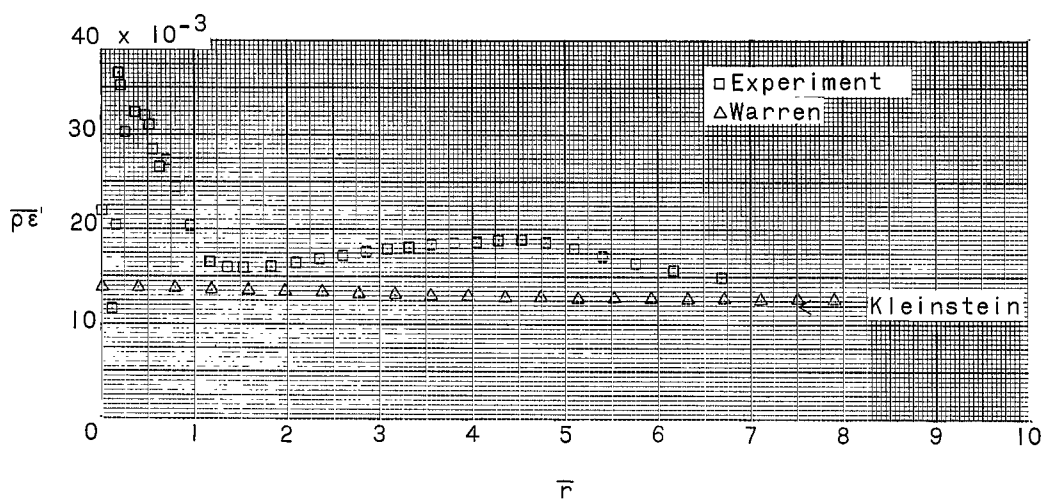

(c) $\bar{x}$ = 65.7.

Figure 15.- Eddy viscosity distributions for the developed region of the Mach 2.22 jet, with the eddy viscosity coefficient expressed as $\overline{\rho\varepsilon}$.

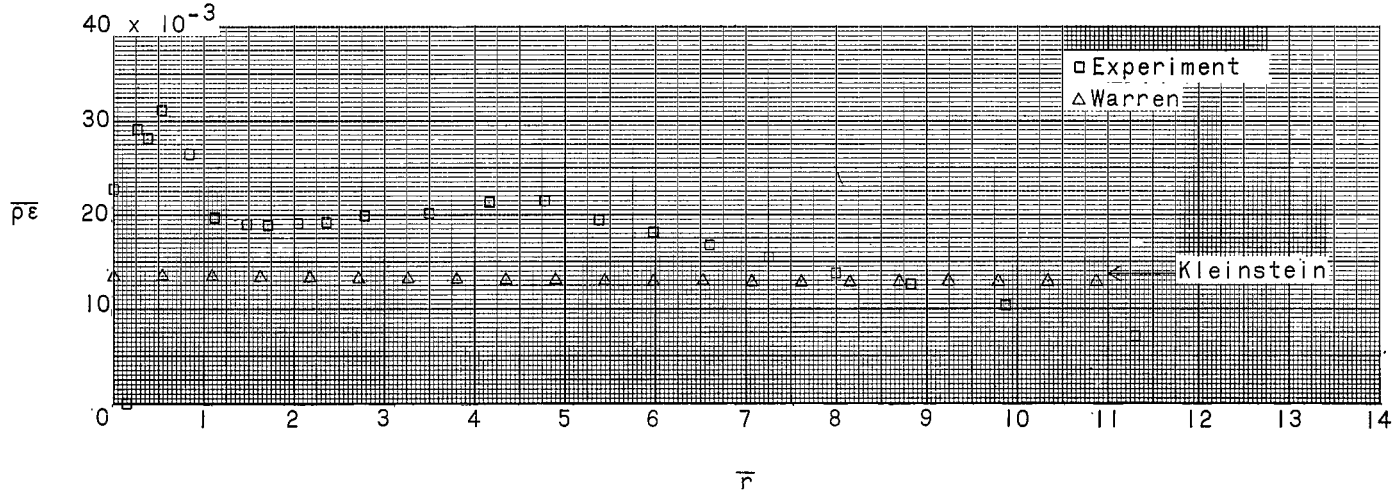

(d) $\bar{x}$ = 90.9.

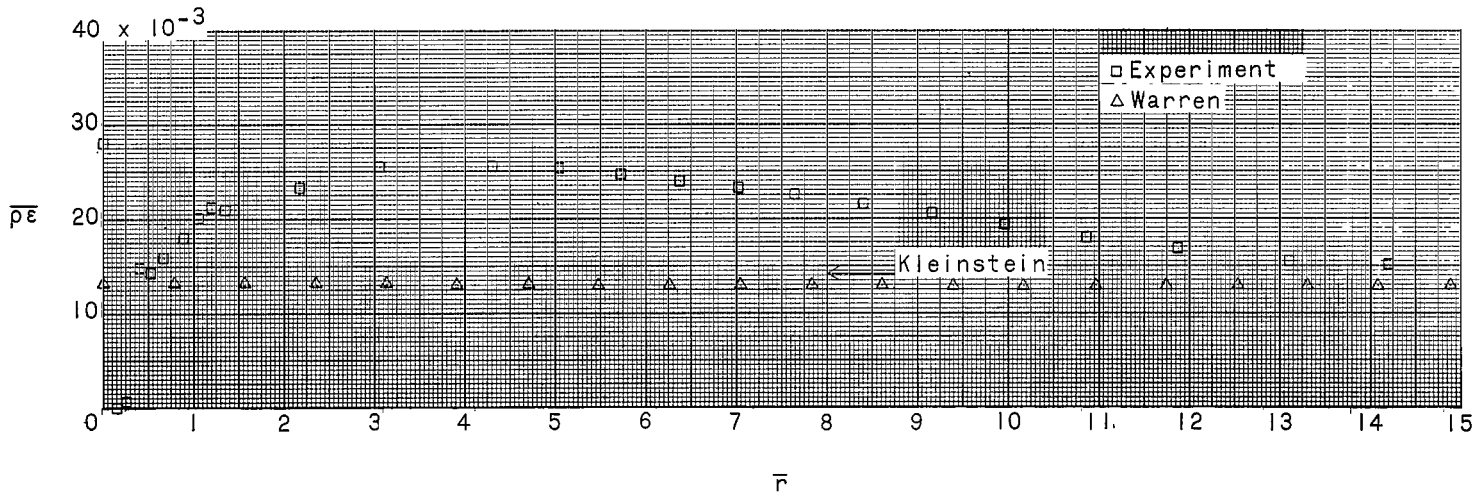

(e) $\bar{x}$ = 127.3.

Figure 15.- Concluded.

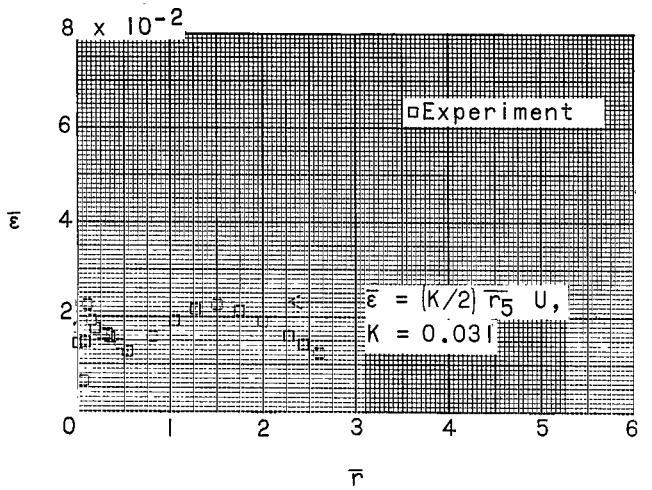

(a) $\bar{x} = 28.9$.

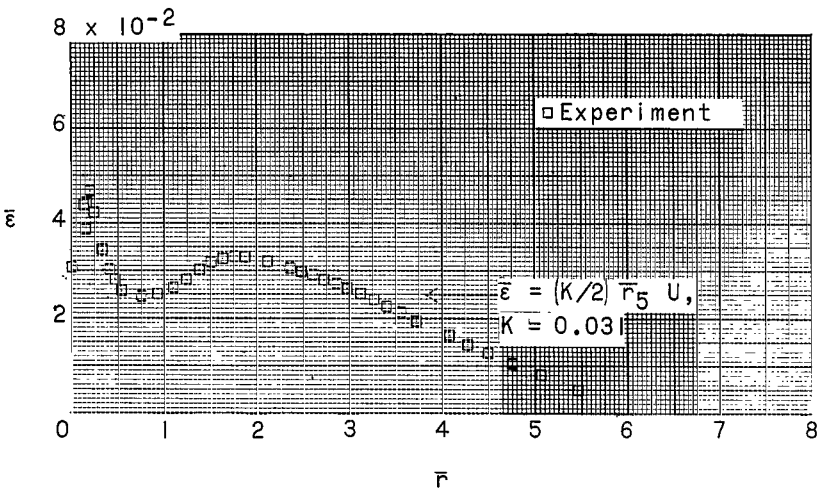

(b) $\bar{x} = 47.9$.

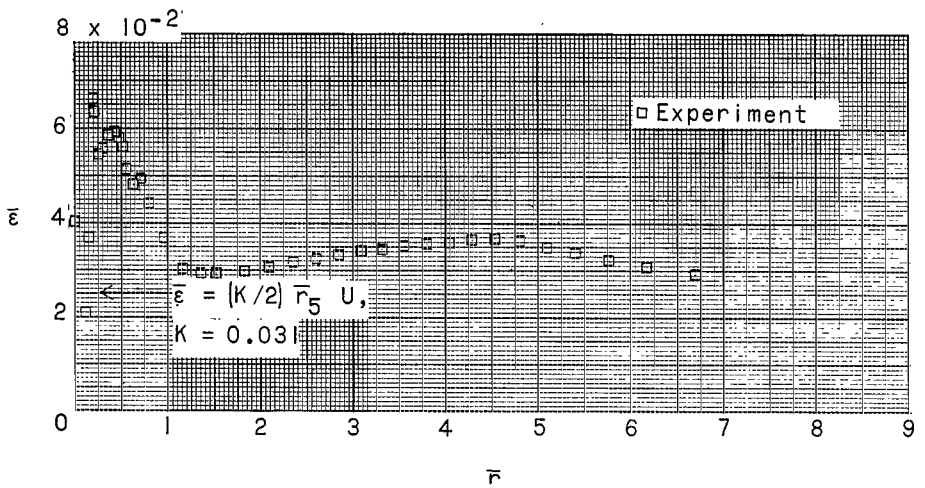

(c) $\bar{x} = 65.7$.

Figure 16.- Eddy viscosity distributions for the developed region of the Mach 2.22 jet, with eddy viscosity coefficient expressed as $\bar{\varepsilon}$.

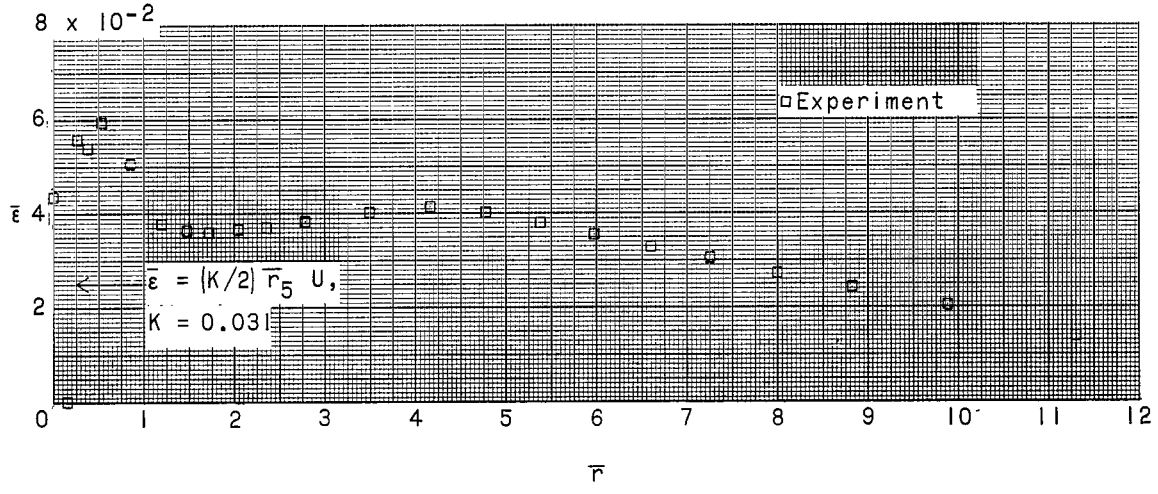

(d) $\bar{x} = 90.9$.

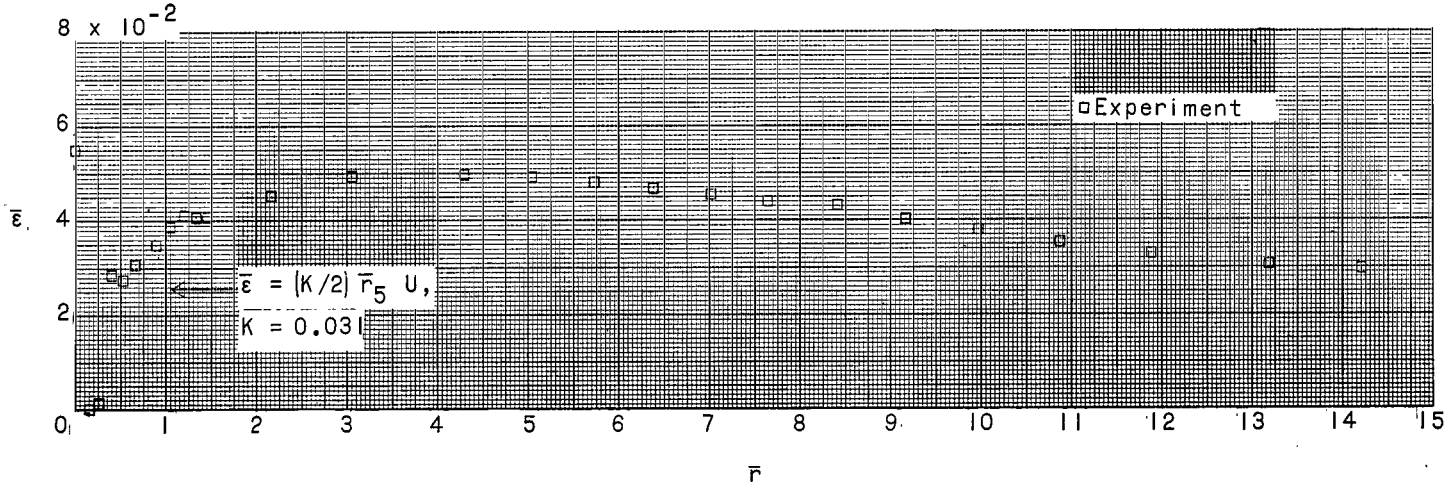

(e) $\bar{x} = 127.3$.

Figure 16.- Concluded.

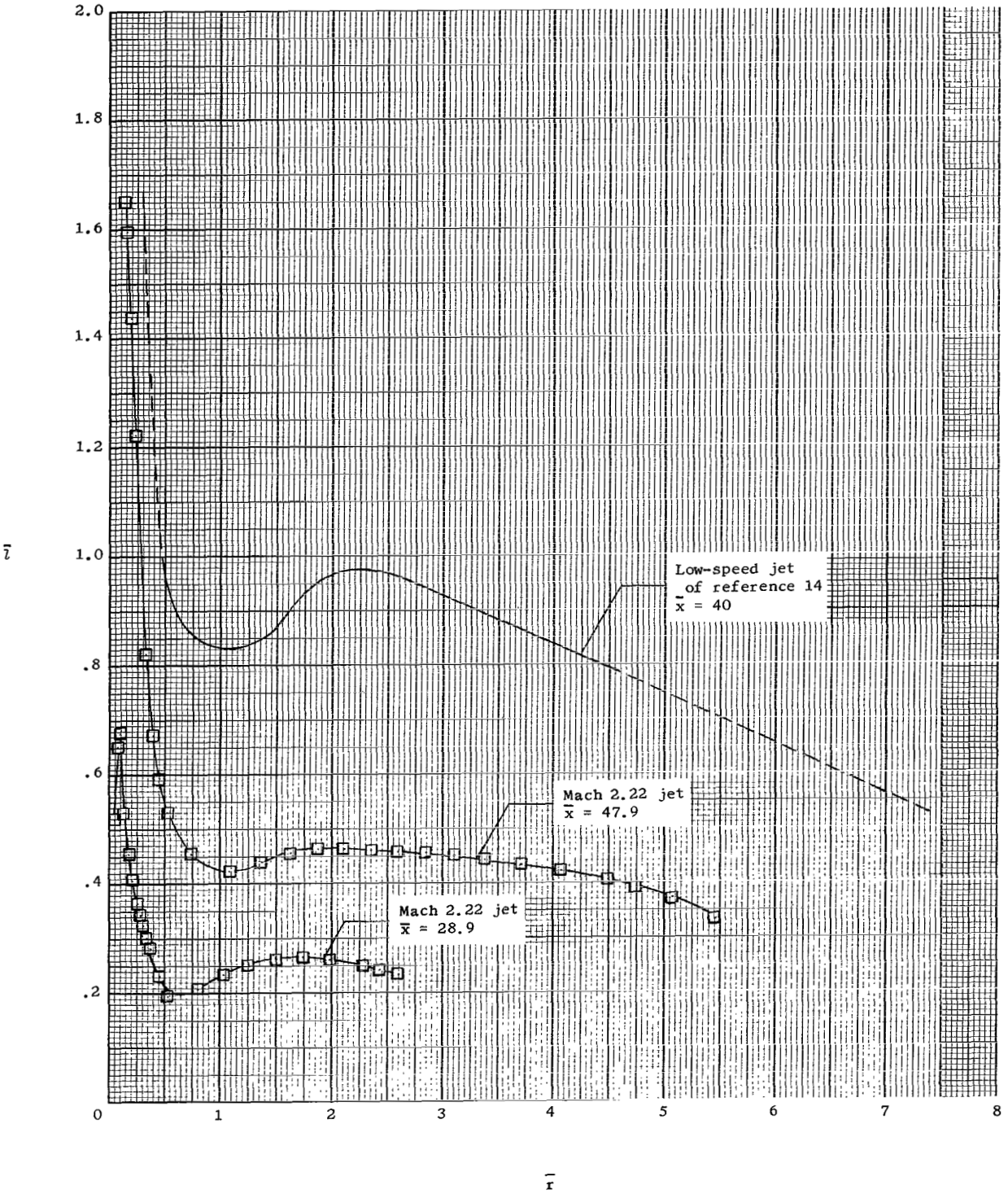

Figure 17.- Prandtl mixing length distributions.

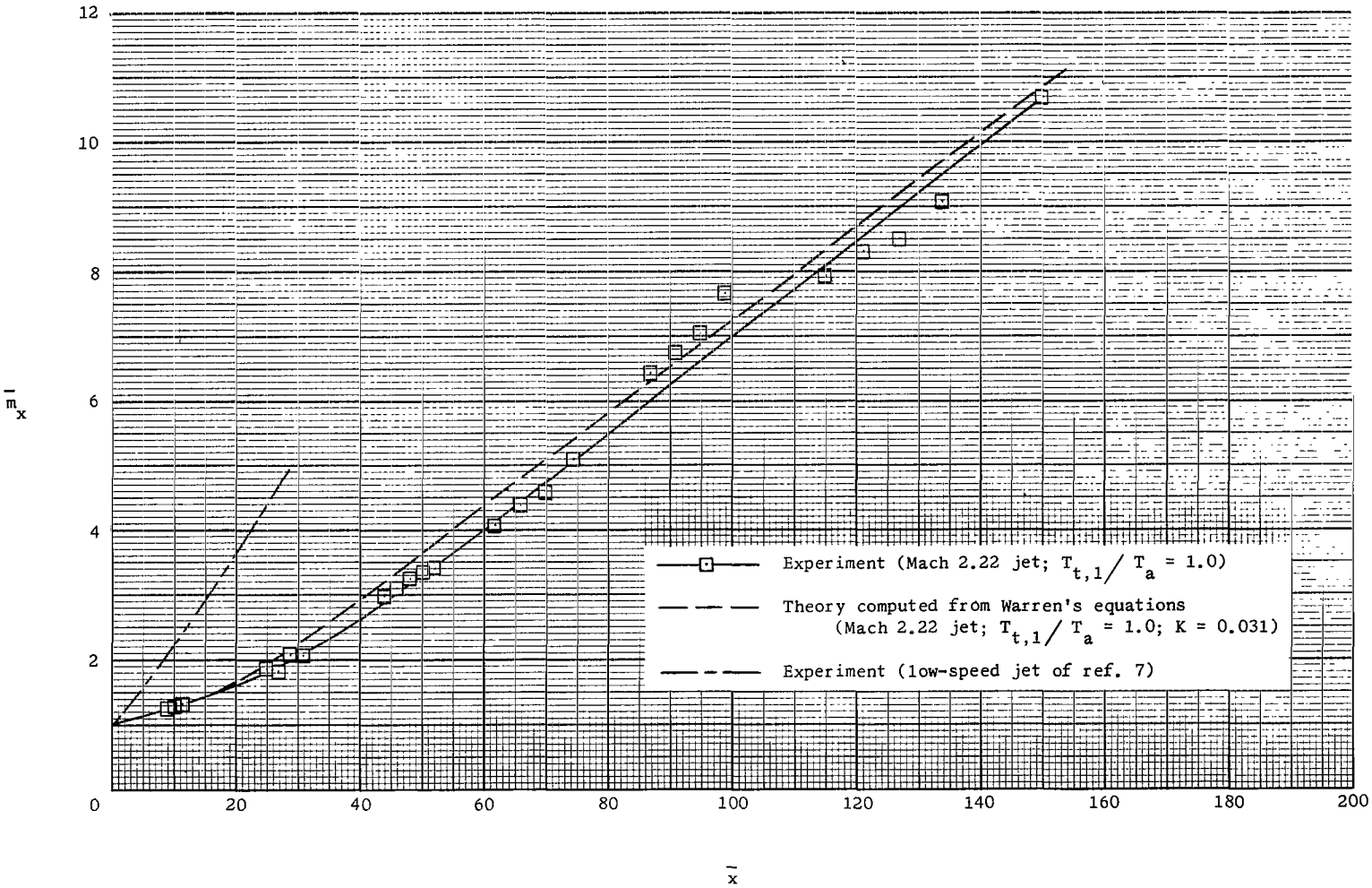

Figure 18.- Entrainment.

"The aeronautical and space activities of the United States shall be conducted so as to contribute . . . to the expansion of human knowledge of phenomena in the atmosphere and space. The Administration shall provide for the widest practicable and appropriate dissemination of information concerning its activities and the results thereof."

—NATIONAL AERONAUTICS AND SPACE ACT OF 1958

NASA SCIENTIFIC AND TECHNICAL PUBLICATIONS

TECHNICAL REPORTS: Scientific and technical information considered important, complete, and a lasting contribution to existing knowledge.

TECHNICAL NOTES: Information less broad in scope but nevertheless of importance as a contribution to existing knowledge.

TECHNICAL MEMORANDUMS: Information receiving limited distribution because of preliminary data, security classification, or other reasons.

CONTRACTOR REPORTS: Technical information generated in connection with a NASA contract or grant and released under NASA auspices.

TECHNICAL TRANSLATIONS: Information published in a foreign language considered to merit NASA distribution in English.

TECHNICAL REPRINTS: Information derived from NASA activities and initially published in the form of journal articles.

SPECIAL PUBLICATIONS: Information derived from or of value to NASA activities but not necessarily reporting the results of individual NASA-programmed scientific efforts. Publications include conference proceedings, monographs, data compilations, handbooks, sourcebooks, and special bibliographies.

Details on the availability of these publications may be obtained from:

SCIENTIFIC AND TECHNICAL INFORMATION DIVISION

NATIONAL AERONAUTICS AND SPACE ADMINISTRATION

Washington, D.C. 20546